EVALUATION OF TIME RATE OF CONSOLIDATION AND UNDRAINED SHEAR STRENGTH OF HYDRAULICALLY PLACED FINE COAL REFUSE

Cyrus Jedari Sefidgari
University of Tennessee, cjedaris@vols.utk.edu

Follow this and additional works at: https://trace.tennessee.edu/utk_graddiss

EVALUATION OF TIME RATE OF CONSOLIDATION AND UNDRAINED SHEAR STRENGTH OF HYDRAULICALLY PLACED FINE COAL REFUSE

A Dissertation Presented for the
Doctor of Philosophy
Degree
The University of Tennessee, Knoxville

Cyrus Jedari Sefidgari
May 2019

DEDICATION

I dedicate my work to my beloved wife
Mina for her endless love and support.

ACKNOWLEDGEMENTS

ABSTRACT

Fine coal refuse (FCR) refers to the fines generated during the processing of raw coal. FCR is usually mixed with flocculant and water and hydraulically placed behind impoundments. It is generally assumed that the FCR in these impoundments will consolidate over time due to the overburden weight of the materials above, losing some of the fluid-like properties that it possessed when initially placed. However, some in situ observations have shown that there exists under-consolidated material within slurry impoundments even after many decades of deposition. These under-consolidated materials can be prone to destabilization and flow, which can result in fatalities and environmental disasters. The purpose of this study is to investigate the consolidation behavior and effect of flocculant on the material properties and flowability of the FCR.

Traditional consolidation tests were conducted on in situ FCR samples obtained from a range of depths behind an impoundment. The consolidation response of the in situ samples was compared with companion samples of fresh liquid slurry pre-consolidated to stresses corresponding to the depths of the recovered in situ samples. A finite difference model used to calculate time rate of consolidation of the FCR using variable coefficient of consolidation which was obtained by consolidating FCR slurry under different pressures. The results were compared to traditional Terzaghi method with constant coefficient of consolidation. Laboratory vane shear tests were conducted to study the influence of flocculant on undrained shear strength of the FCR and modified flow table tests performed on consolidated FCR slurry samples prepared with different background fluids.

The results suggest that the variable coefficient of consolidation method may best predict the time rate of consolidation for the FCR slurry compared to traditional methods which use the in situ coefficient of consolidation. Although the particle size analysis revealed that the effect of flocculant degrades over the time, vane shear results suggest that the flocculant increases the undrained shear strength and can improve the FCR resistance to flow at early stages of consolidation. The results of this study give a better understanding of the consolidation behavior and undrained shear resistance of the hydraulically placed FCR behind impoundments.

TABLE OF CONTENTS

LIST OF TABLES

LIST OF FIGURES

CHAPTER I
INTRODUCTION

1.1 PROBLEM STATEMENT

According to the U.S. Energy Information Administration Statistics (2017), coal is one of the major sources of energy in the U.S. Approximately 720 million tons of coal was produced in the U.S. during 2017, 92% of which was used in coal fired power plants to generate 30.1% (~1208 million MWh) of the total U.S. power production in 2017 (USEIAS, 2017). Coal is processed to remove impurities before transporting to the power plants, leaving behind waste materials described as coarse or fine refuse. Fine coal refuse (FCR) refers to the fines generated during the processing of raw coal and is considered a waste material. FCR is typically stored behind on-site impoundments constructed primarily with the coarse refuse. This FCR is typically hydraulically placed by mixing the fines with water and a chemical flocculent and then pumping the resulting slurry through a series of pipelines. The flocculent is added to promote rapid settling of the solids once the slurry is placed in the impoundment. There are more than 1,170 tailing dams in US, of which approximately 700 are coal refuse impoundments (U.S Army Corps of Engineers, 2017). These on-site impoundments are essentially tall dams (60 to 240 meters tall) behind which the FCR is allowed to settle and dewater. Hundreds of these impoundments are in the Appalachia region.

The most common method of constructing impoundments is the upstream method (Figure 1-1). During the initial stage in this method of construction, the fine coal refuse slurry is hydraulically discharged from the top of the starter dike and forms a delta. The deposited fine refuse then becomes the foundation for the second stage of embankment construction with additional coarse refuse used to construct the next dike followed by additional slurry placement. Construction continues in this manner until the desired and/or permitted impoundment height is reached. While the upstream construction method is typically depicted as shown in Figure 1-1, it has been suggested that during the placement of the coarse refuse on top of the underlying fine refuse some coarse refuse may displace the underlying soft FCR increasing the depth to the fine refuse and perhaps creating a zone of mixed material (Kalinski and Phillips, 2008).
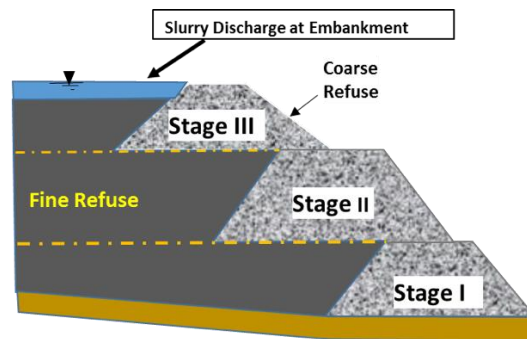
Figure 1-1. Upstream method of construction of FCR impoundments.

One of the most critical concerns of impounded mine waste material is whether or not the materials are prone to destabilization, i.e. flow. Destabilization of the FCR impoundment can result in severe and unpredictable fatalities and environmental disasters. The failure of FCR impoundments is in the form of dam failures (Coarse Refuse) and/or breakthrough of FCR slurry into adjacent underground mines (FCR flow). As mentioned above, hundreds of these impoundments exist in the Appalachia region, and while many are well constructed and routinely inspected, there have been cases in which slurry destabilization resulted in loss of life, injury, significant environmental degradation of the downstream surface waters, and property loss. One such event occurred at Buffalo Creek in 1972 (Logan County, WV) where approximately 132 million gallons of FCR was released, resulting in the deaths of 125 people, the loss of 16 local communities, and more than $75,000,000 in damages (Kelley et al., 1973). In 2000 in Martin County (KY), a breakthrough occurred causing an estimated 306 million gallons of water and slurry to drain from an impoundment into an adjacent underground mine (Mine Safety and Health Administration, 2009).

The rate at which the FCR consolidates is one of the most critical characteristics of impounded mine waste material related to destabilization, i.e. flow. The general assumption is that the fine refuse in these impoundments will consolidate over time due to the overburden weight of the material above, losing some of the fluid-like properties that it possessed when initially placed. This consolidation process decreases the volume of the slurry, as the water is squeezed out, with the water pressure in the pores between solid particles decreasing over time. This consolidation and dissipation in pore pressure is accompanied by an increase in strength. Yet, the consolidation behavior of fine coal slurry has not been fully investigated. There are limited observations of the characteristics of slurry in place and its variation with depth within slurry impoundments. Furthermore, there is no generally agreed upon model for the consolidation behavior of these materials, which would define under what conditions they are being consolidated.

One other factor that may influence behavior is the influence of the flocculent added to the FCR slurry. The flocculent is added to the FCR to promote rapid settling of the solids once the slurry is placed in the impoundment. Solid particle suspensions may exhibit a wide range of rheological responses. The response depends on the particle size and shape, solids content, particle interactions in the surrounding fluid, fluid viscosity, and inter-particle forces, and colloidal suspensions often exhibit Bingham plastic flow (van Olphen, 1977). Effect of pore fluid on viscosity and rheological behavior of the FCR has been studied in this research. Coal slurries with high particle concentrations dispersed in water have been observed to follow the Bingham plastic behavior model as well as the Ostwald-de Waele (power law) model (Singh et al., 2016)

The effects of the flocculant, compared to a dispersant, on the particle structure and material response and its subsequent effects on particle size, shear strength and flowability of the FCR is also addressed in this study.

The purpose of this investigation is to contribute to the understanding of the compression and flow characteristics of fine coal refuse placed in impoundments by: (1) characterizing the in situ properties of fine coal refuse at an existing impoundment, (2) relating the background fluid chemistry with rheological response, particle and floc size (3)relating the staged deposition and evolving compression properties (i.e. coefficient of consolidation) to the time rate of consolidation of fine coal refuse slurry, and (4) studying the influence of background fluid chemistry on shear strength and flowability of fine coal refuse. These objectives were addressed through both field and laboratory testing as well as finite difference modeling of FCR consolidation. Field testing consisted of both traditional Standard Penetration Tests (SPT) and Cone Penetration Tests (CPT) to obtain measurements of in situ properties as a function of depth. Samples were obtained both from the impoundment as a function of depth, and fresh coal refuse slurry collected from the discharge pipe as it was being placed behind an adjacent active FCR impoundment.

1.2 OBJECTIVES

This research addresses the following specific objectives:

- Synthesize information found in the literature pertaining to the behavior of fine coal refuse.
- Determine, based on the field exploration of an existing slurry impoundment, the variation of in situ properties with depth.
- Investigate the laboratory rheological behavior and particle/floc size distribution of fine coal refuse as a function of background fluid chemistry using traditional hydrometer analysis and laser diffraction methods.
- Predict time rate of consolidation of the FCR slurry with a new approach by incorporating the time and stress dependency of the coefficient of consolidation to improve the traditional Terzaghi method of prediction of time rate of consolidation.
- Determine the influence of pore fluid chemistry on flowability and undrained shear strength of the FCR.

1.3 RESEARCH QUESTIONS

This study focuses on the in situ behavior of fine coal refuse based on the findings from laboratory experiments. Rather than following hypothesis-driven research, many avenues of engineering research are explored on the basis of identifying number of pertinent research questions. For the research described here, the following research questions were identified

1- How do the in situ properties of fine coal refuse change with the depth?
2- How does pore fluid chemistry affect the particle size distribution and rheology?

3- Has the fine coal refuse in an old inactive impoundment reached to the end of primary consolidation?

4- How does loading/staging sequencing affect the consolidation process/time?

5- How does the added flocculant influence the shear strength and flowability of fine coal refuse?

1.4   ORGANIZATION

This proposed work is divided into seven chapters summarized here.

- Chapter One defines the problem, research objectives and outline of this research.
- Chapter Two includes a detailed literature review on the fine coal refuse material
- Chapter Three includes the investigation of the in situ characteristics on fine coal refuse
- Chapter Four describes the study of rheology and the particle and floc size distribution of fine coal refuse
- Chapter Five describes a detailed investigation of the consolidation properties and the time rate of settlement and introduces a finite difference method to predict time rate of consolidation that accounts for the spatial and temporal variation of the coefficient of consolidation.
- Chapter Six includes the study of the influence of a flocculant and other background solutions on the undrained shear strength and flow behavior of fine coal refuse
- Chapter Seven concludes the findings of this research and provides recommendations for future research.

1.5   REFERENCES

Kalinski, M.E., Phillips, J.L., 2008. Development of Methods to Predict the Dynamic Behavior of Fine Coal Refuse: Preliminary Results from Two Sites in Appalachia, Geotechnical Earthquake Engineering and Soil Dynamics Congress IV. ASCE, Sacramento, CA.

Kelley, J.H., Kealy, D., Hylton, J., C.D., Hallanan, E.V., Ashcraft, J., Murrin, J.F., Davies, W.E., Erwin, R.B., Latimer, J., I.S. , 1973. The Buffalo Creek Flood and Disaster: Official Report from the Governor's Ad Hoc Commission of Inquiry 1973.

Mine Safety and Health Administration, M., 2009. Engineering and Design Manual: Coal Refuse Disposal Facilities, 2nd ed. Department of Labor, Prepared by D'Appolonia Engineering.

U.S Army Corps of Engineers, N.I.o.D., 2017. National Inventory of Dams

USEIAS, 2017. U.S. Energy Information Administration Statistics https://www.eia.gov/tools/faqs/faq.cfm?id=427&t=3

van Olphen, H., 1977. An Introduction to Clay Colloid Chemistry, 2nd ed. Krieger Publishing Company, Malabar, Florida, USA.

CHAPTER II
LITERATURE REVIEW

Disclaimer: Portions of this chapter will be repeated in subsequent chapters.

According to the U.S. Energy Information Administration Statistics (2017), coal is one of the major sources of energy in USA. Approximately 720 million tons of coal was produced in the U.S. during 2017, 92% of which was used in coal fired power plants to generate 30.1% (~1208 million MWh) of the total U.S. power production in 2017 (USEIAS, 2017). Coal is processed to remove impurities before transporting to the power plants, leaving behind waste materials described as coarse or fine refuse. Fine coal refuse (FCR) refers to the fines generated during the processing of raw coal and is considered a waste material. FCR is typically stored behind on-site impoundments constructed primarily with the coarse refuse. This FCR is typically hydraulically placed by mixing the fines with water and a chemical flocculant and then pumping the resulting slurry through a series of pipelines. The flocculant is added to promote rapid settling of the solids once the slurry is placed in the impoundment. There are more than 1170 tailing dams in US, of which ~700 are coal refuse impoundments (U.S Army Corps of Engineers, 2017). Hundreds of these impoundments are in the Appalachia region, and many have heights exceeding 600 feet.

The flowability or rheology of impounded coal refuse, and the stability implications and potential for this material to break through into mine workings below and adjacent to the impoundment has been recognized as an issue for some time. Michael et al. (2005) conducted a comprehensive literature review on the behavior of coal-refuse, and documented feedback from engineers and geologists. BilBao et al. (2011) reviewed the literature and identified problems related to the flowability fine refuse slurry and how these materials might be tested.

Currently, there are no established methods for determining the rheology of coal refuse material. It has been suggested by BilBao et al. (2011) that the liquid limit (LL) test (ASTM-D4318, 2010) may be of value in determining if the material is flowable or non-flowable. The LL is one of several arbitrary index measurements of water content known as the Atterberg Limits that is used in soil mechanics to define the water content boundary between the plastic and liquid behavioral states of a fine-grained material. Soils at the liquid limit have a shear strength between 1.3 and 2.4 kPa (0.2 to 0.35 psi) (Wroth and Wood, 1978). The shear strength of a fine-grained material at its liquid limit depends on the particle associations as well as particle shape since the particles or aggregates interact to resist shear (Mitchell, 1993).

The BilBao et al. (2011) suggestion of the LL/water content as a tool for investigating the stability of fine refuse is based on the defining characteristic of a particulate material whose moisture content is above the LL, i.e. the material behaves as a liquid with the ability to flow. Thus, a comparison between the measured in situ moisture content and the LL would indicate if the material in its current state has the potential to flow. Figure 2-1 (BilBao et al., 2011) compares measured values of water content from a slurry impoundment as a function of depth with an assumed liquid limit. Those zones where the water content approaches or exceeds the LL are suggested to be zones where the material may act similar to a liquid.
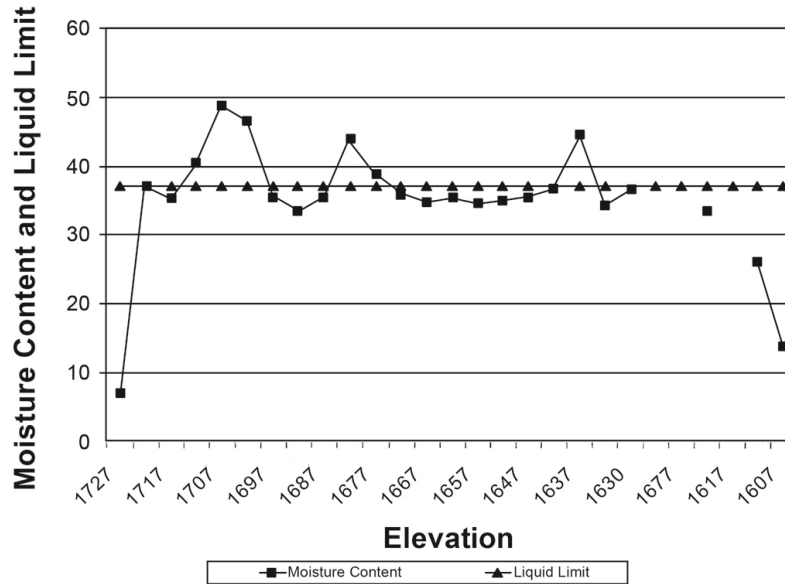
Figure 2-1. Variation of Measured Water Content with Depth and Comparison with an Assumed Liquid Limit Value of 37 (BilBao et al., 2011).

Rather than comparing the in situ water content with the liquid limit as above, the liquidity index (LI) may be a practical term to estimate the in-place flowability of the materials. The liquidity index is defined as:

$$LI = \frac{w - PL}{PL - LL}$$

Equation 2-1

Where w is the in situ water content, LL is the liquid limit, and PL is the plastic limit of the soil (ASTM D 4318). Thus, values of LL > 1 indicate the material is at water content above the LL, and LI = 0 indicates that the material is at the PL.

2.1. PHYSICAL CHARACTERIZATION AND INDEX PROPERTIES OF FCR

A number of studies have focused on characterizing FCR, while others have focused on application of coal waste as a construction material. For instance, Hu et al. (2017) investigated the feasibility of using coal tailings as a landfill liner material. Often, standard test methods developed for the testing of soils (Table 2-1) are used.

9

Table 2-1. **Common Material Characterization Techniques for Soil which may be Applicable for FCR**

Property	Measurement Technique(s)	Comments
Particle Size Distribution	ASTM D 422	Distribution of coarse materials is determined by sieve analysis, while distribution of fine materials is determined using a hydrometer.
Liquid Limit	ASTM D 4318; BS1377 (BSI, 1990)	The British Standard offers improved repeatability and ease of conducting relative to the Casagrande Dish method (ASTM D 4318).
Plastic Limit	ASTM D 4318	--
Undrained Shear Strength	Unconsolidated-Undrained (ASTM D 2850) or Consolidated Undrained (ASTM D 4767) Triaxial Testing	Test method depends on the number of viable undisturbed samples obtained. Would include pore water pressure measurements.

Physical properties of fine coal refuse including Atterberg limits, grain size distribution and specific gravity have been investigated by some researchers (e.g. Hegazy et al. 2004 and Yu 2014). Despite the variation of characteristics of FCR regionally and from one mine to another (Backer et al. 1977) or even from one coal seam in an individual mine to another, physical characteristics of the FCR are in a specific range suggesting similarities in their properties. Table 2-2 is a summary of specific gravity, plastic limit, and liquid limit ranges of FCR from different coal mines in the United States and Great Britain. Although these values vary according to the location of the coal mine and the method of processing, the variation within each property is in a narrow range.

As noted in Table 2-2, the specific gravity of FCR is less than that of most common soil minerals, which typically ranges from about 2.6 to 2.8 (Budhu, 2011). This would suggest that the overburden stresses in FCR are lower than those in typical soils at the same depth. Zeng et al. (2008) performed Atterberg limit tests on fine and coarse coal refuse on undisturbed tube samples collected from an eastern Kentucky coal mine. The results are shown in Table 2-3. The coarse refuse is a mixture of sand and gravel sized particles with a small fraction of fine grains and is classified as clayey sand with gravel. The FCR is typically a mixture of sand and silt and clay sized particles with low plasticity. Consistent with the results of Table 2-2, the specific gravity was much less than common soil mineral constituents.

Table 2-2. Specific Gravity, Plastic Limit and Liquid Limit of Fine Coal Refuse (after Vick, 1983)

Location	Specific Gravity of Solids	Liquid Limit (%)	Plasticity index	Source
Eastern U.S.	1.5-1.8	33-50	0-13	Busch et al., 1975
Western U.S.	1.4-1.8	-	-	Backer et al. (1977)
Buffalo Creek, W.V.	1.4-1.6	20-40	2-12	Wahler, 1973
Great Britain	1.7-2.4	30-60	3-30	Wimpey, 1972

Table 2-3. Index Properties of Fine and Coarse Coal Refuse (Zeng et al. 2008)

	Fine Coal Refuse				Coarse Refuse
Sample No.	1	2	3	4	
Water Content (%)	13.5	13.6	8.7	12.5	11.2
Wet Unit Weight (kN/m^3)	15.2	16.5	17.0	15.7	19.2
Liquid Limit	36	27	32	34	31
Plastic Limit	26	24	21	23	20
Plasticity Index	10	3	11	11	11
Specific Gravity	2.02	2.02	2.16	2.10	2.5
Soil Classification (USCS)	sandy silt (ML)	silty sand (SM)	sandy lean clay (CL)	sandy lean clay (CL)	clayey sand with gravel (SC)

As noted previously, the physical characterization of fine coal refuse varies with coal mine location. As a manufactured material, this variation in properties depends on rock strata, coal seam, coal extraction and processing method, and impoundment depositional characteristics. Table 2-4 presents summary of physical and mechanical properties of FCR from different studies.

Stewart and Daniel (1992) investigated physical and chemical properties of coal refuse from Southwest Virginia. They investigated the clay mineralogy of the <2-mm fraction of three different samples. X-ray diffraction method was used to identify the mineralogy of the clay particles. As summarized in Table 2-5, they estimated the relative amounts of kaolinite, muscovite, vermiculite, and chloritized vermiculite using relative peak areas.

Table 2-4. Fine Coal Refuse Characterization Summary of Average Values (MSHA, 2009)

Reference	Location	Grain Size		Atterberg Limits			Specific Gravity, G_s	Effective Shear Strength	
		Pass. No. 40 (%)	Pass. No. 200 (%)	LL	PL	PI		ϕ' (degrees)	c' (psf)
Almes & Butali (1976)	PA, KY, VW, VA	64-100	36-47	20-40	NR	<10	1.55-1.65	29-34	0
McCutcheon (1983)	OH	81	46	29	22	7	1.85	36	0
Qiu & Sego (2001)	Western Canada	90	66	40	24	16	1.94	32	200
Hegazy et al. (2004)	PA	65-100	58	31	20	11	1.52	33	230
Genes et al. (2000)	WV	NR	16-90	NR	NR	<12	1.44-2.37	23-36	0
Cowherd & Corda (1998)	NR	NR	24-91	23-39	NR	0-9	1.4-2.1	NR	NR
Huang et al. (1987)	KY, WV, PA, TN, WV, VA	NR	27-95	22-44	NR	0-12	1.52-2.14	NR	NR
Busch et al. (1974, 1975)	WV	50-98	10-60	34-51	NR	0-13	1.45-2.07	NR	NR
Becker et al. (1977)	UT, NM	60-100	16-98	NR	NR	NR	1.33-2.07	NR	NR
Ullrich et al. (1991)	KY, TN, OH	45-95	25-85	31-44	NR	0-31	1.8-2.5	NR	NR
Zeng & Globe (2008)	Appalachian Region	75-85	40-62	27-36	21-26	3-11	2.02-2.16	NR	NR

Table 2-5. Clay Mineralogy of Three Refuse Samples (Stewart & Daniel 1992)

Site	Mica	KaO	Smec	Chl	Qz	RIMV
			Minerals (%)			
1[*]	25	25	25	10	ND	10
2	45	30	ND	10	5	10
3[**]	55	20	ND	5	5	10

KaO= kaolinite, Smec= smectite, Chl=chlorite, ND= Not detected, Qz= quartz, and RIMV= regularly interstratified mica/vermiculite.

[*]Also contained 5% chloritized vermiculite

[**] Also contained 5% vermiculite

Grain size distribution analysis was performed to classify FCR in different studies. The particle size distribution is one of the most significant properties having strong influence on the strength, compressibility, and seismic behavior of the impounded coal refuse material. Wakeley and Peterson (2004) indicated that the geological location of the mine contributes to the mineralogy, grain size and shape and other physical characteristics of mine waste. For instance, coal refuse obtained from cyclothem sedimentary rock is relatively rich in clay minerals and clay sized particles.

Hegazy et al. (2004) studied physical, mechanical, and hydraulic properties of coal refuse. They performed a series of comprehensive laboratory tests to evaluate physical properties of coarse and fine coal refuse. Table 2-6 presents the size distribution analysis done on different samples. They showed that there was relatively high variation in the percent passing sieve #200. This variation was between 18% and 92% with the average of 58%. Based on their findings, the classification of fine refuse ranged from silty clayey sand and clayey silty sand to sandy clayey silt and sandy silty clay. This was consistent with what other researchers have published that shows fine coal refuse are a silt size material that contain low plastic clays. Hegazy et al. (2004) also showed that the coarser materials were generally found in the locations closer to the impoundment delta, or at locations where the slurry was pumped into the impoundment.

Several grain size distribution curves from the available literature are summarized below in Figure 2-2. It can be seen that the size range of fine coal refuse is relatively narrow. It should be noted that the method of mining affects the grain size distribution of fine coal refuse.

All but one of the grain size distribution curves in Figure 2-2 show that more than 50% of the refuse material passes the #200 sieve (< 75μm). In some cases, more than 90% of the fine refuse material is < 75μm.

Hui Wu et al. (2017) studied the feasibility of using coal gangue (tailing material) as a landfill liner material. They characterized coal refuse as a geotechnical material. Table 2-7 presents the geotechnical properties of coal gangue which they studied.

Table 2-6. Summary of FCR Sieve Analysis (Hegazy et al. 2004)

Equivalent Particle Size or % passing	Average	Standard deviation	Coefficient of variation
D_{10}	0.010 (mm)	0.015	1.50
D_{30}	0.037 (mm)	0.055	1.49
D_{50}	0.127 (mm)	0.128	1.01
D_{60}	0.196 (mm)	0.209	1.07
Passing sieve 200 (0.075 mm)	57.7 (%)	25.0	0.43
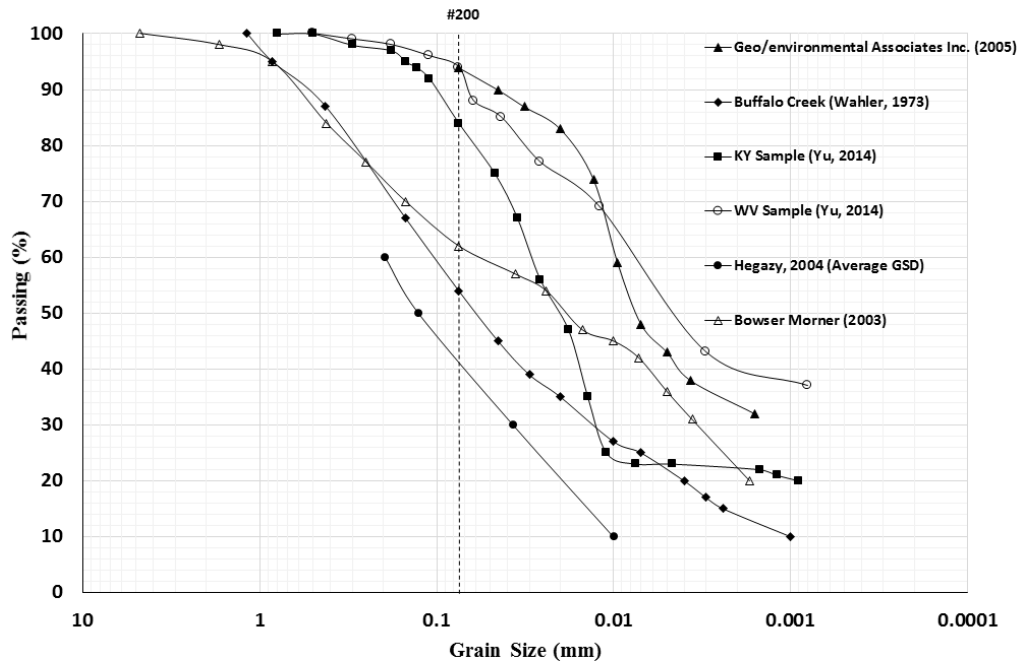
Figure 2-2. Comparison of GSD curves of FCR from the Literature.

Table 2-7. Geotechnical Properties of Coal Gangue (Wu et al. 2017)

Specific Gravity	Liquid Limit (%)	Plastic Limit (%)	Plasticity Index (%)	Optimum Water Content (%)	Specific Surface (m²/g)	pH	Carbon Content (%)
2.54	28.3	17.2	11.1	17.8	8.01	6.14	3.49

14

2.1 RHEOLOGICAL BEHAVIOR OF FCR

Coal refuse slurries are likely to exhibit non-Newtonian rheological behavior. A Newtonian fluid (such as water) is considered an ideal fluid in which the relationship between the applied shear stress and resulting shear strain is linear. The slope of this relationship is the viscosity, and in a Newtonian fluid the viscosity is constant for a wide range of rate of shear. Non-Newtonian fluids, such as catsup or blood, display a different viscosity depending on the rate at which the shear is applied. The literature generally refers to fine coal slurry as displaying non-Newtonian rheological behavior, yet there is limited data to substantiate this. Much of the literature (BilBao et al. 2011; Michael et al. 2005; and Hunter 2001) suggests that fine slurry exhibits a Bingham–type non-Newtonian flow.

Bingham plastic flow occurs in solid-liquid (two-phase) systems with extensive structure but not in pure fluid systems. Bingham plastic flow is characterized by a minimum stress, or yield stress, that must be exceeded in order for flow to take place. The system acts as an elastic solid below this yield stress (Munson et al., 1994; Patton, 1979). Figure 2-3 depicts Bingham behavior for both the ideal and non-ideal cases.

Aktasa and Woodburn (2000) investigated the effect of coal concentration and particle size on the viscosity of coal water suspensions. Figure 2-4 shows the dependency of the slurry viscosity on coal solids concentration for the two samples of the same coal but with different particle size distributions. They illustrated that the suspension with particles less than 48μm in size reached a much higher viscosity when compared to the unscreened sample at similar coal solids concentrations.
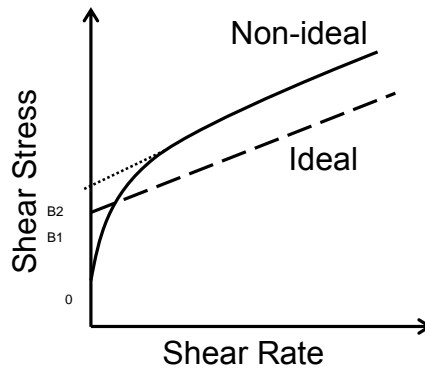
Figure 2-3. Schematic of Ideal (Bingham) and Non-Ideal Plastic Behavior. S_0 is the Primary Yield Value, and S_{B1} and S_{B2} are the Bingham Yield Values for the Ideal and Non-Ideal Cases, Respectively (after Hunter, 2001). For a Newtonian Fluid, the Response is More Like the "Ideal" Behavior, Except the Value of S_{B1} is Very Nearly Zero.
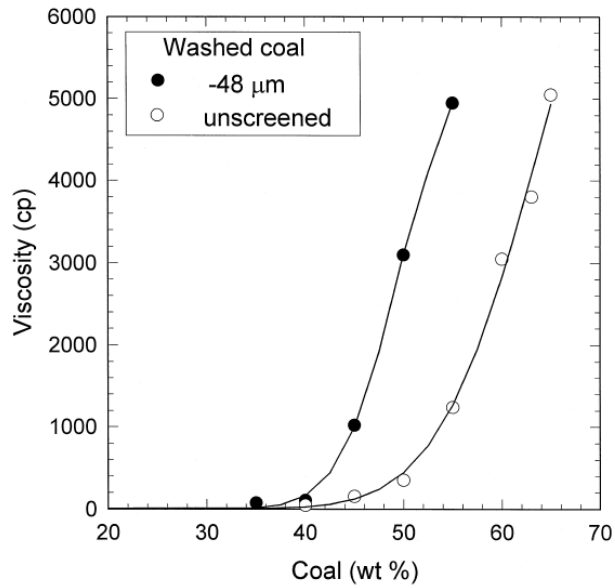
Figure 2-4. Dependency of Slurry Viscosity on Coal Loading and Particle Size (Aktasa & Woodburn 2000)

Mishra et al. (2002) investigated the effect of pH on the rheological behavior of coal-water suspensions CWS). The coal water suspension is different from coal refuse slurry and is not refuse material. It is basically used as a fuel in a highly concentrated form of suspension. Mishra et al. (2002) showed that pH has an important effect on the viscosity of the tested coal-water suspensions (CWS), Figure 2-5. They reported high apparent viscosity in acidic medium, the highest viscosity they reported was around pH 6 for all three types of coal samples and the lowest was around pH 8. They also observed that coal-water suspensions have non-Newtonian behavior at low pH.
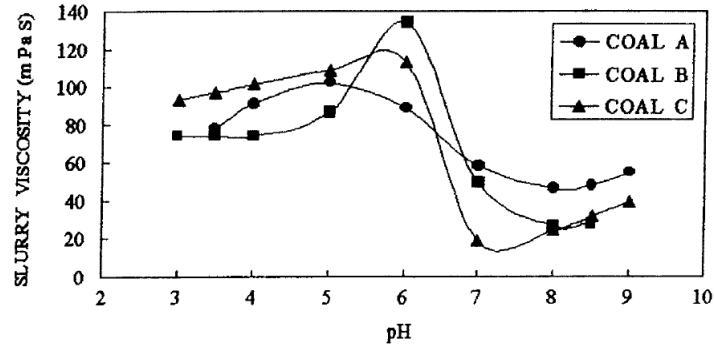
Figure 2-5. Apparent Viscosity of CWS (50% w/w) as a Function of pH at a Shear Rate of 100 (1/sec). (Mishra et al. 2002)

Atesok et al. (2002) measured the viscosity of coal-water suspensions including different types of coal from Turkey with different mean particle sizes. As shown in Figure 2-6, they concluded that in CWSs with less than 50% solids, the viscosity values were more than 1000cp. They suggested that for preparing coal-water suspensions with viscosity values less than 1000cp, the solids percentage must be less than 50%.

The rheological behavior of a suspension, captured as shear stress vs. shear strain, can take several forms depending on both the characteristics of the solid particles and the fluid phase. For example, if the particles develop a net surface charge when hydrated with a polar fluid, then they are susceptible to flocculation and/or aggregation for certain fluid conditions (e.g., moderate pH or high ionic concentration). These flocs/aggregates tend to increase the resistance to shear of the suspension. Furthermore, these flocs or aggregates may deflocculate or deaggregate under certain fluid conditions (e.g. change in pH or decrease in ionic concentration) or applied shear stresses. Thus, the rheological behavior depends on the interaction between the particles and the chemical composition of the fluid. Michael et al. (2005) reference previous studies that have suggested that flow-controlling admixtures in the slurry used to improve the fluid transport properties may impact slurry particle sedimentation, thus the water chemistry of the transport fluid should also be investigated as a variable impacting the rheological behavior. However, once placed in the impoundment, the influence of these additives may degrade over time. So, the properties of the transport fluid with time are also important.

17
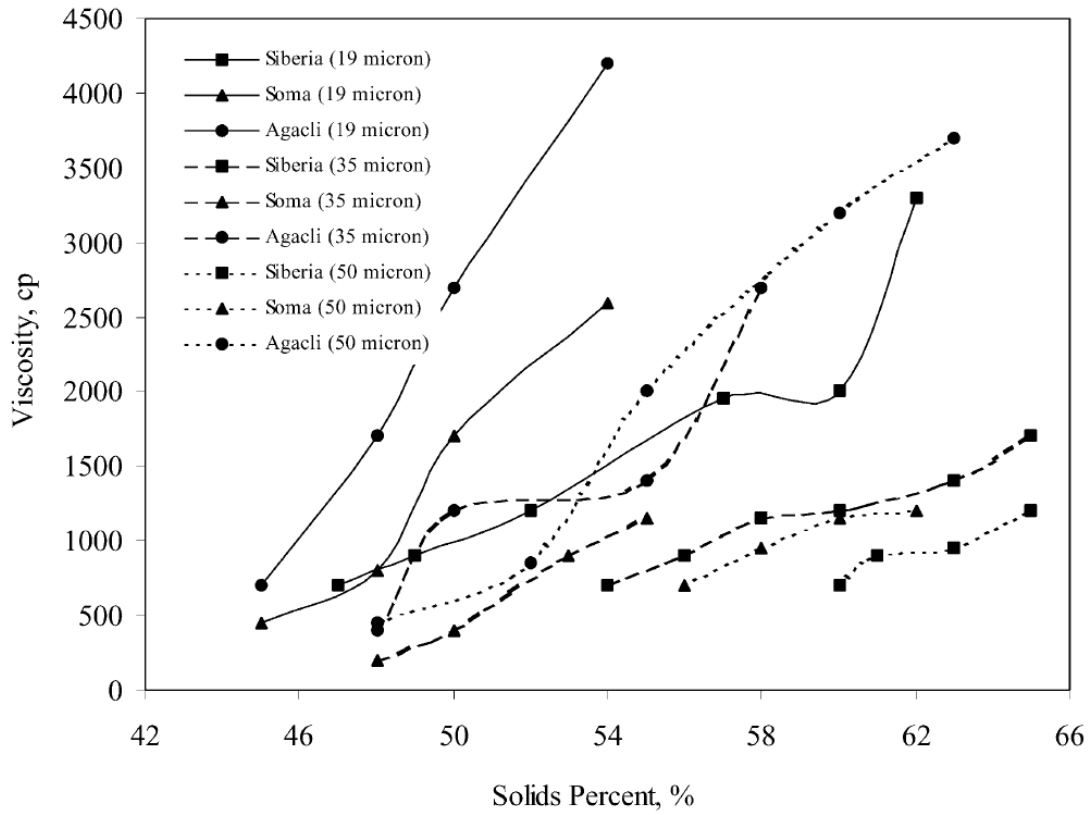
Figure 2-6. Viscosity Measurement of Coal Samples having Different Mean Particle Size (Atesok et al. 2002)

2.2 CHARACTERISTICS OF IN-PLACE REFUSE

There have been several reported investigations of in situ measurements of FCR impoundments, and there is likely a large database of in situ information in the permit files and files of coal operators. The most common in situ test method is the Standard Penetration Test (SPT). SPTs are a simple, cost effective means to indirectly assess the consistency of the refuse as a function of depth. The STP-N value (which can be correct for depth effects and is referred to as N60) provides an indirect measure of the in-place consistency, which is related to the strength, and may be valuable to infer the stability of the material with depth. In addition to providing a penetration or N value, the SPT provides a disturbed sample that can be evaluated for in situ water content and index (Atterberg limits) properties. Depending on the nature of the material retrieved, it may be possible to determine the particle size distribution, which is likely to govern the rheology as well as the index properties.

Often during the drilling for the SPT's, undisturbed tube samples are obtained. These can be to determine the density and void ratio, and may be used for strength determination. When extremely soft materials (like flowable FCR) are encountered, a piston or GUS (e.g. Acker Drill Company) sampler is often used due to the additional suction provided.

From the literature, Hegazy et al. (2004) reported a decrease in undrained shear strength, C_u with depth as determined from Cone Penetration Testing (CPT) ASTM D-3441 testing (Figure 2-7) and presented a relationship between the drained friction angle and corrected STP blow count N_{60}.
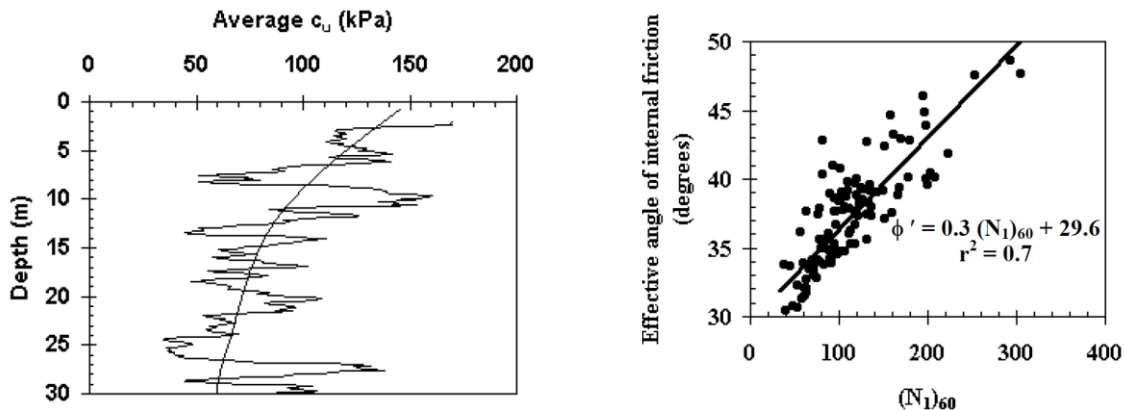
Figure 2-7. In situ testing of FCR a) Observed Decrease in Undrained Shear Strength with Depth and b) Relationship between SPT N and Friction Angle Obtained from CPT (Reference Hegazy et al. (2004)).

Kalinski and Phillips (2008) reported on a study focused on the seismic stability of refuse impoundments, and presented data from the upstream toe of an embankment that also suggested a decrease in strength with depth (Figure 2-8). They also suggested that during upstream construction, the coarse refuse may displace the underlying fine refuse increasing the depth to the fine refuse and perhaps creating a zone of mixed material near the crest of the embankment.

One of the other important characteristics of fine coal refuse is hydraulic conductivity. Hydraulic conductivity has a direct effect on the consolidation rate of impounded refuse material. Hegazy et al. (2004) used the CPTu method to measure the horizontal hydraulic conductivity of fine coal refuse based on piezocone pore water pressure dissipation. Table 2-8 presents the results of CPTu testing. They concluded that the range of estimated horizontal conductivity (k_h) indicates that the FCR behaves very similar to fine sands, silts and mixtures of sand, silt and clay.
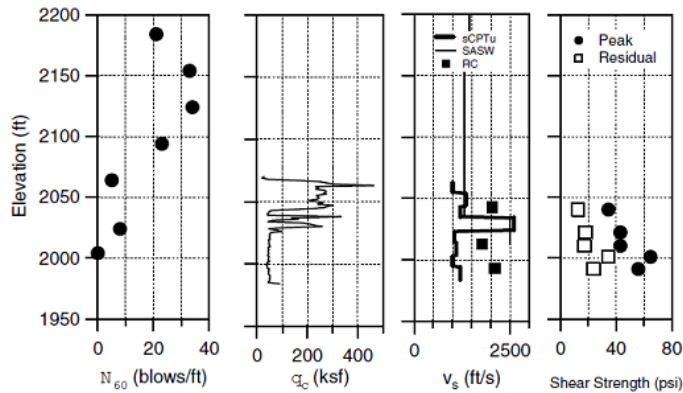
b. from upstream toe of dam (fine refuse from 1984-2064 ft)

Figure 2-8. Observed Decrease in SPT N_{60} and Cone Tip Resistance, q_c with Depth from CPT in Fine Refuse from Kentucky (Reference Kalinski and Phillips (2008).

Table 2-8. Hydraulic Conductivity of Fine Coal Refuse Based on CPT Piezocone Dissipation (Hegazy et al. 2004)

Piezocone	Depth (m)	t_{50} (sec)	c_h (cm^2/s)	k_h(cm/s)
PCPT1	7.9	800	15E-3	1.21E-5
PCPT1	19.2	30,000	0.4E-3	0.03E-5
PCPT1	22.9	40	301E-3	24.30E-5
PCPT3	13.3	128	94E-3	7.59E-5
PCPT4	21.9	300	40E-3	3.24E-5

Note: Groundwater level was approximately 3 meters below ground surface.

20

2.3   MECHANICAL PROPERTIES OF FCR

As discussed previously, fine coal refuse in the impoundment is often used as the foundation material of a tailings dam in the upstream placement method. So, it is very important to investigate mechanical behaviour and strength of FCR under different loading conditions.

Zeng et al. (2008) evaluated the liquefaction potential of FCR under dynamic loading conditions by performing resonant column tests and cyclic triaxial tests. They concluded that no liquefaction was observed during cyclic triaxial tests for samples obtained from the minefield in eastern Kentucky. They discussed that even though they did not observe liquefaction in their samples, this may be due to the high confining pressures experienced in the field.

Yu (2014) performed direct shear tests on samples collected from two impoundments in West Virginia and Kentucky. It was observed that the in situ moisture content of impounded FCR plays a critical role in the shear strength of the refuse material. As water content increases, the undrained shear strength of FCR decreases (Figure 2-9).
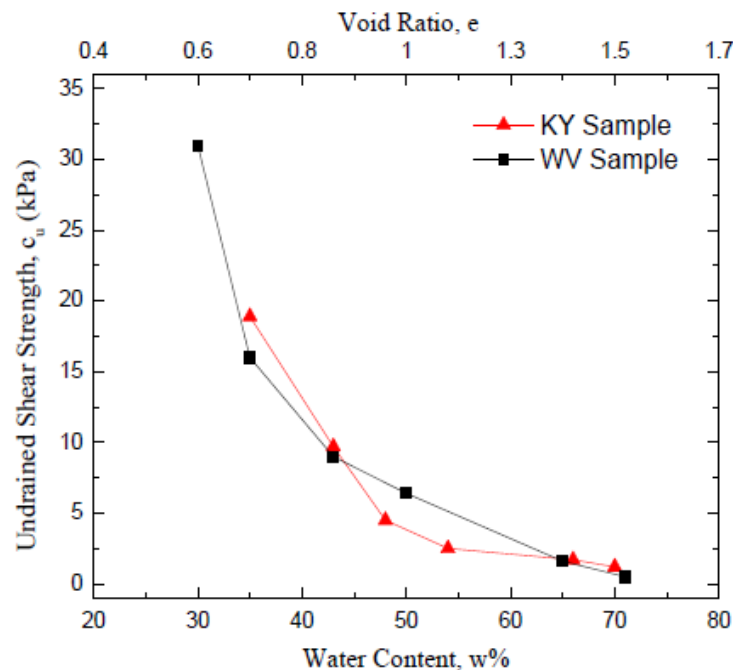
Figure 2-9. Undrained shear strength vs. water content (Yu 2014).

Hegazy et al. (2004) estimated the shear strength of FCR using laboratory and in situ tests. They determined drained shear strength parameters using consolidated isotropic undrained compression (CIUC). They also performed triaxial tests in which the pore pressure was measured in consolidated isotropic drained compression condition (CIDC).

Hegazy et al. (2004) collected undisturbed Shelby Tube samples from the upstream stages of the tailing dam which were built over the FCR in the impoundment. Summarized results of the strength tests are presented in Table 2-9. The drained angle of internal friction ($\emptyset'$) and drained cohesion (c') are shown. Table 2-9 also shows that the variability of drained friction angle ($\emptyset'$) is low to moderate, but the change in the range of drained cohesion c' is relatively high. The shear strength parameters are peak values, which were found to decrease with increasing fines contents (Figure 2-10).

Table 2-9. Strength Parameters of FCR (Hegazy et al. 2004)

Parameter	Average	Standard Deviation	Coefficient of Variation
$\emptyset'$	33 (degrees)	4	0.12
c'	11 (kPa)	14	1.30
$\emptyset'(c' = 0)$	35 (kPa)	4	0.11
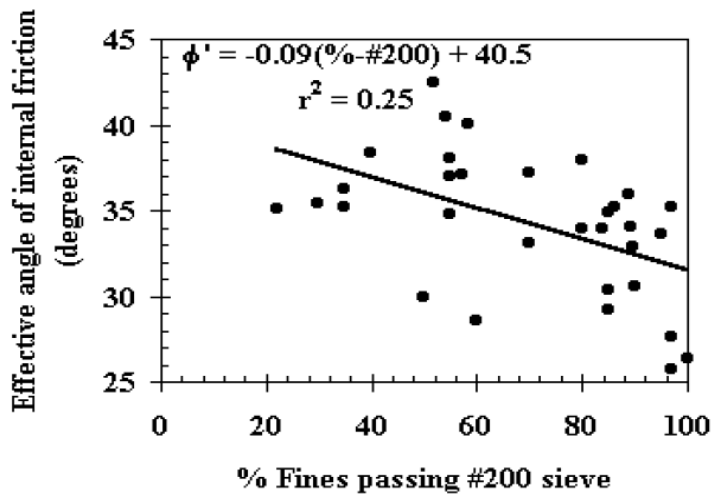
Figure 2-10. Variation of Effective Friction Angle with Fines Percentage (Hegazy et al. 2004)

22

2.4   EFFECTS OF FLOCCULANTS AND DISPERSANTS ON SOIL STRUCTURE AND ASSOCIATED MATERIAL RESPONSE

Particulate material properties, e.g. soil, are a function of the particle-level arrangement, or fabric. Two common fabric types are dispersed and flocculated in which the particles either remain as individual units or bind together to form larger structures, respectively. Fabric, in part, determines the mechanical properties such as shear strength, compressibility, and hydraulic conductivity (Mitchel and Soga 2005). A summary of the known relationships between clay particle fabric and selected soil properties is shown in Figure 2-11. In nature, the difference in clay particle associations (dispersed vs. flocculated) depends on the surrounding pore fluid chemistry, namely pH and ionic concentration. These associations can be altered by purposefully exposing the materials to chemical additives. For example, the compressibility of clays can be significantly reduced by adding salt, which changes the soil fabric from flocculated to dispersed by reducing the interparticle spacing (Di Maio et al. 2004).

One common type of chemical dispersant is sodium hexametaphosphate. This additive is used in the hydrometer analysis method of ASTM D422 Standard Test Method for Particle-Size Analysis of Soils for breaking down any larger aggregated or flocculated structures into individual grains. Sodium hexametaphosphate disperses particles by providing both cationic and anionic species that bind to charged sites on the particles, rendering the particle neutral in charge. The particles then remain dissociated (Wintermyer and Kinter 1955).

Clay Particle-Level Arrangement

	Dispersed	Edge-to-Face Flocculated
Permeability :	low	high
Compressibility :	low	high
Shear resistance :	high or low	very high
Water retention :	low	high
Surface area :	low	high

Impact on Material Properties
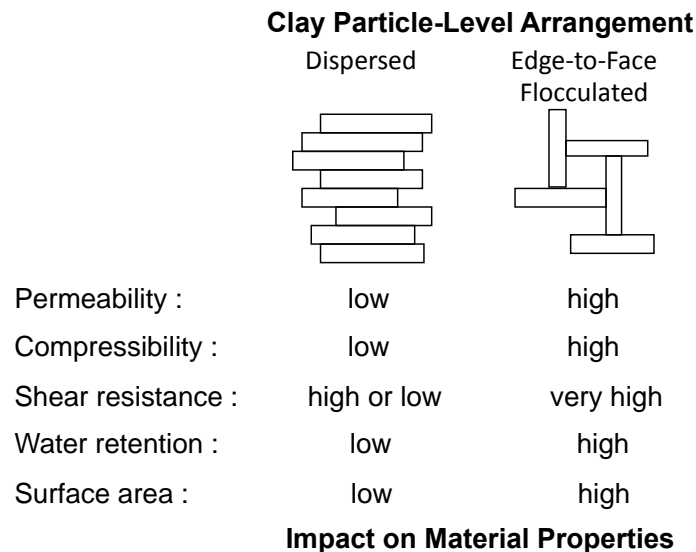
Figure 2-11. Relationship between Clay Particle Fabric and Material Properties.

23

Polymer flocculants are another type of chemical additive used to manipulate particle interactions. The fine particles in FCR slurries tend to remain as individual particles in suspension, i.e. dispersed. These dispersed particles take a very long time to settle (weeks to months). Polymer flocculants are used to bind these particles creating larger formations that settle at a faster rate. These loose bonded particle structures are called flocs. The mechanism(s) by which the polymer binds to the particle surface depends on the particle surface characteristics (existence of charged sites) and the polymer type, anionic (negatively charged), cationic (positively charged), or non-ionic. The bond types include Coulombic, dipole, hydrogen bonding, and van der Waals. Flocs form when the polymer molecules bind to the surface sites of two or more particles as shown in Figure 2-12 (Hunter 2001). In order to easily distribute the polymer flocculant into a slurry system, the polymer should be water-soluble. Thus, these flocculants are likely to be highly hydrophilic.

A flocculated particulate system tends to have a higher void ratio, higher compressibility, higher hydraulic conductivity, and higher shear strength than a dispersed one (Lambe and Whitman 1969).

However, for a particulate system flocculated with a polymer-based additive, very little is known about the evolution of these properties if the flocculant degrades over time. In particular, many FCR slurry impoundments are decades old, and any benefits the flocculants provided when the slurry is initially placed may decrease with time.
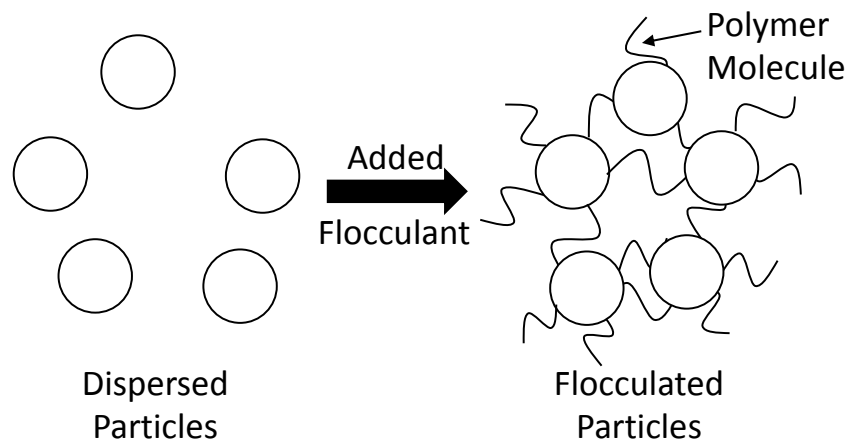
Figure 2-12. Floc Formation from Dispersed Particles Induced by a Polymer Flocculant.

2.5   ACCELERATION OF CONSOLIDATION USING WICK DRAINS

Synthetic wick drains are widely used in to consolidate saturated fine grain soils by providing a number of high permeability flow paths to more quickly reduce the build-up of pore water pressure in the soil allowing consolidation to occur more quickly. The application of wick drains in FCR impoundments and tailing dams has been described (Thacker et al. 1988; Liu et al. 1999). However, as suggested by Michael et al. (2005), for these systems to be effective a surcharge of some type is required to produce an elevated pore water pressure to drive the water through the drains. This may be cost prohibitive for many FCR impoundments.

2.6   SITE INFORMATION

The sampling and subsurface investigation of the fine coal refuse in this study was performed at a slurry impoundment in Martin County, KY. The impoundment was first constructed in the 1970s by the upstream method of construction. While the impoundment is still permitted and open, slurry from the nearby preparation plant is no longer being placed in this impoundment. Slurry from the plant is now being placed behind a newer impoundment, which is where fresh slurry samples investigated in the study were obtained. Figure 2-13 is a cross section of the impoundment with the approximate location of the August 2016 subsurface investigation which is described in the next section.

25
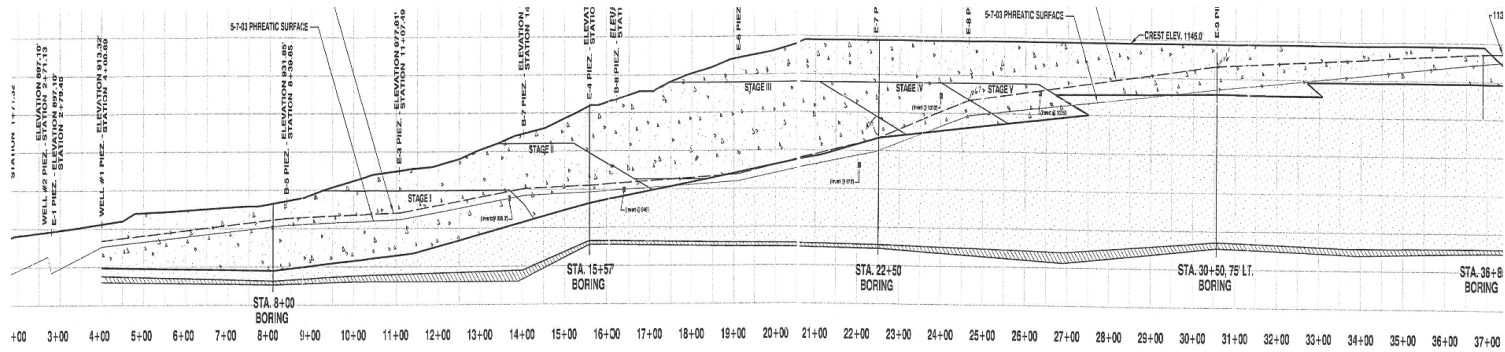
a)
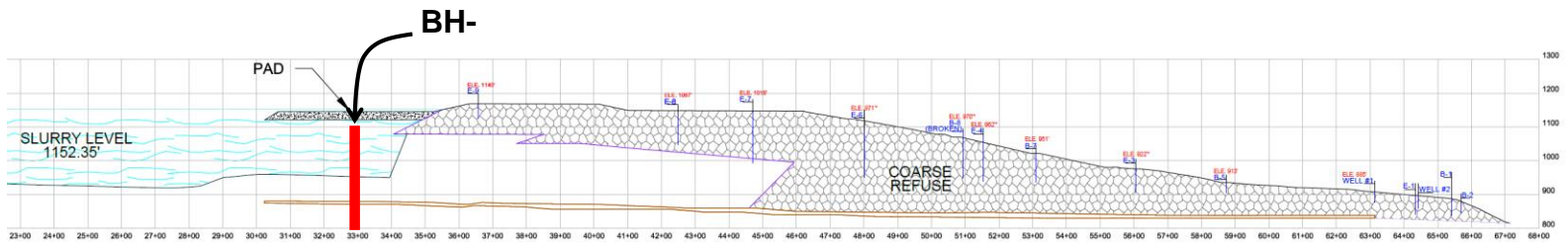
b)

Figure 2-13. Two Cross section views of the impoundment, with the approximate boring locations from this study shown in red. a) Section looking south, depicting early stages of impoundment development; b) Section looking north with some boring locations from previous investigations. (Bowser Morner Co. 2003)

26

2.7 REFERENCES

Acker Drill Company, 2015. "GUS Sampler (Gregory Undisturbed Sampler)" (BSI), B.S.I., 1990. Methods of Test for Soils for Civil Engineering Purposes, BS 1377, "Determination of the Liquid Limit".

Aktasa, R.G., Woodburn, E.T., 2000. Effect of addition of surface active agent on the viscosity of a high concentration slurry of a low-rank British coal in water. Fuel processing Technology 62, 1-15.

Almes, R.G., Butail, A., 1976. Coal Refuse: Its Behavior Related to the Design and Construction of Coal Refuse Disposal Facilities, Proceedings of the Seventh Ohio Valley Soils Seminar on Shales and Mine Wastes, Lexington, KY.

ASTM-C230/C230M, 2014. Standard Specification for Flow Table for Use in Tests of Hydraulic Cement.

ASTM-D422, 2007. Standard Test Method for Particle-Size Analysis of Soils. American Society for Testing Materials, 1-8.

ASTM-D2850, Standard Test Method for Unconsolidated-Undrained Triaxial Compression Test for Cohesive Soils.

ASTM-D3441, Standard Test Method for Cone Penetration Testing.

ASTM-D4318, 2010. Standard Test Methods for Liquid Limit, Plastic Limit, and Plasticity Index of Soils. 1-16.

ASTM-D4767, Standard Test Method for Consolidated Undrained Triaxial Compression Test for Cohesive Soils.

Atesok, G., Boylu, F., Sirkeci, A.A., Dincer, H., 2002. The Effect of Coal Properties on the Viscosity of Coal- Water Slurries. Fuel 81, 1855-1858.

Backer, R.R., Busch, R.A., Atkins, L.A., 1977. Physical Properties of Western Coal Waste Materials, Report of Investigations 8216. U.S. Department of the Interior, Bureau of Mines, Spokane, WA.

Becker, E., Chan, C.K., Seed, H.B., 1972. Strength and Deformation Characteristics of Rockfill Materials in Plane Strain and Triaxial Compression Tests. California Department of Water Resources.

BilBao, Li, T., S., Lane, D.E., Michael, P.R., Richmond, M.W., Stoltz, J.R., Stumpt, D.E., Superfesky, M.J., 2011. Potential of Impounded-Coal-Waste-Slurry Breakthroughs Into Underground Mines, Issues and Answers. Technical Position Paper - U.S. Department of the Interior, Office of Surface Mining Reclamation and Enforcement, Appalachian Region.

Bowser Morner Compony, 2003. Liquefaction Susceptibility Assessment Report for a Coal refuse Impoundment,

Boylu, F., Dicer, H., Atesok, G., 2004. Effect of coal particle size distribution, volume fraction and rank on the rheology of coal– water slurries. J. Fuel processing technology 85, 241-250.

Budhu, M., 2011. Soil mechanics and foundations, 3rd ed. Wiley, New York.

Busch, R.A., Backer, R.R., Atkins, L.A., Kealy, C.D., 1975. Physical Property Data on Fine Coal Refuse. USDI Bureau of Mines.

Cowherd, D.C., Corda, I.J., 1998. Seismic Considerations for Upstream Construction of Coal Refuse Dams, Annual Conference, Association of State Dam Safety Officials, Lexington, KY, pp. 523-534.

Di Maio, C., Santoli, L., and Schiovone, P. (2004), "Volume Change Behavior of Clays: the Influence of Mineral Composition, Pore

Fluid Composition, and Stress Rate", Mechanics of Materials, 36, 435-451.

Genes, B.E., Keller, T.O., Laird, J.P., 2000. Steady State Liquefaction Susceptibility of High Hazard Upstream-Constructed Coal Refuse Disposal Facilities, Tailings Dams 2000. ASDSO/USCOLD, Las Vegas, NV, pp. 47-58.

Hegazy, Y.A., Cushing, A.G., Lewis, C.J., 2004. Physical, mechanical, and hydraulic properties of coal refuse for slurry impoundment design. Geotechnical and Geophysical Site Characterization Vols 1 and 2, 1285-1291.

Hiemenz, P.C., 1988. Principles of Colloid and Surface Chemistry, 2nd ed. Marcel Dekker, Inc., New York.

Hu, L., Wu, H., Zhang, L., Zhang, P., Wen, Q., 2017. Geotechnical Properties of Mine Tailings. Journal of Material in Civil Engineering 29, 1-10.

Huang, Y.H., Li, J., Weeratunga, G., 1987. Strength and Consolidation Characteristics of Fine Coal Refuse. Office of Surface Mining, Department of the Interior.

Hunter, R.J., 2001. Foundations of Colloid Science, 2nd ed. Oxford University Press, New York.

Kalinski, M.E., Phillips, J.L., 2008. Development of Methods to Predict the Dynamic Behavior of Fine Coal Refuse: Preliminary Results from Two Sites in Appalachia, Geotechnical Earthquake Engineering and Soil Dynamics Congress IV. ASCE, Sacramento, CA.

Kelley, J.H., Kealy, D., Hylton, J., C.D., Hallanan, E.V., Ashcraft, J., Murrin, J.F., Davies, W.E., Erwin, R.B., Latimer, J., I.S. , 1973. The Buffalo Creek Flood and Disaster: Official Report from the Governor's Ad Hoc Commission of Inquiry 1973.

Lambe, T.W. and Whitman, R.V. (1969), *Soil Mechanics*, John Wiley & Sons, New York, 553 p.

Liu, B.Y., McKenna, G., 1999. Application of Wickdrains in Composite Tailings, 52nd Canadian Geotechnical Conference. Canadian Geotechnical Society, Regina, SK, pp. 487-494.

Ltifi, M., Abichou, T., Tisot, J.P., 2014. Effects of Soil Aging on Mechanical and Hydraulic Properties of a   Silty Soil. Geotechnical and Geological Engineering 32, 1101-1108.

McCutcheon, H.P., 1983. Liquefaction and Cyclic Mobility of Coal Refuse Material. Carnegie Mellon University, Pittsburgh, PA.

Michael, P., L., C., 2008. Environmental Risks Associated with Coal Refuse Impoundment Reclamation: An Assessment of the Possibility of an Underground Mine Breakthrough Occurring as a Result of   the Impoundment Reclamation Process. U.S. Office of Surface Mining Appalachian Region Management Council Open-File Report, Pittsburgh, PA.

Michael, P., Murguia, R., Kosare, L., 2005. The Flowability of Impounded Coal Refuse - A review of recent   work and current ideas in the engineering profession. Technical Assistance Report-U.S. Department of the Interior, Office of Surface Mining. The Appalachian Region Management Council.

Mine Safety and Health Administration, 2009. Engineering and Design Manual: Coal Refuse Disposal Facilities, 2nd ed. Department of Labor, Prepared by D'Appolonia Engineering.

Mishra, S.K., Senapati, P.K., Panda, D., 2002. Rheological Behavior of Coal-Water Slurry. Energy Sources 24, 159-167.

Mitchel, J.K., 1993. Fundamentals of Soil Behavior. John Wiley & Sons, New York.

Mitchell, J.K. and Soga, K. (2005), Fundamentals of Soil Behavior, 3rd ed., John Wiley & Sons, Hoboken, New Jersey, 592 p.

Munson, B.R., Young, D.F., Okiishi, T.H., 1994. Fundamentals of Fluid Mechanics, 2nd ed. John Wiley & Sons, New York.

National Research Council "Coal Waste Impoundments: Risks, Responses, and Alternatives" (2002). National Academy Press, Washington D.C.

Patton, T.C., 1979. Paint Flow and Pigment Dispersion, 2nd ed. John Wiley & Sons, New York.

Qiu, Y., Sego, D., 2000. Engineering Properties of Mine Tailings, 51st Canadian Geotechnical Conference: Canadian Geotechnical Society, Vancouver, B.C, pp. 149-155.

Stewart, B.M., Atkins, L.A., 1982. Engineering Properties of Combined Coarse and Fine Coal Wastes, Report of Investigations 8623. U.S. Department of the Interior, Bureau of Mines, Pittsburgh, PA.

Suthaker, N., Scott, J., 1996. Measurement of hydraulic conductivity in oil sand tailings slurries. Canadian Geotechnical Journal 33, 642-653.

Suthaker, N., Scott, J., 1997. Thixotropic strength measurement of oil sand fine tailings. Canadian Geotechnical Journal 34, 974-984.

Thacker, B.K., Ullrich, C.R., Athanasakes, J.G., Smith, G., 1988. Evaluation of a Coal Refuse Impoundment Built by the Upstream Method. Geotechnical Special Publications, ASCE, 730-749.

U.S Army Corps of Engineers, N.I.o.D., 2017. National Inventory of Dams

Ullrich, C.R., Thacker, B.K., Roberts, N.R., 1991. Dynamic Properties of Fine-Grained Coal Refuse, Second International Conference on Recent Advances in Geotechnical Earthquake Engineering and Soil Dynamics, St. Louis, Missouri.

USEIA, 2018. U.S. Energy Information Administration / Monthly Energy Review March 2018. USEIA.

USEIAS, 2017. U.S. Energy Information Administration Statistics https://www.eia.gov/tools/faqs/faq.cfm?id=427&t=3

Wakeley, L., Peterson, R., 2004. The Flowability of Impounded Coal Refuse. U.S. Army Engineer R&D Center Vicksburg, MS.

Wintermyer, A.M. and Kinter, E.B. (1955), "Dispersing Agents for Particle-Size Analysis of Soils", Highway Research Board Bulletin, 95, 1-14.

Wroth, C.P., Wood, D.M., 1978. The correlation of index properties with some basic engineering properties of soils. Canadian Geotechnical Journal 15, 137-145.

Wu, H., Wen, Q., Hu, L., Gong, M., Tang, Z., 2017. Feasibility study on the application of coal gangue as landfill liner material. Journal of Waste Management 63, 161-171.

Yu, H., 2014. Geotechnical Properties and Flow Behavior of Coal Refuse under Static and Impact Loading, Civil engineering. Case Western Reserve University, Cleveland, OH.

Zeng, X., FGlobe, J.A., 2008. Dynamic Properties of Coal Waste Refuse in A Tailings Dam. ASCE Geotechnical Special Publication, 181.

Zeng, X., Wu, J., Rohlf, R.A., 1998. Seismic Stability of Coal waste Tailing Dams. Geotechnical Earthquake Engineering and Soli

Dynamics III 1, 950-960.

CHAPTER III
IN SITU CHARACTERISTICS OF FINE COAL REFUSE

Portions of this chapter have been accepted as a conference paper:

3.1 ABSTRACT

A field exploration study was performed on an inactive coal refuse impoundment in the Appalachian region (USA) to investigate in situ characteristics of fine coal refuse (FCR). A series of standard penetration tests (SPT) were conducted from the crest of the impoundment and relatively undisturbed Shelby tube samples were obtained from various depths within the impoundment to a depth of about 60 meters (m). The SPT blow counts (N_{60}-values) in the FCR ranged from 7 to 15 blows per foot suggesting medium to stiff material consistency. The split-spoon samples revealed intermittent layering over short intervals, with thin layers of coarser FCR separated by layers of the finer very soft FCR. Particle size analyses identified two groupings of material, a "sandy" FCR and a "silty" FCR, with no apparent trend with depth. Index testing identified a few locations where the liquidity index was greater than one. It appears thin layers of coarser FCR material produce blow counts that obscure the presence of the soft layers of FCR. This suggests the SPT is not an effective means to investigate these slurry placed materials, if the intent is to identify flowable, under-consolidated materials.

3.2 INTRODUCTION

Fine coal refuse (FCR) refers to the fines generated during the processing of raw coal and stored behind on-site impoundments constructed primarily with the coarse refuse. This FCR is typically hydraulically placed by mixing the fines with water and a chemical flocculant and then pumping the resulting slurry through a series of pipelines. The flocculant is added to increase the apparent particle size and promote rapid settling of the solids once the slurry is placed in the impoundment. There are more than 1,170 tailing dams in US, of which approximately 700 are coal refuse impoundments (U.S Army Corps of Engineers, 2017). Hundreds of these impoundments are in the Appalachia region. These on-site impoundments are essentially tall dams (60-240 m tall) behind which the FCR is allowed to settle and dewater. The most common method of constructing impoundments is the upstream method (Figure 3-1). In this method of construction, during the initial stage, the fine refuse slurry is hydraulically discharged from the top of the starter dike and forms a delta. The deposited fine refuse then becomes the foundation for the second stage of embankment construction with additional coarse refuse used to construct the next dike followed by additional slurry. Construction continues in this manner to reach the desired and permitted height of impoundment. While the upstream construction method is typically depicted as shown in Figure

32

3-1, it has been suggested (Kalinski and Phillips, 2008) that during the placement of the coarse refuse on top of the underlying fine refuse some coarse refuse may displace the underlying soft FCR increasing the depth to the fine refuse and perhaps creating a zone of mixed material.

One of the most critical concerns of impounded mine waste material is whether or not the materials are prone to destabilization, i.e. flow. Destabilization of the FCR impoundment can result in severe and unpredictable fatalities and environmental disasters. As mentioned above, hundreds of these impoundments exist in the Appalachia region, and while many are well constructed and routinely inspected, there have been cases in which the slurry destabilizes resulting in loss of life, injury, significant environmental degradation of the downstream surface waters, and property loss. One such spill occurred at Buffalo Creek in 1972 (Logan County, WV) where approximately 132 million gallons of FCR material was released, resulting in the deaths of 125 people, the loss of 16 local communities, and more than $75,000,000 in damages (Kelley et al., 1973) In 2000 in Martin County (KY), a breakthrough occurred causing an estimated 306 million gallons of water and slurry to drain from an impoundment into an adjacent underground mine (Mine Safety and Health Administration, 2009).

There have been several reported investigations of in situ measurements of FCR impoundments (Thacker et al. (1988); Ullrich et al. (1991); Hegazy et al. (2004); Kalinski and Phillips (2008)), and there is likely a large database of in situ information in the permit files and files of coal operators. However, not much of this data has not found its way into the geotechnical engineering literature. In this study, an inactive FCR impoundment in the commonwealth of Kentucky has been studied and the FCR has been characterized using in situ exploration methods. In order to characterize the FCR, the crest of the impoundment was drilled and series of standard penetration tests (SPT) were performed.
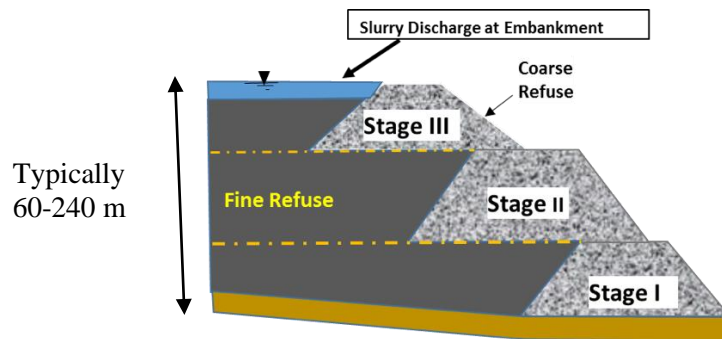
Figure 3-1. Upstream Method of Construction of FCR Impoundments

3.3 EXPERIMENTAL METHODS

The sampling and subsurface investigation of the fine coal refuse was performed at an inactive slurry impoundment in Kentucky. The impoundment was constructed in 1970s by the upstream method of construction, and permitting records suggest the slurry in the impoundment was slightly over 60 m (200 feet) thick.

Field testing consisted of traditional Standard Penetration Tests (SPT) to obtain measurements of in situ properties down to a depth of approximately 60 m, and undisturbed Shelby tube samples were collected to conduct laboratory testing. Figure 3-2, shows the drill rig in place working at a depth of at least 49 m (note the drill stem on the ground that has been removed for sampling).

After first passing through about 25 m of coarse coal refuse that had been placed as a cap, a total of 10 SPT tests were performed in a single borehole to a depth of 60 m. Eight undisturbed Shelby tube samples were collected with a piston sampler. Tube samples were sealed with paraffin wax and stored at room temperature before transferring to the laboratory. From each SPT test, a split spoon sample was collected. An attempt was made to measure the field water content of the collected split spoon samples, and selected spoon samples were collected for later laboratory testing.
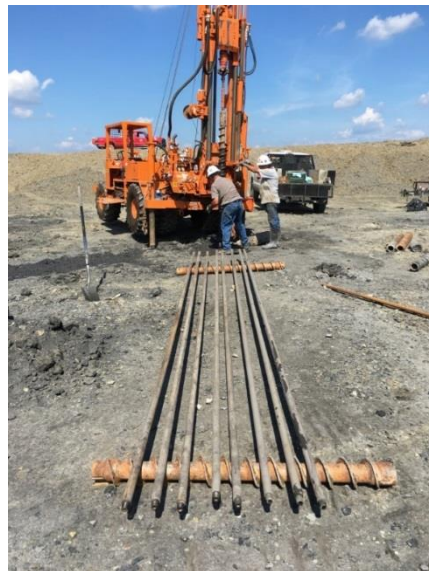
Figure 3-2. Drill Rig Used for this Study. Note: The Drill Stem on the Ground Suggests a Working Depth at the Time of about 49 m (160 feet); Each Assembled Length Consists of 4 Segments 5 feet Long for a Total Working Depth of 160 feet.

3.4   RESULTS AND DISCUSSION

Table 3-1 summarizes the depths at which SPTs were conducted (with corresponding split-spoon samples) and the locations where Shelby tube samples were obtained. At depths of 32 m, 42 m, and 56 m the split spoon sampler was observed to penetrate 50 to 75 mm under the weight of the center rods alone before the hammer was placed on the anvil (referred to as WOT = weight of tools).

Figure 3-3 shows split spoon samples representing samples from eight different depths. As shown in Figure 3-3, there are several clearly observable soft, high water content areas within the split spoon samples from upper depths of 27.4 m, 36.7 m and 39.8 m. Also observed were the predominant firmer more competent samples of the FCR. One key observation which was noted while inspecting the split spoon samples was the variation in grain size of the FCR (thin alternating layers of course and fine material) even within the length of the split spoon. This may be observed in Figure 3-3, and indicates that the deposited material may have highly variable properties within short intervals of depth, including particle size distribution, moisture content and shear strength. The layering over very short vertical distances is likely a result of the slurry placement process, creating deltas with various particles sizes accumulating in proportion to the velocity of the slurry as it settles. This deposition process can produce the alternating layers of finer and coarser materials, and the variation in grain size may affect the rate of consolidation resulting in layers of both stiff and very soft materials. Figure 3-4 illustrates this fine interlayering in a bulk sample which was obtained from a depth of about 5 m by a track hoe during the recovery of a broken auger. About 44 m of auger was in the ground when the auger broke, but fortunately the break occurred only about 5 m from the surface allowing recovery and replacement of the auger. Figure 3-5 shows the auger retrieval tool which also broke during the attempted recovery.

Table 3-1. Depths of Shelby Tube Sampling and Standard Penetration Tests

Type of Sampling	Top Depth of Obtained sample (m)									
Shelby Tube			28.2	32.9	36.1	39	42.1	46.3	52.6	58.8
Split Spoon	24.4	27.4	31	36.7	39.8	42.8	47.2	53.3	55.8	59.4
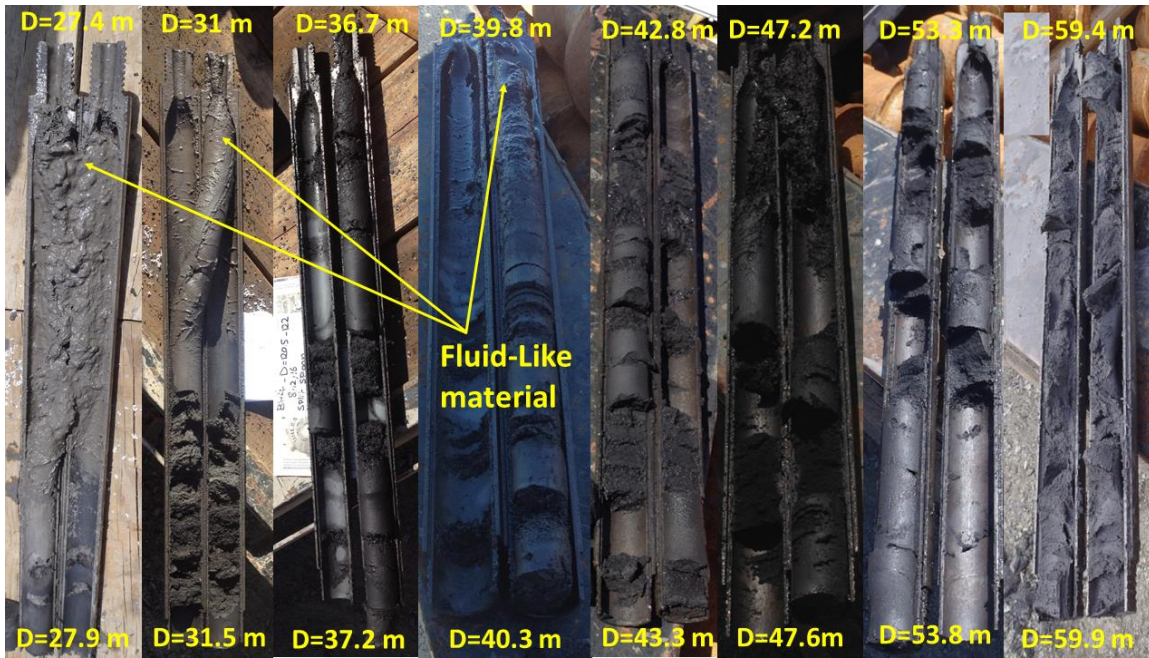
Figure 3-3. Heterogeneity within Split Spoon Samples from Various Depths

Figure 3-4. Bulk Sample Obtained from Approximately D = 5 m when a Track hoe was required to   Extract a Broken Auger. The Knife Included for Scale has a Length of Approximately 250   mm (5 inches).

Figure 3-5. Broken Auger Recovery Tool Resulting from Attempted Recovery of Broken Auger. Total Depth of Augers in the Ground at the Time of the Break was 44 m; Auger Breakage (Segment at Right) Occurred at about 5m.

The drilling difficulties, the medium consistency of the bulk sample obtained from 5 m, and the nature of the materials retrieved from the split-spoon sampler suggest the thin layers of very soft materials are not readily identified by standard exploratory methods and have the potential to be overlooked or never realized during analyses.

The grain size distribution was determined for each of these depths, as shown in Figure 3-6. Although the Atterberg limits suggest the FCR can be categorized as low plasticity clay (CL), the behavior of the material is different from clay and for the purpose of this study we are categorizing these materials according to relative grain size distribution. These particle size results show the FCR can be practically grouped into two different particle size distributions, with no apparent relationship with depth: a coarser FCR (with a diameter corresponding to 50percent finer = $D_{50} \approx 0.2$ mm referred to here as a "sandy" FCR, and a finer FCR ($D_{50} \approx 0.01$ mm) referred to as a "silty" FCR. Also shown for comparison is the particle size distribution of the fresh slurry taken from the discharge pipe during FCR placement.
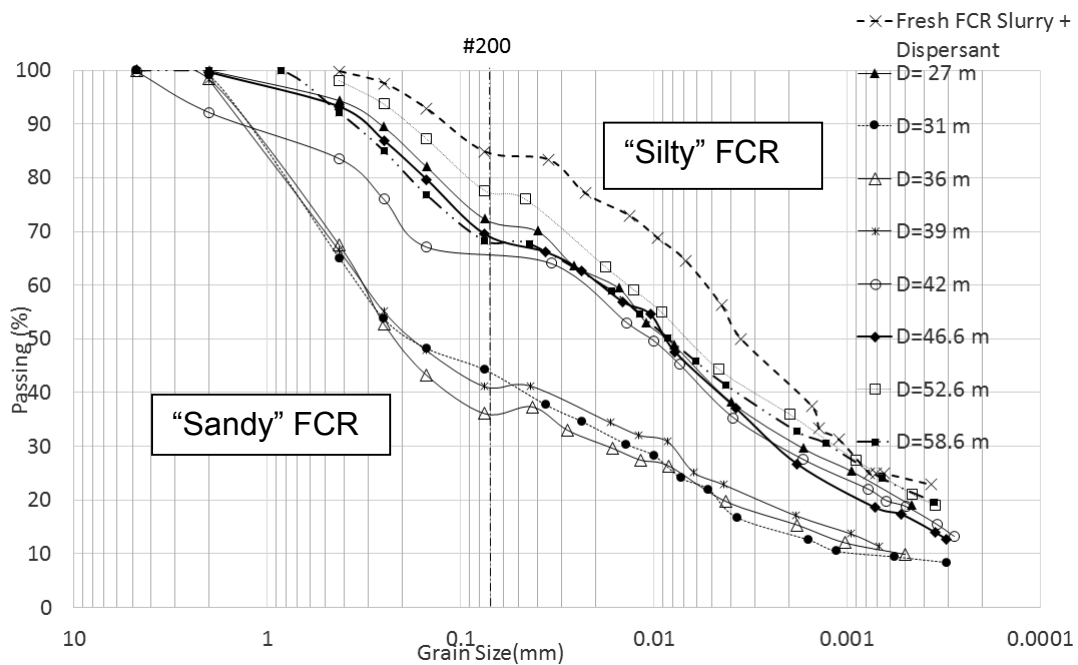
Figure 3-6. Grain Size Distribution of In situ Consolidation Samples from Various Depths. Note the Distinct Groupings of "Sandy" FCR and "Silty" FCR.

Figure 3-7 illustrates the results of standard penetration tests over the range of depth. Complete boring logs are provided in the Appendix. The SPT blow counts (N-values) in the FCR range from 7 to 15 blows per foot suggesting that the material would generally be classified as varying from "firm" to "stiff" by many traditional schemes. But these blow counts do not seem to reflect the soft materials observed in the split-spoon samples and the recorded WOT materials, nor are they consistent with what would be expected from the measured consolidation test data which indicated an under-consolidated behavior. It appears that the coarser FCR materials produce blow counts that obscure the presence of the thin soft layers of under-consolidated FCR. This suggests the SPT is not an effective means to identify thin layers of very soft material.
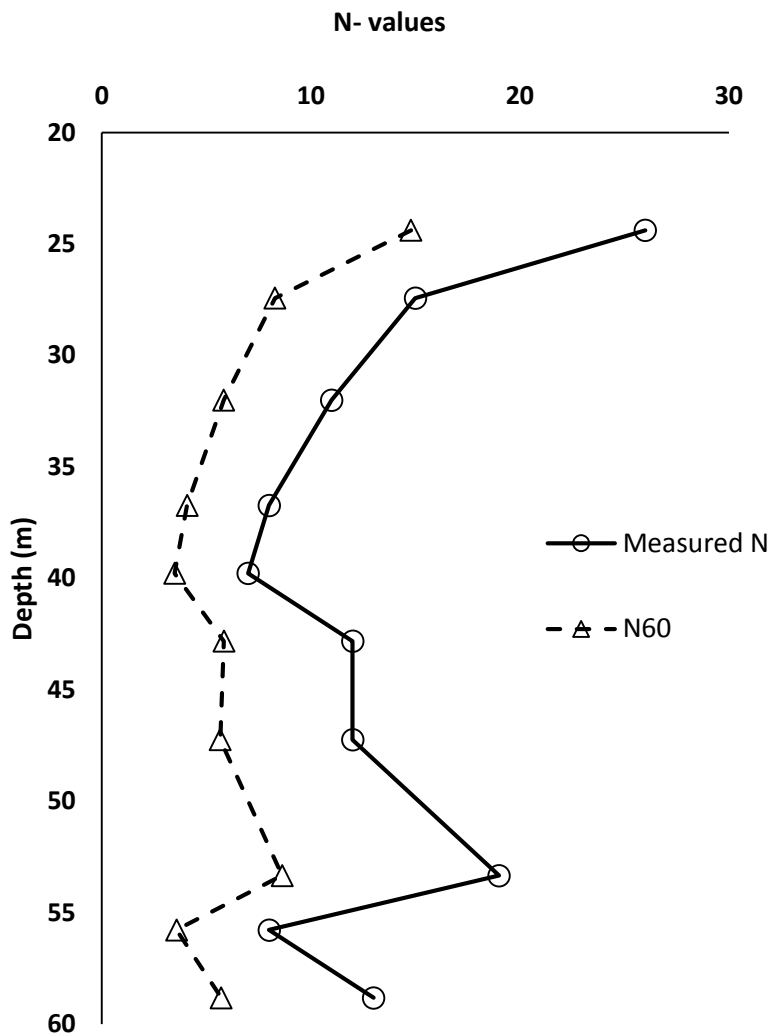
Figure 3-7. Standard Penetration Test Results (Both Measured and Corrected for Depth, D_{60}) from FCR Impoundment

The liquid limit and plastic limit of in situ samples of FCR were measured using the Casagrande method (ASTM-D4318, 2010), and the results are summarized in Table 3-2. Although the in situ water content can be compared with the liquid limit (LL) as an indicator of how flowable the material may be, since the LL will vary with depth, it is more convenient to compare the water content with the liquidity index (LI):

$$LI = (w - PL)/(LL - PL) \qquad \textbf{Equation 2-2}$$

where w is the in situ water content, PL is the Plastic Limit, and LL is the liquid Limit of a given sample.

The liquidity index (LI) is useful in that it scales the water content of a sample relative to the PL and LL. Thus, a liquidity index of 0 means the sample is at the PL, and a LI of 1 indicates the sample is at the LL. Values of LI above 1 indicate the material is at a water content above the LL. A value of the LI between 0 and 1 suggests that the soil deforms like a plastic material (Budhu, 2011).

Figure 3-8 summarizes the liquid index determined from the in situ FCR samples as a function of depth, along with the corrected blow count data from Figure 3-7. The LI (and PL and LL) were obtained from samples which were recovered from Shelby tube samples or split spoon samples. Also shown are the depths (depicted in Figure 3-3) which were observed to be very soft but not recoverable (e.g. D=27 m), and the three depths at which WOT material was detected. The data shown in Figure 3-8 suggest that the SPT is not useful for the identification of these relatively thin soft zones. The undrained shear strength values of the undisturbed FCR samples obtained by pocket penetrometer are also shown in Figure 3-8

Table 3-2. Atterberg Limits of the In situ FCR Samples

Depth(m)	w (%)	LL	PL	PI	LI	FCR type
28.2	27.9	36.2	22.8	13.4	0.38	Silty
32.9	30	33.5	15.3	18.2	0.81	Sandy
36.1	28.2	39.5	18.8	20.7	0.45	Sandy
39	35.3	35.9	20.6	15.3	0.96	Sandy
42.1	37.1	36.3	24.9	11.4	1.07	Silty
46.3	33.4	47.7	20.2	27.5	0.48	Silty
52.6	36.1	44.4	31.4	13	0.36	Silty
58.6	34.8	44.4	24.6	19.8	0.52	Silty

.
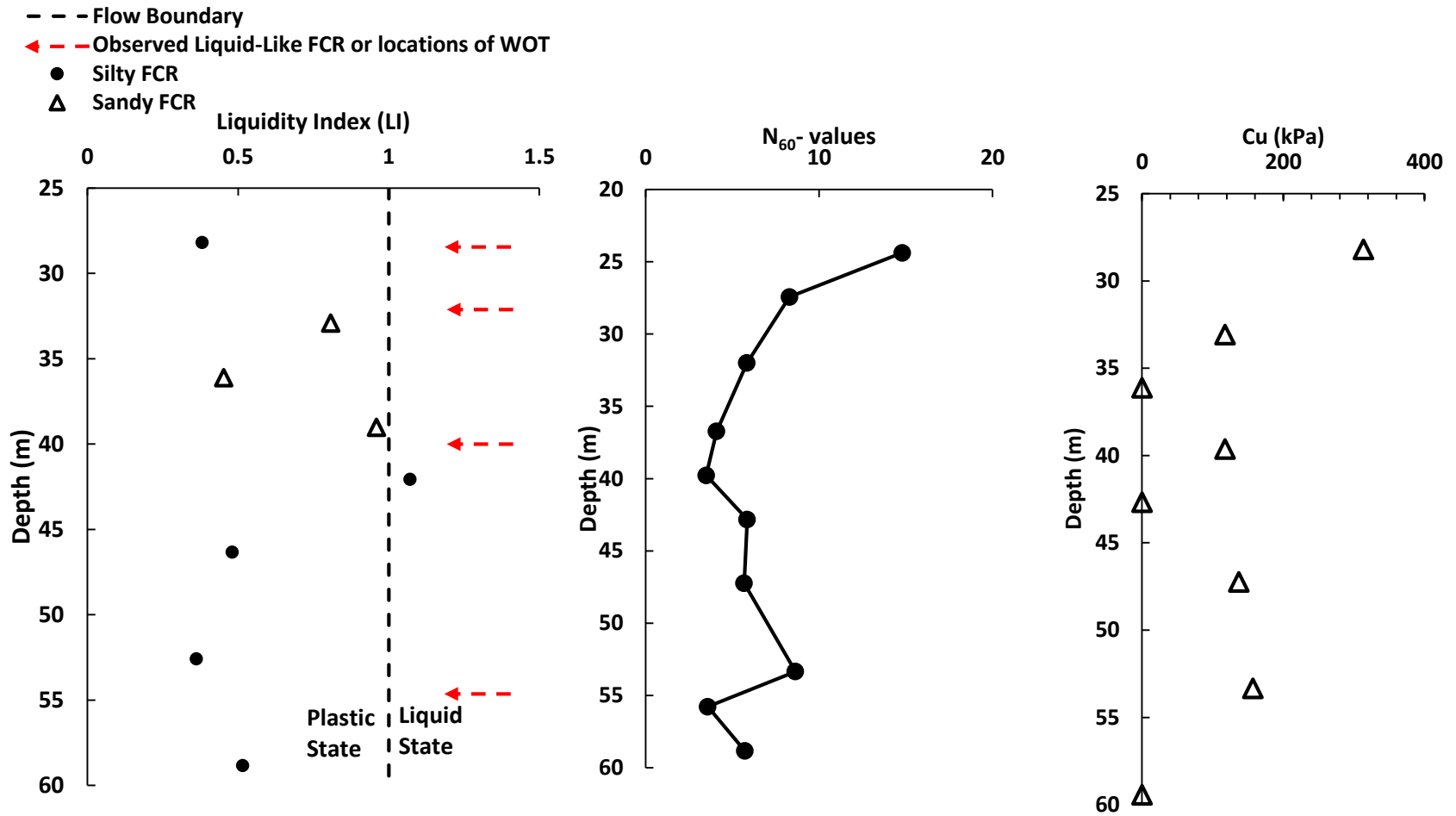
Figure 3-8. Liquidity Index of the In Situ FCR at Different Depths and Depths Where Fluid-Like Materials were Observed, N_{60} Values with Depth, and Shear Strength Values of Undisturbed Shelby Tube Samples Measured by Pocket Penetrometer

3.5 CONCLUSIONS

Fine coal refuse is a pre-combustion byproduct of coal processing which is usually mixed with water and flocculant and hydraulically placed behind on-site impoundments. In this study, the in situ characteristics of FCR in an inactive impoundment were investigated through a geotechnical exploration to a depth of about 60 m. Results show that in spite of being hydraulically placed, the FCR materials are very heterogeneous and the grain size distribution curves indicated there are two major groups of material referred to as "sandy" and "silty" fine coal refuse. The Atterberg limits of the FCR from different depths found scattered values for moisture content, liquid limit and plastic limit, and in some zones values of liquidity index which were greater than 1 suggesting the potential of local flowable material. Despite a long time of deposition and consolidation (approximately 40 years), some thin "fluid-like" zones were observed in the split-spoon. The SPT blow counts (N_{60}-values) in the FCR range from 7 to 15 blows per foot suggesting medium to stiff material consistency, which does not reflect the presence of the observed thin layers of very soft material, nor the WOT materials recorded or the measured liquidity index values greater than 1. It appears the stiffer and coarser FCR materials produce N-values which represent the material consistency over the length of the sampler, and may obscure the presence of the short intervals of very soft material. This suggests the SPT is not an effective means to investigate slurry placed materials if the intent is to identify thin zones of very soft, potentially flowable under-consolidated materials.

3.6 REFERENCES

ASTM-D4318, 2010. Standard Test Methods for Liquid Limit, Plastic Limit, and Plasticity Index of Soils. 1-16.

Budhu, M., 2011. Soil mechanics and foundations, 3rd ed. Wiley, New York.

Hegazy, Y.A., Cushing, A.G., Lewis, C.J., 2004. Physical, mechanical, and hydraulic properties of coal refuse for slurry impoundment design. Geotechnical and Geophysical Site Characterization Vols 1 and 2, 1285-1291.

Jedari, C., Palomino, A.M., Drumm, E.C., 2018. Compressibility of Fine Coal Refuse. IFCEE 2018,   Geotechnical Special Publications, ASCE 296, 455-462.

Kalinski, M.E., Phillips, J.L., 2008. Development of Methods to Predict the Dynamic Behavior of Fine Coal Refuse: Preliminary Results from Two Sites in Appalachia, Geotechnical Earthquake Engineering and Soil Dynamics Congress IV. ASCE, Sacramento, CA.

Kelley, J.H., Kealy, D., Hylton, J., C.D., Hallanan, E.V., Ashcraft, J., Murrin, J.F., Davies, W.E., Erwin, R.B., Latimer, J., I.S. , 1973. The Buffalo Creek Flood and Disaster: Official Report from the Governor's Ad Hoc Commission of Inquiry 1973.

Mine Safety and Health Administration, M., 2009. Engineering and Design Manual: Coal Refuse Disposal Facilities, 2nd ed. Department of Labor, Prepared by D'Appolonia Engineering.

Thacker, B.K., Ullrich, C.R., Athanasakes, J.G., Smith, G., 1988. Evaluation of a Coal Refuse Impoundment   Built by the Upstream Method. Geotechnical Special Publications, ASCE, 730-749.

U.S Army Corps of Engineers, N.I.o.D., 2017. National Inventory of Dams

Ullrich, C.R., Thacker, B.K., Roberts, N.R., 1991. Dynamic Properties of Fine-Grained Coal Refuse, Second International Conference on Recent Advances in Geotechnical Earthquake Engineering and Soil Dynamics, St. Louis, Missouri.

CHAPTER IV
RHEOLOGY AND THE PARTICLE AND FLOC SIZE DISTRIBUTION OF FCR

Portions of this chapter were submitted to Geotechnical Testing Journal (ASTM):

Jedari, C., Palomino, A.M., Drumm, E.C. (2018), Cyr, H. J. "Comparison of Hydrometer Analysis and Laser Diffraction Method for Measuring Particle and Floc Size Distribution Applied to Fine Coal Refuse", Geotechnical Testing Journal (Under Review)

4.1 ABSTRACT

Traditional grain size distribution measurement techniques assume that the obtained particle diameters are of individual grains. However, for suspended particulate materials, particles may be dispersed or associated in flocs. Further, particle-level associations depend on the surrounding fluid chemistry which may change over time. The purpose of this study is to compare two different methods of grain size analysis for detecting particle and floc sizes in suspensions of fine coal refuse (FCR): hydrometer analysis, the well-known traditional method, and laser diffraction, a lesser known method. The influence of background solution – flocculant, dispersant, or distilled water – on the apparent grain size of FCR was also investigated. Analogous slurry suspensions made from a well-characterized kaolin were analyzed for comparison. Results from the grain/floc size analysis indicate that there are several advantages of laser diffraction over hydrometer analysis including a short measurement period, small sample size requirement, and the ability to measure a wide range of particle sizes in the same analysis. Moreover, this study highlights the ability of the PSA to accurately measure changes in particle size over time for the same suspension and thereby indicate the presence of flocs. Finally, the PSA has the capability of capturing dynamic particle interactions – flocculation and deflocculation in real time.

Keywords: Fine coal refuse, particle size, floc size, grain size distribution, laser diffraction

4.2 INTRODUCTION

The behavior of a particulate slurry and resulting sediment is a function of the particle-level interactions. This is especially true for fine-grained soils made up predominately of clay minerals in which the particle associations are controlled by the surrounding fluid chemistry (van Olphen 1977). Different particle associations lead to very different settling behavior and resulting sediment fabric. For example, dispersed clay particles settle much more slowly and form denser sediments, while flocculated particles settle much faster and form more open, voluminous sediments (Michaels and Bolger 1962, Imai 1980, Pierre et al. 1995, Pierre and Ma 1999, Palomino and Santamarina 2005). Sediment fabric in part determines macro-scale sediment properties and behavior, e.g. sediments formed from flocculated particles tend to have higher shear strength than dispersed sediments (Mitchell and Soga 2005) .While many such studies focus on clay mineral particles, less is known about the particle associations that form in suspensions and

46

corresponding sediment fabric of waste materials derived from energy production processes since many of these materials contain little to no clay minerals. Further, these materials are often impounded in slurry form with added chemical flocculants. Thus, standard characterization techniques, such as for grain size distribution, may not be reliable for predicting or estimating the material properties of the final sediment.

One such waste material is fine coal refuse (FCR), a by-product of the coal preparation process. FCR is typically hydraulically placed in on-site impoundments, and the predominant silt-sized material usually contains significant amounts of coal which yields a low specific gravity. In the energy production industry, waste products such as fly ash and fine coal refuse are often impounded in slurry form. The challenge during the placement process is to induce rapid settling and sediment formation such that consolidation can take place as quickly as possible. Furthermore, the rheology and flowability of impounded FCR slurry is influenced by particle size distribution and how much flocculation has taken place in the suspension (Logos and Nguyen 1996, Atesok et al. 2002, Boylu et al. 2004). Chemical flocculants are added to the FCR slurry to flocculate fine particles and accelerate settlement and subsequent consolidation after placement. As a result, the effective particle size distribution of the FCR is altered, potentially impacting the properties of the placed material such as rheology, consolidation time (Jedari et al. 2018), and void ratio. For example, particle size distribution is one of the most important factors controlling the viscosity of coal-water suspensions (Fidleris and Whitamore 1961). Thus, having a method that more accurately describes the apparent grain size distribution of the solids – flocculated or dispersed – in suspension will provide a greater insight into the predicted behavior of these impounded materials.

The ability to accurately measure particle size distribution of FCR, which consists of at least some flocs, is not straight forward. Furthermore, flocculation and deflocculation of FCR particles over time is likely dependent on the concentration and effectiveness of the added flocculant. Hence, selection of an appropriate grain size analyses technique must include the ability to observe or infer the presence of flocs. In this study, we compare two different methods of grain size analysis for detecting particle and floc sizes in suspensions of fine coal refuse: hydrometer analysis, the well-known traditional method, and laser diffraction, a lesser known method. Analogous slurry suspensions made from a well-characterized kaolin were analyzed for comparison.

Grain and Floc Size Analysis

Traditional methods of grain size analysis are based on the physical separation of coarse grains (e.g. wet or dry sieve technique) and changes in the specific gravity of a soil suspension through time (e.g. hydrometer technique) (Day 1965). Although established geotechnical quantitative techniques exist (ASTM-D422 2007), these methods have several disadvantages such as the length of time needed to complete the analyses, the dependency of results on laboratory techniques, and operator error (Syvitski and Hein 1991). These methods also require relatively large sample sizes (tens to hundreds of grams). Moreover,

the hydrometer method relies on Stokes' Law to quantify grain size distribution, which introduces assumptions rarely present within natural settings such that all particles are solid spheres and each have the same unit weight (Murthy 2002). Furthermore, the chemistry of the suspending fluid has a significant influence on the sedimentation behavior of many particulate materials (Lambe and Whitman 1969, van Olphen 1977). As shown in Figure 4-1, this dependency of particle interactions on fluid chemistry extends to FCR. These issues make traditional methods less advantageous for rapid and accurate analysis of a large number of particulate samples, especially when dealing with flocculated materials such as FCR, which are artificially produced and contain substantial quantities of carbon (low G_s).
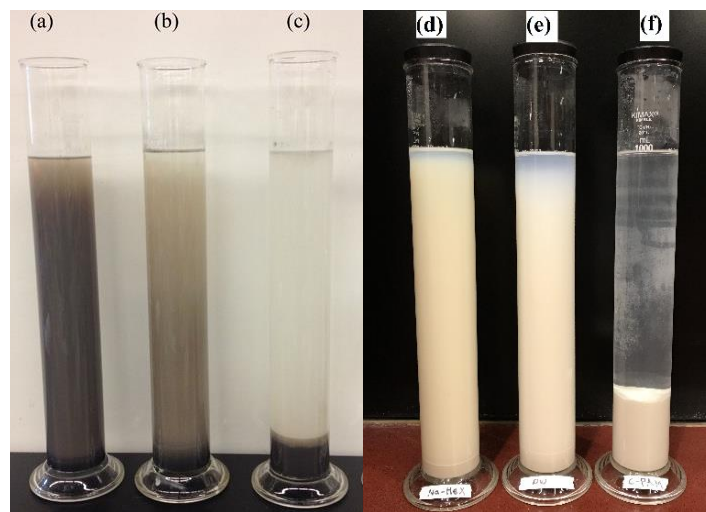
Figure 4-1. Hydrometer Tests with Different Background Solutions: (a) FCR with Dispersant at 3 weeks, (b) FCR in Distilled Water at 3 Weeks, (c) FCR in as-received Supernatant Fluid at 24 hrs, (d) Kaolin with Dispersant at 3 Weeks, (e) Kaolin in Distilled Water at 3 Weeks, (f) Kaolin in a Flocculant Solution at 3 Weeks.

In recent decades, new methods for particle size analysis have been developed. One such method is laser diffraction, which measures particle size distributions by analyzing the angular variation in the intensity of light scattered as it passes through a dispersed particulate sample (Storti and Balsamo 2010). For this study, grain size distribution was measured using a Mastersizer 3000 laser diffraction particle size analyzer (Malvern Instruments Ltd). A major advantage of Malvern's laser diffraction technique is the Mastersizer 3000 provides indirect size measurement of a wide range of particles (0.01 to 3500 µm) in a single sample during the same analysis. The method also requires very little sample material (between 0.2 and 2.0 g) and short measurement times (approximately 10 to 20 seconds per analysis). When using the wet dispersion cell, repeated measurements can be run on the same sample. This not only provides statistical reproducibility but also allows one to accurately measure real-time changes in the grain size distribution through time (i.e. if the sample aggregates or deflocculates during the course of the analysis).

The Mastersizer 3000 employs a blue and red light dual-wavelength single-lens detection system to measure the degree to which light is diffracted by particles distributed within a medium. As shown in Figure 4-2, the Mastersizer 3000 is comprised of the dispersion unit, the sample measurement cell, two light sources, and a series of back scatter detectors, focal plane detectors, and side scatter detectors. Material is added to the dispersion unit using either the wet dispersion or dry dispersion modes. The suspended material is then circulated across the measurement cell and illuminated by a 10mW 470 nm blue LED and a 4 mW He-Ne 633 nm red laser. The blue LED has a greater sensitivity to wide angle diffraction and allows for an accurate measurement of sub-100 nm particles. The red laser provides small angle resolution appropriate for particle sizes greater-than-100 nm. The angular variation in the intensity of scattered light is measured across each detector as energy impulses.

Using Mie theory of light scattering, the Mastersizer 3000 software calculates the particle distribution responsible for creating the measured scatter pattern. Mie theory provides a detailed mathematical description of the correlation between the particle size distribution of a sample and the intensity of the scattered light produced (Hergert and Wriedt 2012). To accurately calculate the grain size distribution, the Mastersizer 3000 software takes into account the optical properties of both the sample material and the dispersing medium in the Mie algorithm. The source of the optical properties used in this study are discussed below. These properties include the refractive and absorption indices of the sample material and the refractive index of the dispersing medium and are entered into the Malvern software operating procedure prior to analysis.

The main differences between the hydrometer analysis and laser diffraction methods are summarized in Table 4-1.
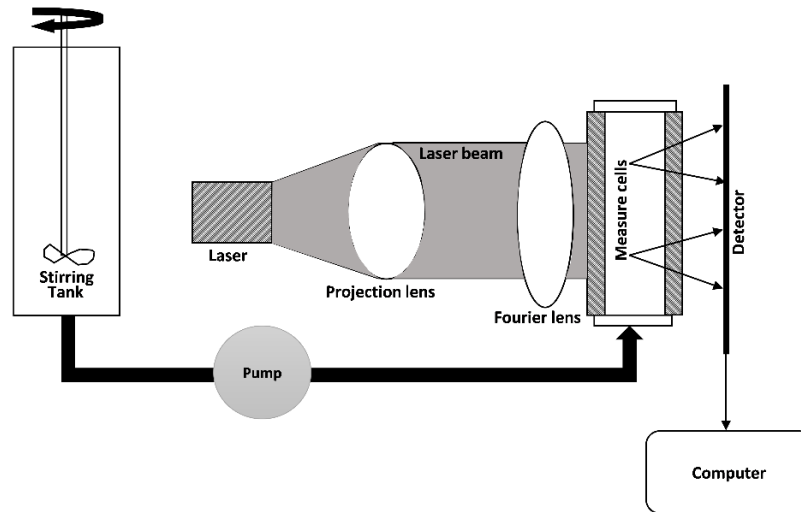
Figure 4-2. Schematic of Laser Diffraction Method (after Storti and Balsamo 2010).

Table 4-1. Comparison of Hydrometer Analysis and Laser Diffraction Methods

| | Test Method | |
	Laser diffraction	Hydrometer
Applied Theory	Mie Theory	Stokes Law
Measurement Time	< minute	Many days
Sample Size	~ 1 gram	50-100 grams

4.3 EXPERIMENTAL METHODS

4.3.1 MATERIALS

For the tests presented here, the material used was FCR suspension obtained in slurry form directly from a discharge pipe at a coal processing facility (Kentucky, US).The FCR suspension was either tested "as-obtained" or reconstituted. For the reconstituted suspensions, the FCR solids were separated from the supernatant, dried, ground with a mortar and pestle, and reconstituted with one of two background solutions to prepare the solid-solution suspensions for measurement: (1) a dispersant solution prepared with sodium hexametaphosphate dissolved in distilled water at a concentration of $40g$ $(NaPO_3)_6$/L water (consistent with ASTM D422) and (2) distilled water. The supernatant solution contains a flocculant (anionic water-soluble polymer) at an unknown concentration. A well-characterized high-purity kaolin was used as a comparison material. The kaolin (Acti-Min® SA-1) was obtained from Active Minerals International, LLC (Georgia, US). A known cationic polyacrylamide (C494; Cytec Industries Inc., West Paterson, NJ) was used as a

flocculant for the kaolin since previous studies with this particular clay-polymer combination resulted in well-flocculated suspensions (Kim and Palomino 2009).

4.3.2 METHODS

Hydrometer Analysis. Traditional hydrometer tests were performed on the FCR according to ASTM D422 with the following suspending fluids: (1) supernatant, (2) dispersant (ASTM D422), and (3) distilled water. The volumetric solids content of the FCR suspensions was kept constant for all tests at solids content = 0.0226, where solids content is defined as:

$$Solids\ Content\ (SC) = \frac{Volume\ of\ Solids}{Total\ Volume\ of\ Suspension}$$
<div align="right">**Equation 3-1**</div>

The moisture content of the as-collected FCR slurry was determined previously. Thus, a given volume of FCR slurry had a known mass of solids. For the supernatant condition, 50 g of FCR was measured in slurry form and placed in a 1000-mL graduated cylinder. Additional supernatant solution, syphoned from as-obtained FCR slurry, was used to increase the total volume of the suspension to 1000 mL. For the dispersant condition, 50 g of oven dried FCR was soaked in 125 mL sodium hexametaphosphate solution for 16 hours prior to the start of the test. For the distilled water condition, 50 g of oven dried FCR was soaked in 125 mL distilled water for 16 hours prior to the start of the test. The soaked materials for each case were then placed in graduated cylinders. Additional corresponding background solution (dispersant or distilled water) was added to the cylinder to increase the total suspension volume to 1000 mL. Each cylinder was shaken for one minute prior to the start of the test to ensure the particles were well-distributed throughout the suspension. At the end of one minute, the cylinder was placed on the benchtop. Hydrometer readings were recorded at time intervals of t = 2, 5, 8, 15, 30, 60, 120, 250, 1440 minutes. Following the 1,440 minute reading, additional hydrometer measurements were taken until the effective diameter (D_{10}) was identified.

Following the hydrometer analysis, each suspension was passed through a series of nested sieves to define the size distribution of particles larger than the sieve #200 (i.e. greater-than-75 μm). The fluid and particles passing the sieve #200 were collected in a plastic bucket. The material retained in each sieve was dried in the oven and weighed.

Laser Diffraction Analysis Particle Size Analyzer (PSA). For this study, a Mastersizer 3000 laser diffraction particle size analyzer (Malvern Instruments Ltd) was used to measure grain and floc size distribution. In this study, the Hydro LV wet dispersion unit was employed, which uses a 600 ml tank equipped with a centrifugal pump system to pass the suspended material through the measurement cell. For the FCR, three different background solutions including distilled water, the supernatant fluid of the FCR slurry, and a 40 g/L sodium hexametaphosphate solution were used to investigate the influence of the

background solution on the particle size distribution and floc size distribution. For each test, approximately 600 ml of the specified background solution was added to the dispersion tank and allowed to circulate. The pump speed was then reduced to 0 rpm and between 1 and 2 g of the slurry matrix was added to the dispersion tank. The pump speed was then increased to 2,200 rpm to circulate the suspended material through the measurement cell. The approximate solids content during the measurements was 1.88×10^{-5}.

Prior to the analyses, material properties specific to bituminous coal were added to the Malvern software measurement settings following Goodarzi and Murchison (1973). These included a refractive index of 1.8, absorption index of 0.1, and density of 2.21 g/cm^3. A total of six measurements were taken for each background solution to investigate the influence of time and pump speed on floc size formation/breakage. Each measurement was conducted with both the blue LED and the red laser for a duration of 10 seconds for each light and then a 40-second waiting period prior to the next measurement. Values of D_{10}, D_{50} and D_{90} were obtained for each of six measurements. Table 4-1 provides a comparison between two techniques of particle size analysis.

For comparison, the same test procedure was used measure particle and floc size of kaolin with different background solutions. A refractive index of 1.57, absorption index of 0.1, and density of 2.6 g/cm^3 were applied to perform PSA experiments. Since the chemical composition and concentration of the flocculant present in the as-received FCR slurry was unknown, a suspension of cationic polyacrylamide (C-PAM) with a concentration of 40 mg/L was used to flocculate the kaolin. The chemical structure of C-PAM is illustrated in Figure 4-3 (Huang et al. 2001). Kim and Palomino (2009) determined the molecular mass of the C-PAM to be $\sim 4 \times 10^6$ $(\frac{g}{mol})$.
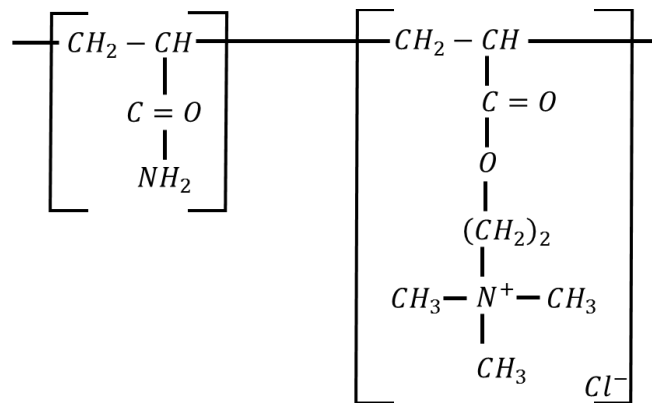
Figure 4-3. Chemical Structure of Cationic Polyacrylamide (C-PAM) (Huang et al. 2001)

The C-PAM concentration was selected based on critical coagulation concentration experiments to ensure flocculation of the kaolin particles. C-PAM concentrations of 0, 20, 30, 40, mg/L were used to observe floc formation and a change in sedimentation behavior. Figure 4-4 shows the settling behavior of kaolin particles in solutions with different concentrations of C-PAM. In order to minimize particle collisions that induce hindered settling sedimentation (Irani and Callis 1963) solutions were prepared with a solids content of 0.02. The kaolin particles form large flocs and settle completely (clear supernatant) in 40 mg/L of C-PAM.
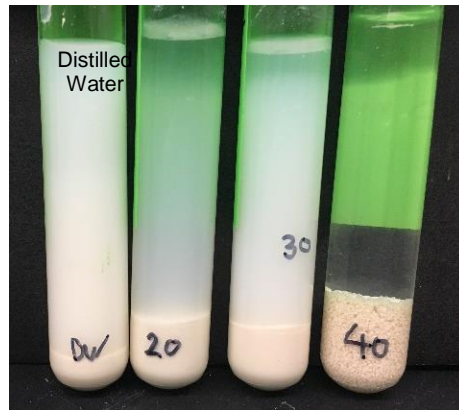
Figure 4-4. Kaolin sedimentation behavior in distilled water, and 20, 30, and 40 mg/L C-PAM after 1 hour of settling.

Scanning Electron Microscopy. Scanning electron micrographs were obtained for freeze-dried samples of FCR and kaolin after exposure to the test solutions. The samples were freeze-dried prior to imaging to maintain the particle arrangement, i.e. fabric, achieved during sedimentation. Scanning electron micrographs were obtained at the JIAM Advanced Microscopy and Imaging Center at the University of Tennessee. A Zeiss Auriga microscope was used for imaging.

Rheology behavior of FCR: The rheology or flow characteristics of coal refuse slurries are not well understood, although BilBao et al. (2011), Mitchell and Soga (2005) and Hunter (2001) suggest that the Bingham plastic model as a likely model describing the flow of coal waste. Bingham plastic flow occurs in solid-liquid (two-phase) systems with extensive structure but not in pure fluid systems. The Bingham plastic flow is characterized by a minimum stress, or yield stress, that must be exceeded in order for flow to take place. The system acts as an elastic solid below this yield stress (Munson et al., 1994; Patton, 1979). Figure 4-5 depicts Bingham behavior for both the ideal and non-ideal cases.
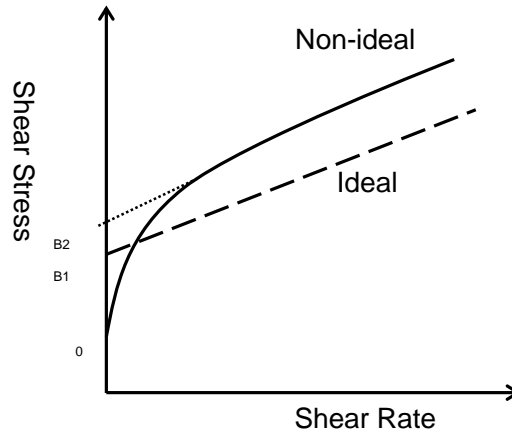
Figure 4-5. Schematic of Ideal (Bingham) and Non-ideal Plastic Behavior. S_0 is the Primary Yield Value, and S_{B1} and S_{B2} are the Bingham Yield Values for the Ideal and Non-ideal Cases, Respectively (after Hunter 2001). For a Newtonian Fluid, the Response is More Like the "Ideal" Behavior, Except the Value of S_{B1} is Very Nearly Zero.

Since the rheological behavior of a particulate material suspension depends on many factors (particle associations, particle shape, gradation, etc.), further study of the flow behavior, including the identification of appropriate models for the behavior, is needed. The change in flow response with variations of particle size distribution and varying moisture contents is especially important.

The rheological behavior of a suspension, captured as shear stress vs. shear strain, can take several forms depending on both the characteristics of the solid particles and the fluid phase. For example, if the particles develop a net surface charge when hydrated with a polar fluid, then they are susceptible to flocculation and/or aggregation for certain fluid conditions (e.g., moderate pH or high ionic concentration). These flocs/aggregates tend to increase the resistance to shear of the suspension. Furthermore, these flocs or aggregates may deflocculate or deaggregate under certain fluid conditions (e.g. change in pH or decrease in ionic concentration) or applied shear stresses. Thus, the rheological behavior depends on the interaction between the particles and the chemical composition of the fluid. Mitchell and Soga (2005) reference previous studies that have suggested that flow-controlling admixtures in the slurry used to improve the fluid transport properties may impact slurry particle sedimentation, thus the water chemistry of the transport fluid should also be investigated as a variable impacting the rheological behavior. However, once placed in the impoundment, the influence of these additives may degrade over time. So, the properties of the transport fluid with time are also important.

Viscosity Measurements. The FCR solids were separated from the as-received FCR slurry, oven-dried at 110°C, ground with a mortar and pestle, and then mixed with each of the background solutions at

54

solids content of 0.129, which is equivalent to the as-received FCR slurry solids content (0.129). Viscosity measurements were also made of the as-received FCR slurry.

The viscosity profiles with increasing shear rate were obtained using a Brookfield LVDV-II+ Programmable viscometer (Figure 4-6) and spindle #LV-1. The viscosity was measured across a range of shear rates applied by varying the spindle rotational speed from 5 rpm to 100 rpm. The viscosity was measured after applying the given rotational speed for one minute, which allows for suspension equilibration and measurement consistency. The viscosity-rotational speed measurements were converted to their corresponding shear stress-shear rate relationships following the procedures described in AMETEK Brookfield (2017).
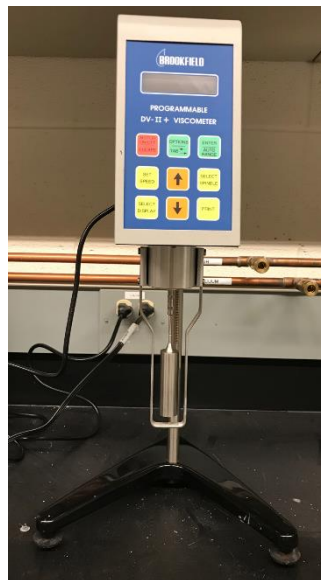
Figure 4-6. Brookfield LVDV-II+ Programmable Viscometer Used to Measure Viscosity of FCR Suspensions.

4.4   RESULTS

4.4.1   HYDROMETER ANALYSIS

Figure 4-7 shows the grain size distribution curves for kaolin and FCR obtained using hydrometer analysis in three different background solutions: a solution containing a flocculant, a dispersant solution, and distilled water. For all FCR cases, approximately 80% of particles/flocs are <75 μm (passing #200). The apparent D_{50} values for FCR in the dispersant solution (Na-Hex), distilled water and supernatant fluid are 6.3 μm, 3.5 μm and 20 μm, respectively. For the kaolin, 100% of particles/flocs are smaller than 75μm. The D_{50} values for kaolin in the dispersant solution, distilled water, and flocculant (C-PAM) solution are 2.4 μm, 1.8 μm and 14 μm respectively.

4.4.2   LASER DIFFRACTION ANALYSIS

Figure 4-8 shows D_{90} values of FCR and kaolin suspensions in each background solution measured using laser diffraction. A total of six measurements were taken of the same suspension sample over time. The apparent D_{90} values are highlighted here as a point of comparison of either floc presence/formation and floc breakage (deflocculation). For example, the D_{90} for kaolin in C-PAM solution is much larger than in distilled water and in dispersant (Na-Hex), indicating the formation of flocs. For the FCR suspension, flocculation is also evident for the supernatant background solution, which contains a flocculant.

For the case of kaolin in FCR supernatant, Figure 4-9 shows the measured D_{90} values over time. The time to reach to stable values of D_{90} was approximately 50 minutes (50 measurements at 1 measurement per minute), much longer than the time for the D_{90} values of kaolin in C-PAM solution to stabilize (Fig. 6a). This implies that the C-PAM is a much stronger flocculant for kaolin particles compared to the flocculant in the FCR supernatant solution. Further, these results highlight the capability of the PSA to capture the dynamic particle interactions, i.e. floc formation in real time.
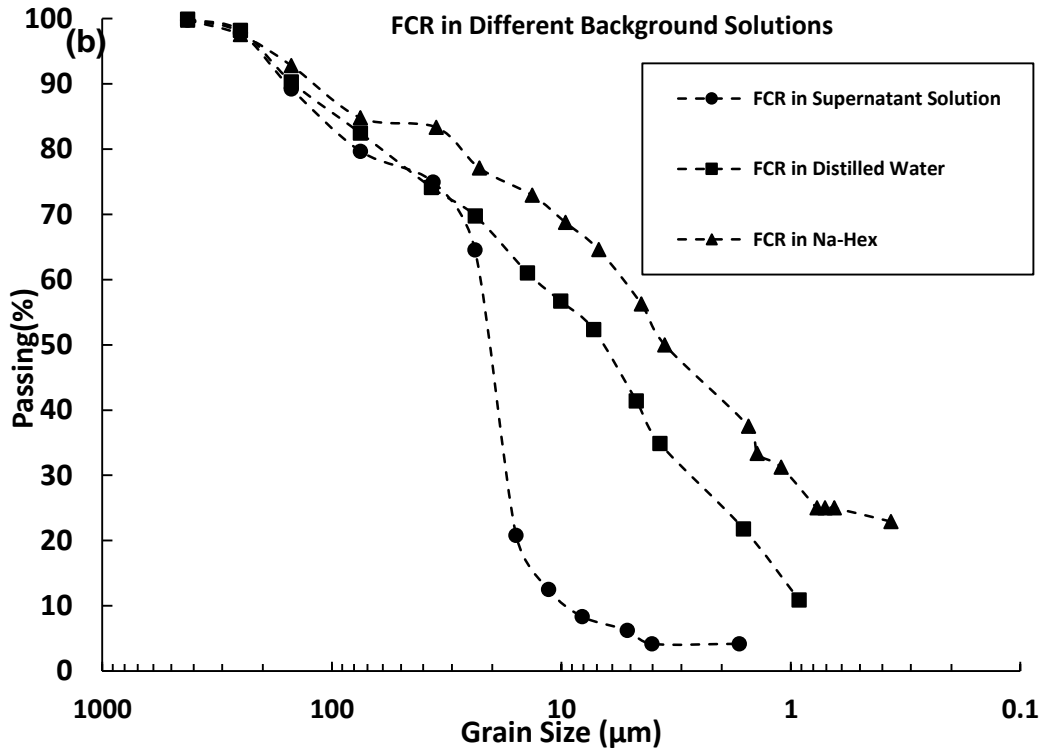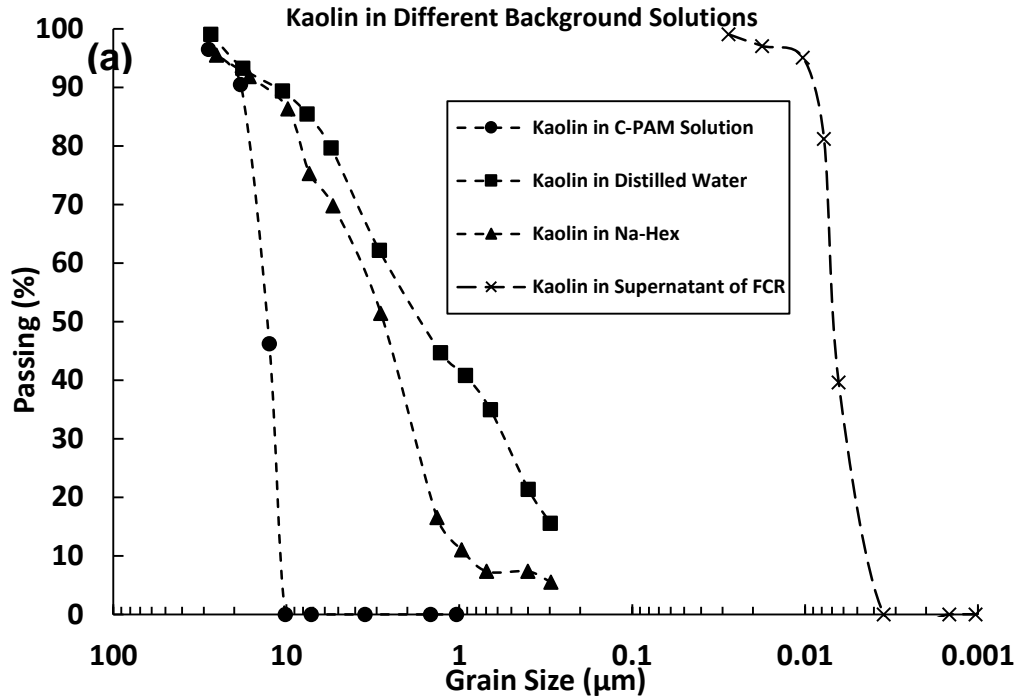
Figure 4-7. Grain size distribution curved obtained using hydrometer analyses of (a) kaolin and (b) FCR in different background solutions.
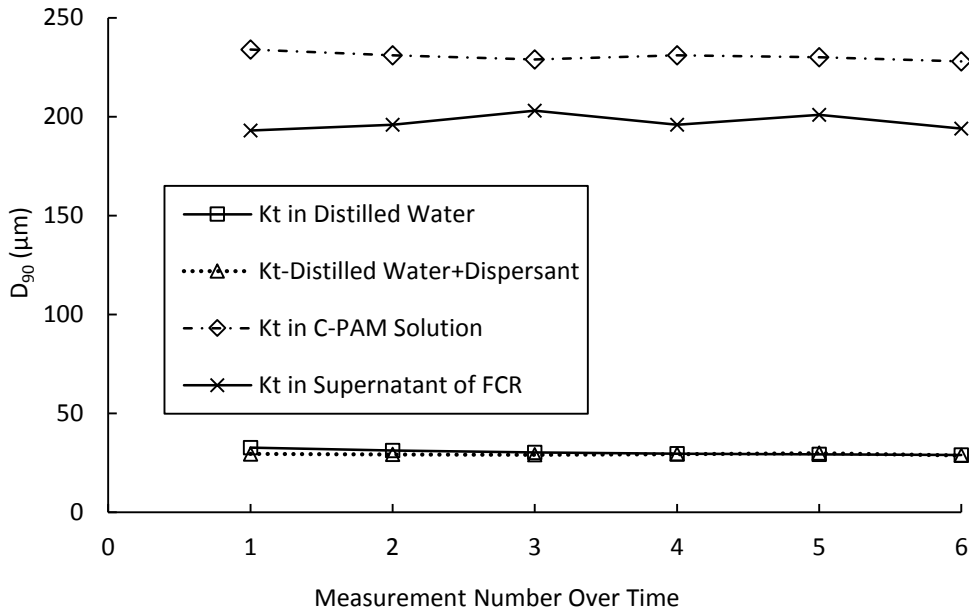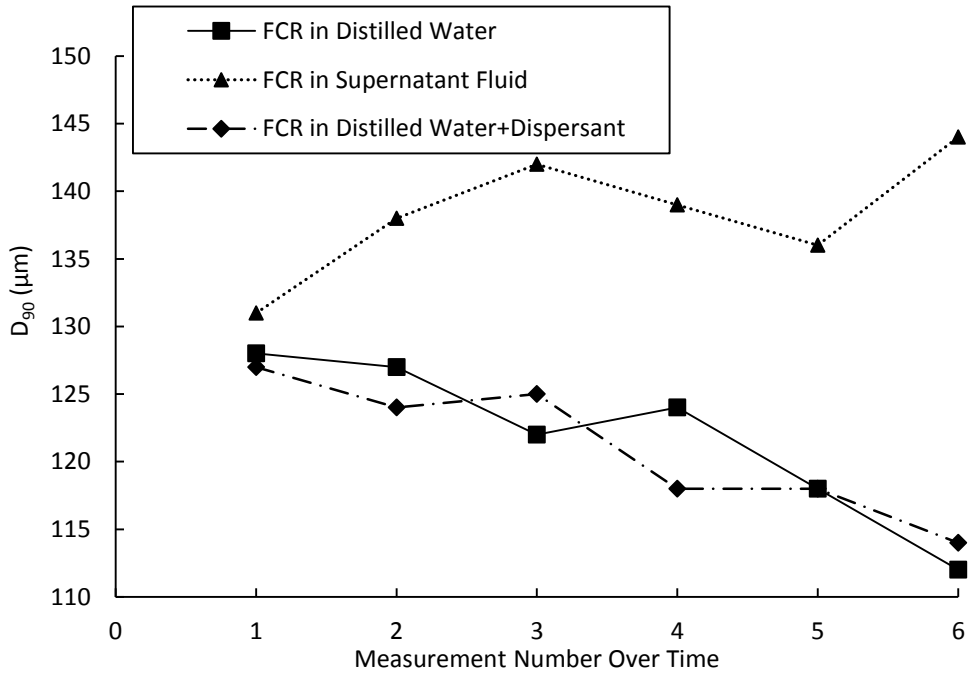
Figure 4-8. D_{90} values of (a) kaolin and (b) FCR measured using laser diffraction in different background solutions.
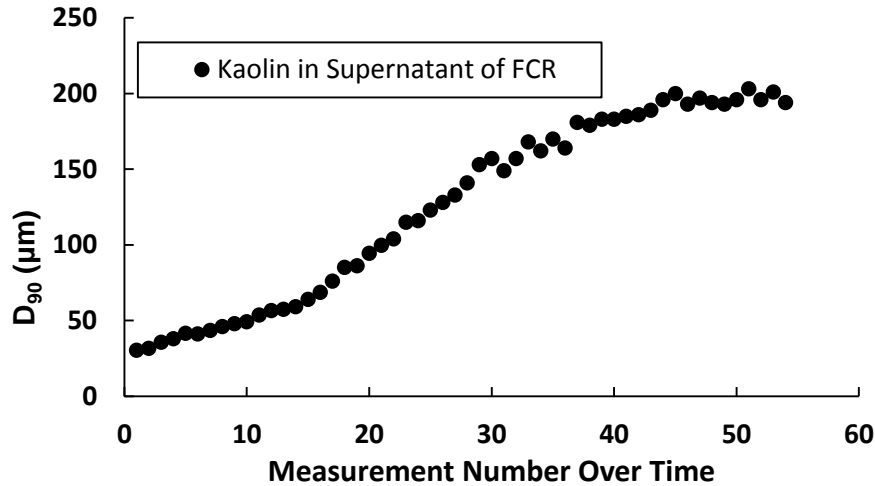
Figure 4-9. Variation of D90 values of Kaolin in Supernatant of FCR

The measured D_{90} values for all tested suspensions were normalized with respect to the corresponding initial measured D_{90} (Figure 4-10). The normalized values emphasize the stability of particle sizes during the measurement time, i.e. measurement #1 to measurement #6. The highest variation of D_{90} values is observed for the FCR in the supernatant solution, while the kaolin in C-PAM solution has the lowest variation. This demonstrates the strong bond between the kaolin particles induced by the cationic polyacrylamide and is consistent with observations made in previous studies (Kim and Palomino 2009). The D_{90} values for FCR suspensions in the dispersant solution and distilled water decrease over time due to deflocculation during the test period. Deflocculation in these cases is most likely attributed to the fluid turbulence caused by the PSA stirrer and pump (Figure 4-8).
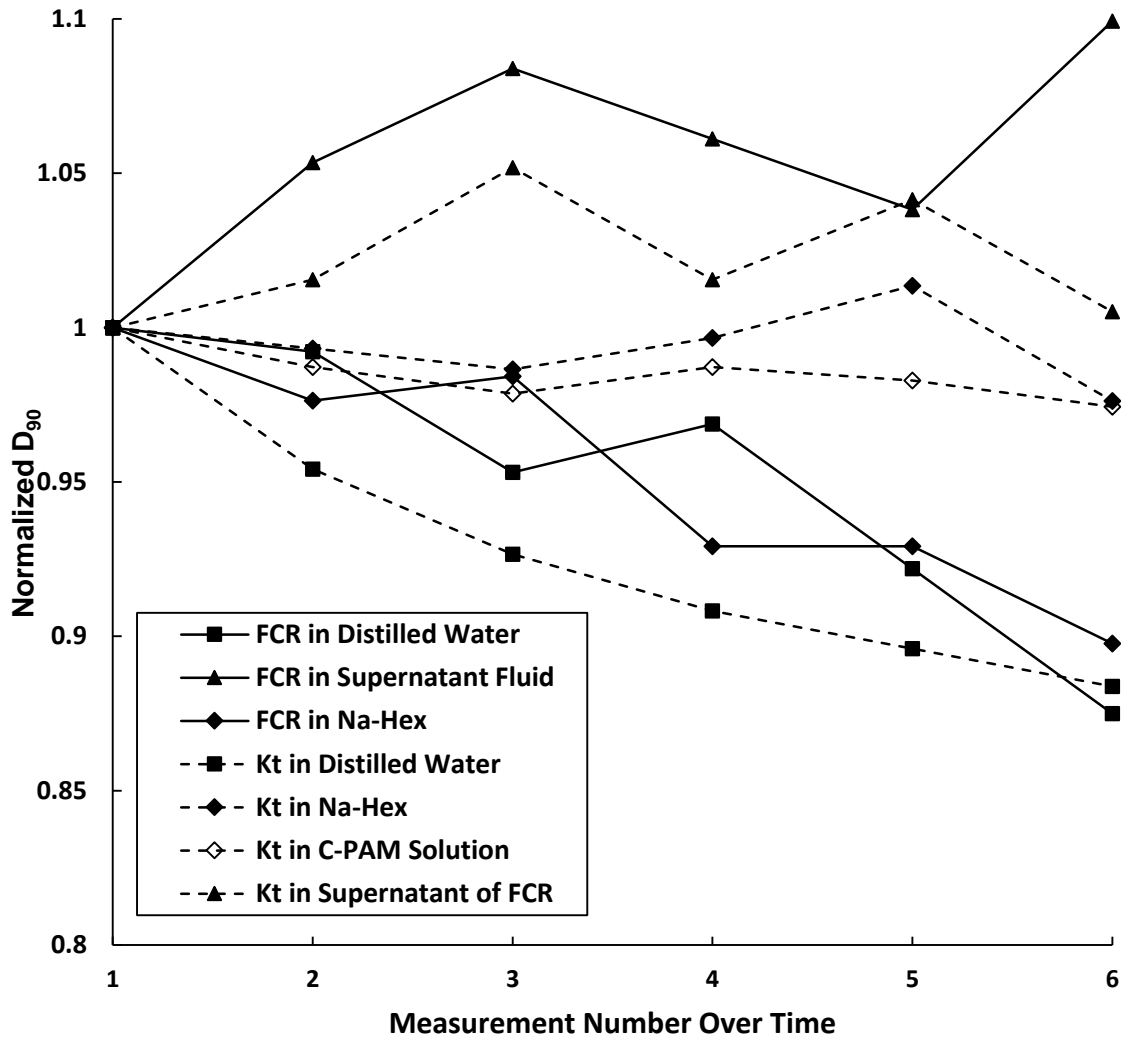
Figure 4-10. D$_{90}$ values normalized with respect to the D$_{90}$ at measurement #1 for FCR and kaolin in different background solutions obtained using the PSA method.

Figure 4-11 shows the frequency of volume density with particle size for FCR in different background solutions for measurement #1 and measurement #6 for each case (left Y-axis). The change in volume density from measurement #1 to measurement #6 for each case is also shown (right Y-axis). A positive change in volume density from measurement #1 to #6 denotes an increase in the number of particles within a given size range (flocculation), while a negative change denotes a decrease of particles within a given size range (deflocculation).

For the FCR in the supernatant fluid, the change in volume density is greater than zero for the size range of 120 μm to 500 μm, indicating flocculation has occurred from measurements #1 to #6. Deflocculation is evident in the size range 3 μm to 120 μm. This shift in grain/floc size distribution occurs only for particle sizes greater than the D_{50} values, which is consistent with the absence of variation in D_{10} and D_{50} values from measurement #1 to #6.

A similar analysis was conducted on kaolin suspensions in different background solutions (flocculant, distilled water, and dispersant). Figure 4-12 shows the frequency of volume density with particle size for kaolin for measurement #1 and measurement #6 for each background solution (left Y-axis). The change in volume density from measurement #1 to measurement #6 for each case is also shown (right Y-axis). When kaolin is mixed with the flocculant (C-PAM) solution, flocs form in the size range of 86 μm to 310 μm (average D_{90} value of 6 measurements is 230 μm). This indicates that the particles form flocs with a wide range of sizes. In distilled water, the flocculation takes place in a narrower particle size range of 1 μm to ~10 μm. The kaolin particles do not flocculate in the dispersant solution (Na-Hex) as indicated by the zero change in volume density across the measured particle size range.
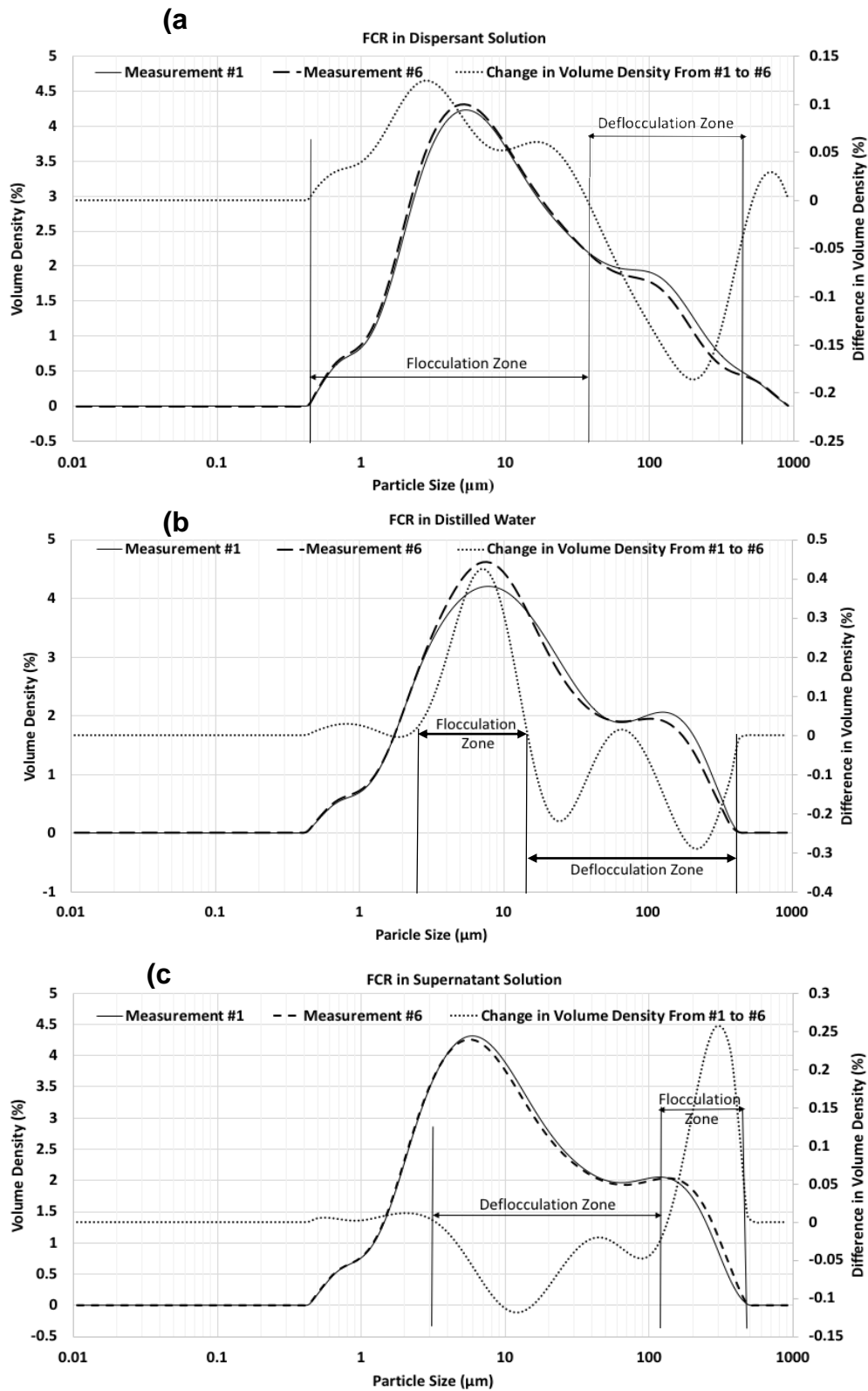
Figure 4-11. Particle size volume density (left axis) and difference in right Particle size volume density (left axis) for laser diffraction measurements #1 and #6 for (a) dispersant solution, (b) distilled water, and (c) supernatant solution.
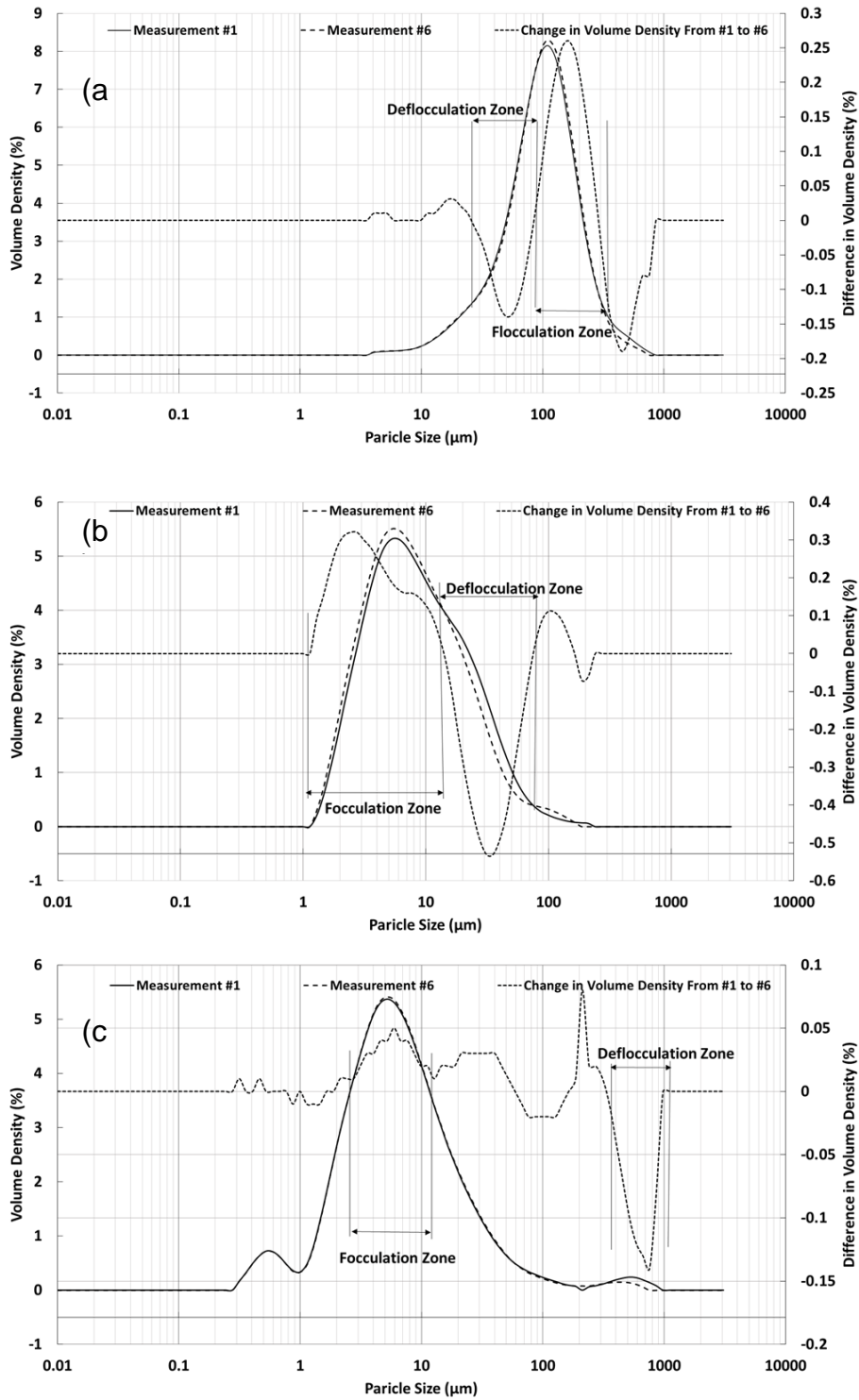
Figure 4-12. Particle size volume density (left axis) and difference in volume density (right axis) for PSA measurements #1 and #6 for (a) flocculant solution (C-PAM), (b) distilled water, and (c) dispersant solution (Na-Hex).

A summary of the D_{90}, D_{50}, and D_{10} obtained using the PSA method and traditional hydrometer analysis is given in Table 4-2.

Figure 4-13 shows grain size distribution curves of both hydrometer and laser diffraction methods in a single plot. For the laser diffraction method (PSA), the average values of D_{10} to D_{100} for six measurements are obtained from the software output of the PSA. Since the standard deviation of the measurements were in range of 4.2 to 5.5 for FCR samples and 0.3 to 1.9 for kaolin samples, the average values are a reasonable representative of particle size measured by the PSA method. The shape of the GSD curves derived from the PSA measurements are smoother, which can be attributed to the ability of PSA to capture any and all grain sizes (continuous measurements) whereas the hydrometer method only captures a selection of particle sizes (discrete measurements).

According to Figure 4-13 and Figure 4-14, in most cases the GSD curves shift to larger particle size ranges when measuring with the PSA compared to hydrometer-based measurements for the same suspensions. This is likely due to the presence of flocs detected by the PSA (and not by the hydrometer). For the kaolin suspensions, all of the D_{90} values measured by the PSA are larger than ones measured by the hydrometer method. This indicates that the kaolin suspensions have at least some flocculation and are not completely dispersed as typically assumed in hydrometer analysis.

The circled data in Figure 4-13 highlight examples of plateaus in the hydrometer data. Plateaus indicate time periods in which the material may flocculate or defloculate during the course of the analysis. Whether the particles flocculate or defloculate is impossible to detect during the hydrometer analysis. However, changes in particle associations can be inferred using PSA analysis (Figures 4-11 and 4-12), where changes can be seen in real time.

Flocculant aging may be observed using laser diffraction analysis by comparing individual apparent grain/floc sizes of the in situ material in distilled water (floc structure maintained) with the same in situ material mixed with a dispersant solution (floc structure decomposed to individual particles). The variation of D_{90} values (ΔD_{90}, Equation 3-2) is the difference in the D_{90} value of in situ material in distilled water and the in situ material in the sodium hexametaphosphate solution (dispersant agent) which is normalized with respect to values in distilled water. As ΔD_{90} decreases, the apparent grain size of the in situ material approaches that of the dispersed material. In other words, as $\Delta D_{90} \rightarrow 0$, the particles of the in situ material (in distilled water) are individual grains rather than flocs. According to Figure 4-15, the in situ material becomes more dispersed with depth, which in this case may be considered a proxy for increasing flocculant age.

$$\Delta D_{90} = \frac{(D_{90})_{DW} - (D_{90})_{NaHex}}{(D_{90})_{DW}} \times 100\% \qquad\qquad\qquad \textbf{Equation 3-2}$$

Table 4-2. Values of D_{10}, D_{50} and D_{90} for PSA and hydrometer analysis in different background solutions.

Background Solution	Measurement Method	FCR			Kaolin		
		D_{90} (μm)	D_{50} (μm)	D_{10} (μm)	D_{90} (μm)	D_{50} (μm)	D_{10} (μm)
Dispersant	PSA*	121	3.83	2.02	27.2	6.39	1.96
	Hydrometer	130	3.5	0.23	9.8	2.4	-
Distilled Water	PSA*	122	11.2	2.31	30.4	8.11	2.84
	Hydrometer	150	6.3	0.9	11	1.8	-
Supernatant or C-PAM	PSA*	138	10.7	2.17	230	107	36.7
	Hydrometer	151	20	10	16	14	10

*Values obtained using PSA are the average of 6 measurements of the same suspension
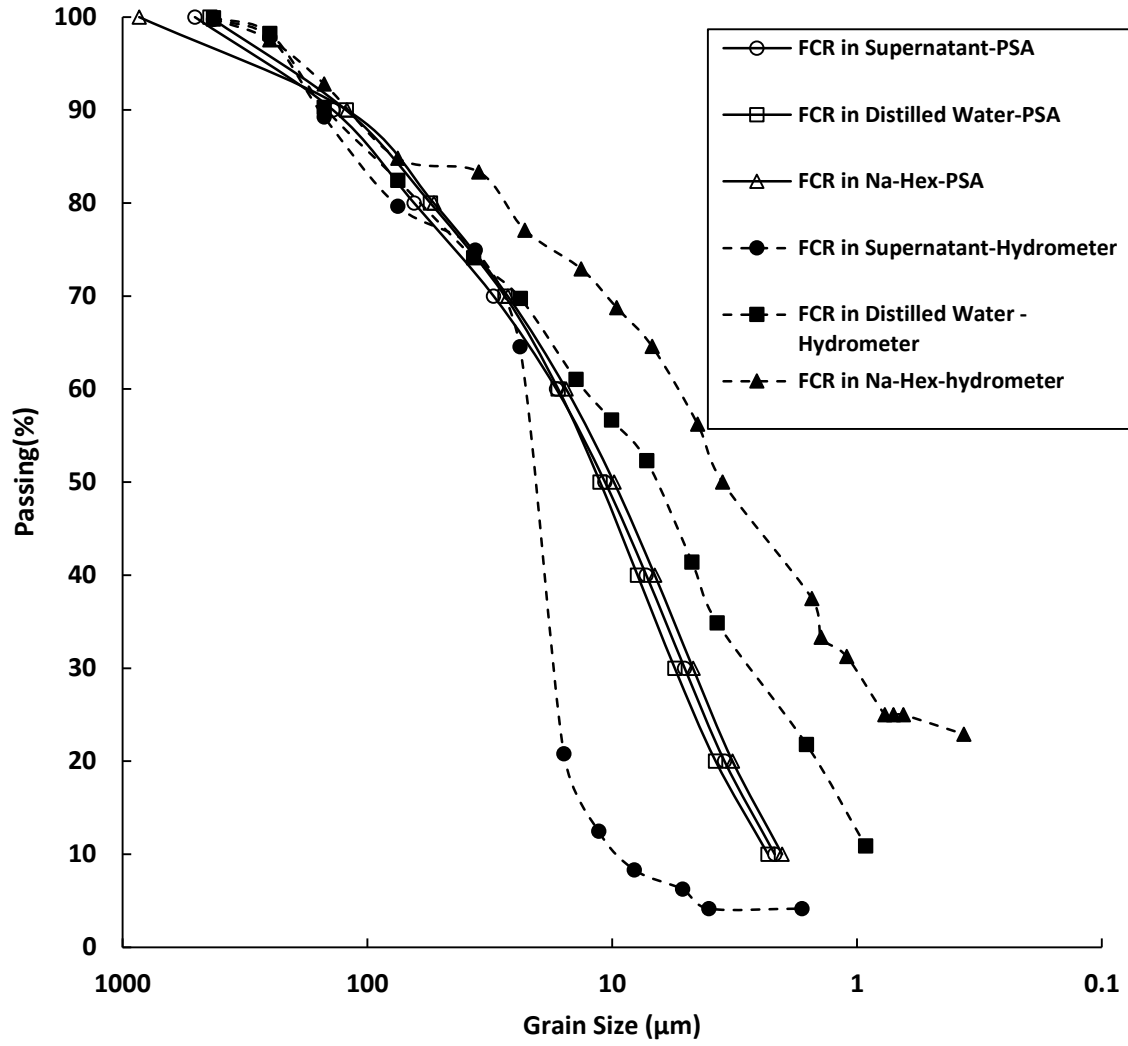
Figure 4-13. GSD of FCR measured by two different methods in different background solutions.
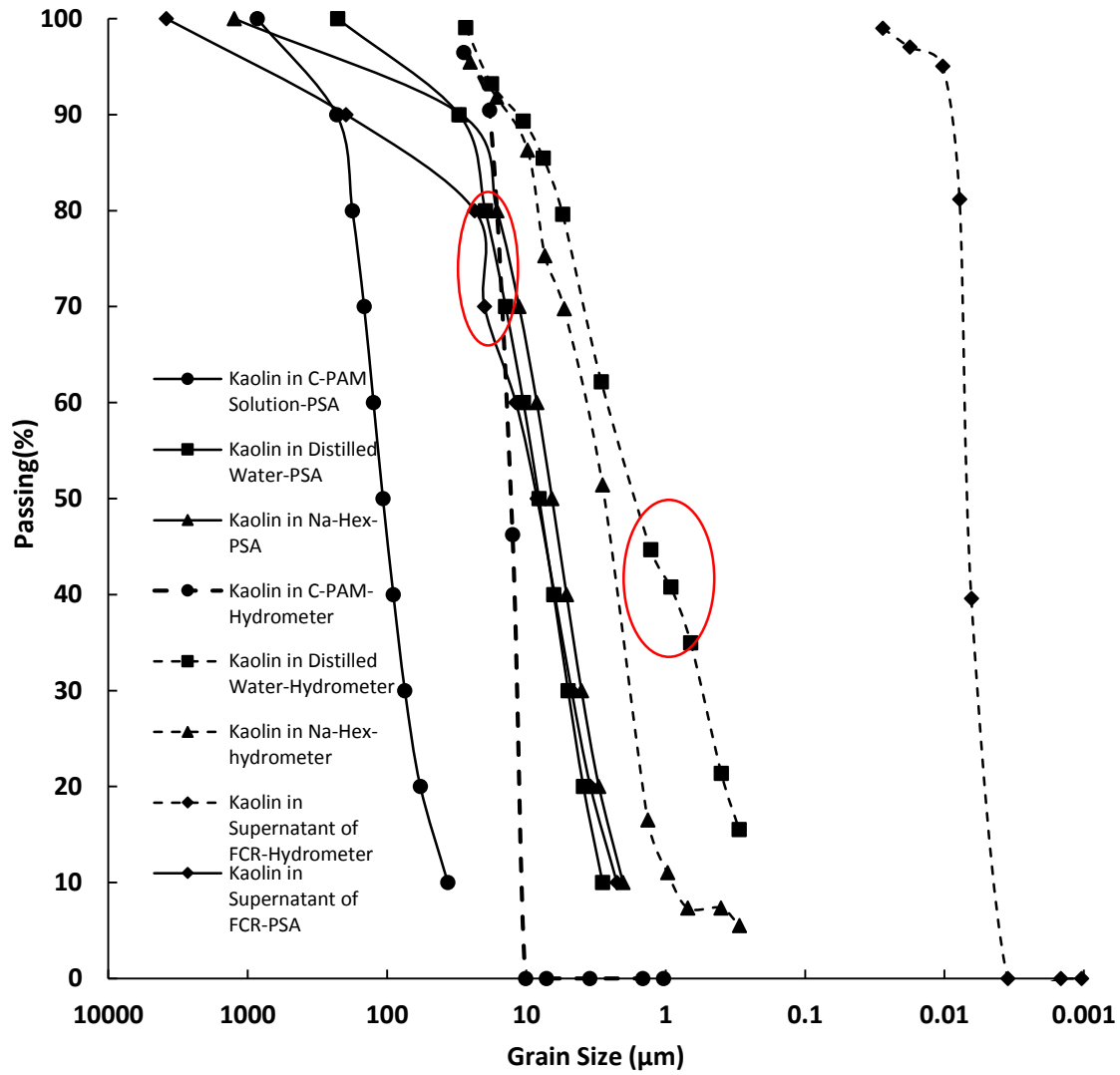
Figure 4-14. GSD of Kaolin measured by two different methods in different background solutions.
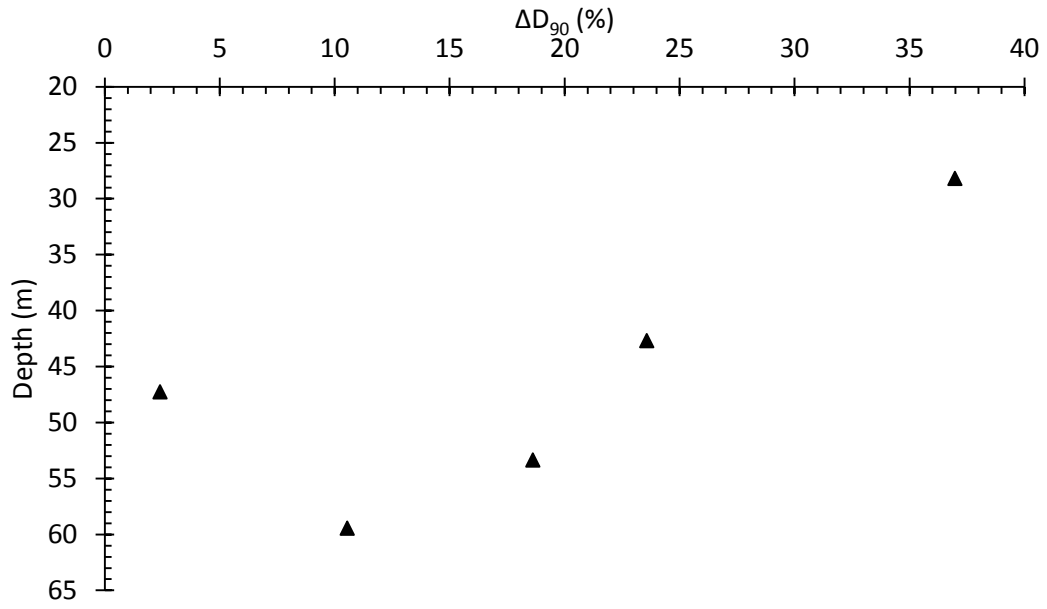
Figure 4-15. D$_{90}$ with depth as an indication of floc degradation with age.

4.4.3 RHEOLOGICAL BEHAVIOR

Solid particle suspensions may exhibit a wide range of rheological responses. The response depends on the particle size and shape, solids content, particle interactions in the surrounding fluid, fluid viscosity, and inter-particle forces, and colloidal suspensions often exhibit Bingham plastic flow (van Olphen, 1977). Coal slurries with high particle concentrations dispersed in water have been observed to follow the Bingham plastic behavior model (Hunter, 2001) as well as the Ostwald-de Waele (power law) model (Singh et al. 2016). For this study, the viscosity measurements at 1 minute for given spindle rotational speeds for FCR suspensions with different background solutions were converted into shear stress-shear rate profiles (following AMETEK Brookfield (2017)) and compared using three flow models: Bingham model, power law model, and Casson model. The Bingham model is expressed as (Hunter, 2001):

$$S = S_B + \eta_{PL}\dot{\gamma} \qquad \textbf{Equation 3-3}$$

where S is the shear stress, S_B is the Bingham yield value, η_{PL} is the plastic viscosity, and $\dot{\gamma}$ is the shear rate.

The power law model is (Hunter, 2001):

$$S = K\dot{\gamma}^n \qquad \textbf{Equation 3-4}$$

where S is the shear stress, K is the consistency coefficient, $\dot{\gamma}$ is the shear rate, and n is the flow behavior index indicating the proximity to Newtonian behavior. The consistency coefficient is equal to the fluid viscosity, η, and $n = 1$ for Newtonian fluids. Shear-thinning fluids have $n < 1$ and shear-thickening fluids have $n > 1$ (Rao, 2014).

The Casson model can be expressed as (Rao, 2014):

$$S^{0.5} = K_{0c} + K_c(\dot{\gamma})^{0.5} \qquad \textbf{Equation 3-5}$$

where S is the shear stress, $\dot{\gamma}$ is the shear rate, and K_{0c} and K_c are the intercept and slope, respectively, of the line resulting from the plot of the square root of shear stress versus the square root of shear rate. This model was developed to describe the rheological behavior of printing inks, but has been used extensively for food dispersions such as chocolate (Rao, 2014).

The rheological profiles for FCR suspensions in distilled water, supernatant solution, and dispersant solution presented according to the flow models of Equations 3-3 through 3-5 are shown in Figure 4-16. The solids content was kept constant for all cases shown (solids content = 0.129). The fitting parameters for each model and the corresponding R^2 values are summarized in Table 4-3.

Table 4-3. Fitting Parameters and R^2 Values of the Rheological Models

Background Solution	Newtonian/Bingham			Power Law			Casson		
	S_B dynes/cm^2	η_{PL} poise	R^2	K poise	n	R^2	K_{0c} (dynes/cm^2)$^{0.5}$	K_c (poise)$^{0.5}$	R^2
Distilled Water	0.2174	0.0132	0.99	0.1650	0.341	0.997	0.3471	0.0784	**0.987**
Supernatant	0.1770	0.0070	**0.71**	0.1676	0.176	0.618	0.3799	0.0383	0.684
Dispersant	0.0078	0.0086	**0.96**	0.0173	0.717	0.939	0.0508	0.0801	0.948
As-received	0	0.0060	0.96	0.0032	1.206	**0.983**	0	0.0730	0.946

Note: Largest R^2 values for each background solution are in bold.
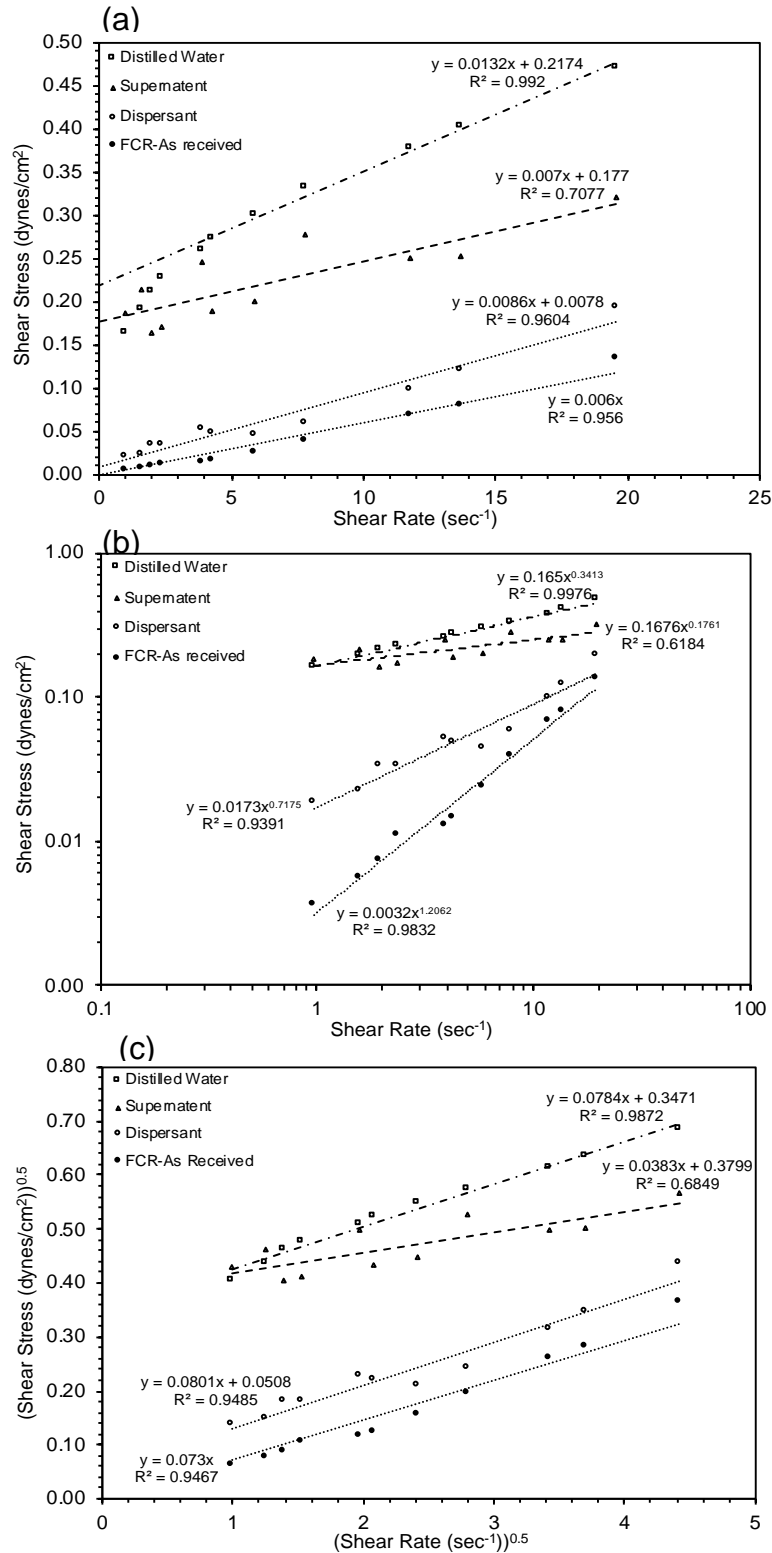
Figure 4-16. Rheological profiles of FCR suspensions with different background solutions with corresponding flow models (a) Newtonian/Bingham plastic model, (b) power law model, and (c) Casson model. The solids content for all cases is 0.129.

The following observations can be made based on Figure 4-16 and Table 4-3:

- The background solution chemistry has an observable influence on the rheological response of the FCR suspension.

- For all tested cases, shear resistance (measured shear stress) across the range of applied shear rates was greatest for the distilled water case, followed by the supernatant, dispersant, and the as-received slurry.

- The as-received FCR slurry behaves as a near-Newtonian fluid (Figure 4-16a). This is consistent with a suspension in which little flocculation has taken place (van Olphen, 1977).

- According to the Bingham model (Figure 4-16-a), the behavior of the distilled water suspension is consistent with a non-ideal plastic behavior. The supernatant and dispersant cases are consistent with ideal plastic behavior (Figure 4-16a).

- According to the power model (Figure 4-16-b), the FCR in distilled water and supernatant background solutions are shear thinning ($n < 1$). This is consistent with a suspension that has at least some flocculation at low shear rates, and deflocculation occurs as the applied shear rate increases (Hunter 2001; van Olphen 1977).

4.5 DISCUSSION

4.5.1 HYDROMETER AND LASER DIFFRACTION ANALYSIS (PSA)

The influence of background solution on particle interactions (fabric) in FCR and kaolin was directly observed through scanning electron microscopy (Figure 4-17). FCR particles form denser aggregates in as-received supernatant solution (Figure 4-17b) compared to the distilled water case.
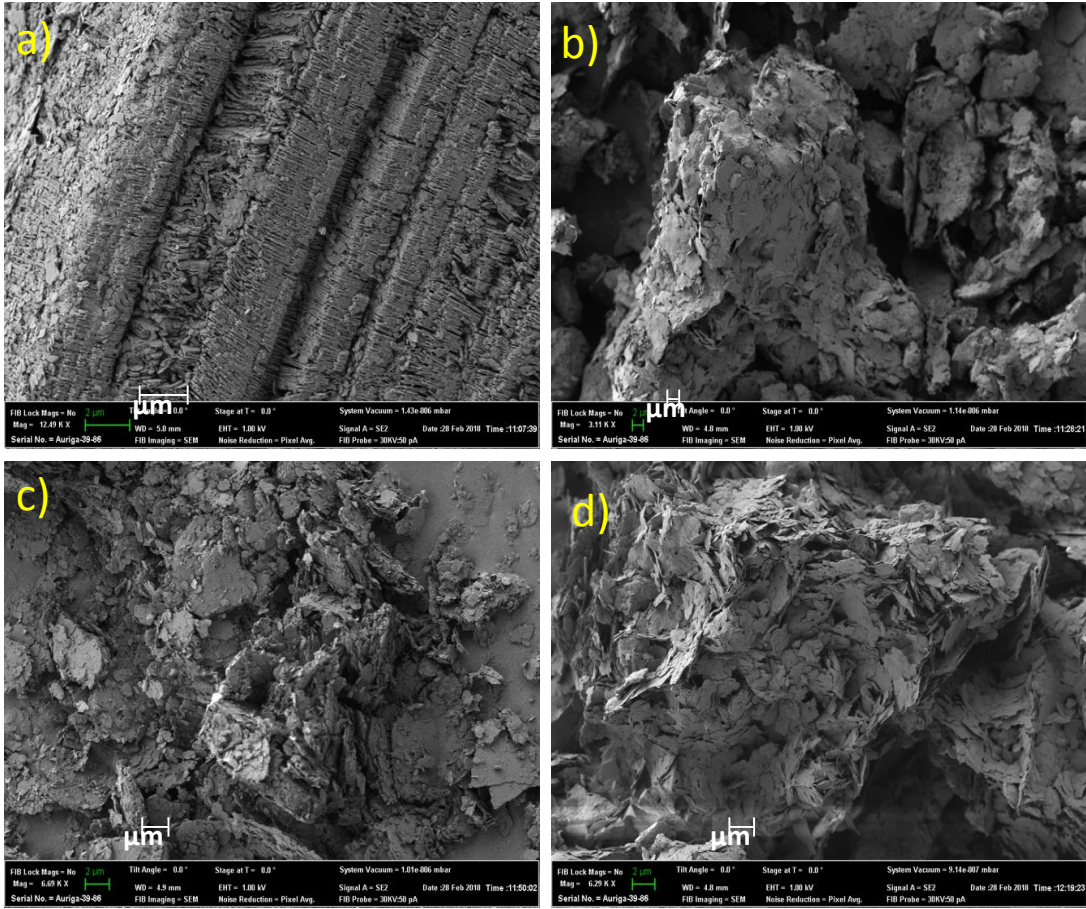
Figure 4-17. SEM images of kaolin and FCR in different background solutions: (a) kaolin in flocculant (C-PAM) solution (40 mg/L), (b) FCR in supernatant solution, (c) kaolin in distilled water, (d) FCR in distilled water.

The distribution curves obtained using hydrometer analysis of FCR suggest the particle size distribution changes over the duration of each test (Figure 4-5b). The curve for FCR in the sodium hexametaphosphate solution shows two measurement plateaus, one at ~82 % passing and one at ~25 % passing. These plateaus are indicative of an increase in the percentage of finer particles over time (i.e. deflocculation). For the FCR in the background solution of supernatant fluid, a significant drop in percent passing from ~65 % to ~21 % may be the result of a significant increase in the percentage of larger particle sizes, which indicates flocculation is likely occurring between these measurement times. Thus, the effective size distribution of the FCR material does not remain constant through the duration of the test, a break of a fundamental assumption for hydrometer analysis (i.e. that the grain sizes remain constant throughout the test). Therefore, hydrometer analysis is not applicable for FCR suspensions if floc stability is in question.

From Table 4-2, the difference between D_{90} values of flocculated and dispersed structures of FCR in the PSA method is 17 μm, while the difference between D_{90} values of flocculated and dispersed structures of kaolin is about 203 μm. This implies the greater influence of C-PAM compared to the flocculant present in the supernatant water of the FCR. The strong interaction between C-PAM and the kaolin particles is consistent with previous studies (Kim and Palomino 2009). The flocculant-induced kaolin particle interactions result in face-to-face aggregates forming higher order structures as evidenced by the observed suspension sedimentation mode (Palomino and Santamarina 2005).

For the kaolin in the C-PAM solution (Figure 4-5a) the hydrometer results show that 100% of particles are finer than 30 μm, and the D_{90} value is ~16 μm. The laser diffraction method results (Figure 4-6a) indicate a relatively high value of D_{90} (~230 μm), which is about 14 times greater than the hydrometer value. This difference may be attributed to the inability of the hydrometer method to accurately detect flocs. The reason for this difference can be related to the mechanism of flocculation of kaolin and the deficiency of the hydrometer method with respect to floc detection. Note that the kaolin-C-PAM flocs are large enough to be observable by eye (Figure 4-4).

Unlike the kaolin in C-PAM solution, the results of hydrometer analysis of kaolin in distilled water and dispersant solutions are relatively consistent with the laser diffraction method. The D_{90} values of kaolin in distilled water and dispersant solutions obtained from hydrometer tests were 11 μm and 9.8 μm, respectively, while the laser diffraction method resulted in values of 30.4 μm and 27.2μm for the distilled water and dispersant cases, respectively.

As shown in Figure 4-6, the flocculant/supernatant water suspension has higher D_{90} values in comparison with FCR in distilled water and the dispersant solution. This relationship suggests the flocculant in the supernatant water causes an increase in floc size, and hence an increase in the D_{90} value over time. For the FCR samples in distilled water and the dispersant solution, the value of D_{90} decreases with time. The decrease of D_{90} in distilled water and dispersant (Na-Hex) solution may be a result of applied energy

74

by stirrer. This trend is consistent with deflocculation, likely due to the decrease in flocculant concentration in the distilled water case and the presence of the deflocculating agent in the dispersant solution (Na-Hex) case.

From Table 4-2, the D_{90} values for FCR obtained from the PSA method are smaller than values of D_{90} obtained from the hydrometer method. This difference is likely due to the transformation of the suspended material during the course of the hydrometer analysis as well as some influence from sampling bias (difference between the larger sample size for hydrometer and smaller sample size for PSA).

Based on measurements made using the PSA method, the D_{90} for each suspension either increased or decreased over the six consecutive measurements of the same sample. Yet, the values of D_{10} and D_{50} for the same suspensions did not show any significant change (measurements not shown here).

4.5.2 RHEOLOGICAL BEHAVIOR

Based on what is known regarding the rheological behavior of colloidal suspensions, two hypotheses were developed for this study. Hypothesis 1 (H1) was that the relative shear stresses would increase with background solution in the following order: dispersant solution, distilled water, and supernatant solution. Hypothesis 2 (H2) was that the flow behavior of FCR suspensions can be predicted by either the Newtonian or Bingham plastic flow models.

H1. Flocculated suspensions have higher resistance to shear (higher shear stress) compared to dispersed suspensions at the same solids content and tend to exhibit shear thinning behavior (Hunter 2001). Yet, the suspension with the highest shear stresses measured across the applied shear rate was for the distilled water case, followed by the supernatant solution, dispersant, and as-received material. Thus, the distilled water case appears to have the most flocculation.

H2. While the as-received FCR slurry follows a near-Newtonian flow model, the remaining suspensions may be predicted using either the Bingham plastic model or the power law model; the differences between the two models for the measured suspensions were not significant.

Based on both the particle size analyses and rheological testing, the background solution composition has a significant influence on the formation of flocs in FCR suspensions. The particle associations and presence of a flocculant have significant impact on the meso-scale properties of FCR, such as consolidation behavior and flow potential. For example, the presence of a flocculant may inhibit flow potential.

4.6 CONCLUSIONS

A series of grain size distribution measurements using traditional hydrometer tests and laser diffraction analysis were performed on fine coal refuse and kaolin suspensions to investigate the capability

of each method for capturing the effective grain size distribution as a function of background chemistry. The results show that (1) the background solution chemistry influences the FCR floc stability and alters the grain size distribution over time and (2) the D_{90}, D_{50}, and D_{10} values obtained from the two methods are not in agreement, with larger D_{90} values reported from hydrometer analysis. The differences between the values obtained highlight one important limitaion of hydrometer analysis, which is the assumption the effective grain size distribution remains constant with time. If grain size changes during the hydrometer analysis, the initial readings represent a different sample than the final readings and may not be comparable. In other words, the hydrometer test may not accurately measure effective grain size distribution over the measurement period.

Laser diffraction offers several advantages over hydrometer analysis including a short measurement period, small sample size requirement, and the ability to measure a wide range of particle sizes in the same analysis. This study highlights another advantage of the PSA method, the ability to accurately measure changes in particle size over time within the same sample. The ability to capture real-time flocculation or deflocculation means this technique can be applied to grain size distribution studies of FCR slurries, and other comparable materials, in their as-placed condition without any pretreatment. This method has the ability to capture dynamic particle interactions over the time.

Based on the particle size analyses, the background solution composition has a significant influence on the formation of flocs in FCR suspensions and thus the effective grain size distribution. However, the effective grain size distribution may also change over time even for the same background solution. These findings are relevant to the overall stability of FCR in impoundments in that particle associations and the presence of a flocculant have a significant impact on the macro-scale properties of FCR, such as consolidation behavior and flow potential.

Three flow models were selected to identify the best fit for predicting the flow behavior of FCR suspensions and identify the presence of flocs: Newtonian/Bingham plastic model, power law model, and the Casson model. The models that best describe the FCR suspensions tested for this study are the (near) Newtonian/Bingham plastic model, with both ideal and non-ideal behavior, and the power law model. Within each model, flocculation was evident in the distilled water and supernatant cases, while very little to no flocculation was observed for the dispersant and as-received suspensions. Note that the as-received material contains a flocculant in the supernatant. Yet, the influence of the flocculant on viscosity was not significantly different than the distilled water case.

4.7 ACKNOWLEDGEMENTS

4.8 REFERENCES

ASTM-D422 2007, "Standard Test Method for Particle-Size Analysis of Soils." American Society for Testing Materials: 1-8.

Atesok, G., Boylu, F., Sirkeci, A. A. and Dincer, H. 2002, "The Effect of Coal Properties on the Viscosity of Coal-Water Slurries." Fuel 81(14): 1855-1858.

Beuselinck, L., Govers, G., Poesen, J., Degraer, G. and Froyen, L. 1998, "Grain Size Analysis by laser diffractometry Comparison with the sieve pipette method.pdf." CATENA 32(3-4): 193-208.

Boylu, F., Dicer, H. and Atesok, G. 2004, "Effect of coal particle size distribution, volume fraction and rank on the rheology of coal–water slurries." J. Fuel processing technology 85: 241-250.

Day, P. R. 1965, "Particle fractionation and particle-size analysis. In Methods of Soil Analysis." American Society of Agronomy: 545-567.

Fidleris, V. and Whitamore, R. L. 1961, "The Physical Interaction of Spherical Particles in Suspension." Rheologica Acta 1(4-6): 573-580.

Goodarzi, F. and Murchison, D. G. 1973, "Oxidized vitrinites — their aromaticity, optical properties and possible detection." Fuel 52(2): 90-92.

Hergert, W. and Wriedt, T. 2012, "The Mie Theory: Basics and Applications". New York, Springer.

Huang, S. Y., Lipp, D. W. and Farinato, R. S. 2001. "Acrylamide Polymers". Kirk-Othmer Encyclopedia of Chemical Technology, John Wiley & Sons: 304-342.

Imai, G. 1980, "Settling behavior of clay suspension", Soils and Foundations." Soils and Foundations 20: 61-77.

Irani, R. R. and Callis, C. F. 1963, "Particle size: measurement, interpretation, and application". New York, John Wiley.

Jedari, C., Palomino, A. M., Cyr, H. J., Drumm, E. C. and Boles, D. 2017," Grain and Floc Size Distribution Analysis of Fine Coal Refuse Slurry". Proceeding of 19th International Conference on Soil Mechanics and Geotechnical Engineering, Seoul, Korea, ISSMGE.

Jedari, C., Palomino, A. M. and Drumm, E. C. 2018," Compressibility of Fine Coal Refuse". International Foundations Congress and Equipment Expo, Orlando, FL, ASCE.

Kim, S. and Palomino, A. M. 2009, "Polyacrylamide-treated kaolin: A fabric study." Applied Clay Science 45(4): 270-279.

Lambe, T. W. and Whitman, R. V. 1969, "Soil Mechanics". New York, John Wiley & Sons.

Logos, C. and Nguyen, Q. D. 1996, "Effect of particle size on the flow properties of a South Australian coal-water slurry." Powder Technology 88(1): 55-58.

Michaels, A. S. and Bolger, J. C. 1962, "Settling rates and sediment volumes of flocculated kaolin suspensions." Industrial and Engineering Chemistry Fundamentals 1: 24-33.

Mitchell, J. K. and Soga, K. 2005, "Fundamentals of Soil Behavior", Wiley.

Murthy, V. N. S. 2002, "Geotechnical engineering : principles and practices of soil mechanics and foundation engineering". New York, Marcel Dekker.

Palomino, A. M. and Santamarina, J. C. 2005, "Fabric map for kaolinite: effects of pH and ionic concentration on behavior." Clays and Clay Minerals 53: 211-223.

Pierre, A. C. and Ma, K. 1999, "DLVO theory and clay aggregate architectures formed with $AlCl_3$." Journal of the European Ceramic Society 19: 1615-1622.

Pierre, A. C., Ma, K. and Barker, C. 1995, "Structure of kaolinite flocs formed in an aqueous medium." Materials Science 30: 2176-2181.

Singh, M.K., Ratha, D., Kumar, S., Kumar, D., 2016. Influence of Particle-Size Distribution and Temperature on Rheological Behavior of Coal Slurry. International Journal of Coal Preparation and Utilization 36, 44-54.

Storti, F. and Balsamo, F. 2010, "Particle size distributions by laser diffraction: sensitivity of granular matter strength to analytical operating procedures." Solid Earth 1(1): 25-48.

Syvitski, J. P. M. and Hein, F. J. 1991, Sedimentology of an arctic basin:Itirbilung Fiord, baffin Island, Northwest teritories, Canada". Canada, Geological survey of Canada.

van Olphen, H. 1977, "An Introduction to Clay Colloid Chemistry". Malabar, Florida, USA, Krieger Publishing Company.

CHAPTER V
TIME RATE OF CONSOLIDATION OF SLURRY-PLACED COAL FINE REFUSE AND DETERMINATION OF APPROPRIATE COEFFICIENT OF CONSOLIDATION

5.1 ABSTRACT

In traditional soil mechanics, the Terzaghi consolidation theory assumes that there will be small strains in the soil due to the applied overburden pressure, and the permeability and thus coefficient of consolidation remain constant during consolidation. While these assumptions may be valid for the consolidation of soft solid soils, in hydraulically placed slurry materials with low solids content such as fine coal refuse, the strains may not be small. Thus, the coefficient of consolidation will likely vary as the material transitions from a fluid to a solid. In this study, the consolidation of fine coal refuse was investigated based on in situ sampling and laboratory measurements of the coefficient of consolidation from both solid and liquid slurry samples. These data are used to predict the time rate of consolidation using classical Terzaghi theory, a finite strain method, and a new method employing a spatial and temporal variable coefficient of consolidation. The results suggest that while the variable coefficient of consolidation method may best reflect the low degree of consolidation at early times when the material is still essentially slurry, a similar response can be obtained using the Terzaghi method with constant value of coefficient of consolidation obtained from measurements of the slurry consolidation at low stress levels. The low value of coefficient of consolidation has little effect on the degree of consolidation at large times due to the nature of the governing differential equation. The consolidation response of hydraulically placed slurry at early times is most important with respect to construction staging and personnel safety.

5.2 INTRODUCTION

Consolidation is the volume change process that takes place in saturated soils as excess pore water pressure dissipates and the external stress is transferred to the particle skeleton. Terzaghi's one dimensional consolidation theory (Terzaghi, 1943) assumes the compressible soil layer is homogenous and fully saturated, and the settlement is assumed to be very small relative to the thickness of the soil layer (infinitesimal strain theory) (Holtz et al., 2011; Schiffman, 1982). Under these assumptions the length of the drainage path remains constant during the consolidation process. It is also assumed that Darcy's coefficient of permeability (k) and consequently the coefficient of consolidation (C_v) remain constant, where

$$C_v \frac{\partial^2 u}{\partial z^2} = \frac{\partial u}{\partial t}$$

Equation 5-1

u: Excess pore water pressure

z: space or depth variable in the soil element

t: time

$C_v = Coefficient\ of\ consolidation$

The coefficient of vertical consolidation (C_v), is the most significant property which affects the

time for consolidation and governs the consolidation process, yet selecting a value of C_v can be difficult (Duncan, 1993). The C_v value may vary substantially in the ground, even in a uniform soil layer (Chang, 1985). The assumption of a constant C_v is generally accepted in spite of common laboratory observations of C_v varying during consolidation testing as the level of stress increases (Duncan, 1993; Elkateb, 2017).

The assumptions of infinitesimal strain and constant C_v may be appropriate for the consolidation of soil deposits. However, the consolidation process for hydraulically placed slurry materials with low solids content, as is the case of impounded fine coal refuse or fly ash, may not be consistent with these assumptions. In addition, Terzaghi's 1-D theory may not be applicable in these cases since the slurry experiences large strains (Schiffman and Cargill, 1981).

Finite strain formulations have been used to calculate the time rate of consolidation in very soft soils where the amount of settlement is significant relative to the layer thickness. Gibson (1958) studied the consolidation progress in a clay layer with increasing thickness with time due to solids deposition. He assumed that the length of the drainage path is not constant during consolidation due to the moving boundary, resulting in a change in C_v, Therefore, an exact solution is difficult to obtain for this case. Cargill (1984) used a finite strain theory of consolidation to predict the time rate consolidation of very soft soils by developing charts based on the dimensionless solution of the Terzaghi consolidation equation (Equation 5-1). The solution considers nonlinear soil properties and accounts for finite strains. Schiffman and Cargill (1981) presented a comparison between a Terzaghi theory and finite strain theory. They showed that for sedimentation of a marine deposit, the finite strain approach leads to shorter consolidation times and lower excess pore water pressures compared to the conventional (linear infinitesimal strain) theory.

The consolidation behavior of soft sedimentary materials such as marine sediments and debris-flow deposits has been studied by different researchers (Bitzer, 1996; Bryant et al., 1975; Karig and Ask, 2003; Major, 2000). Bitzer (1996) developed a mathematical model based on the Terzaghi consolidation equation to calculate fluid flow during the consolidation process and the variation of porosity as a function of change in pore water pressure. They assumed that the permeability, along with compressibility, of the sediment are reduced during consolidation, and hydraulic diffusivity which is the ratio of hydraulic conductivity (k) to specific storage (Chilingarian et al., 1995) remains approximately constant during the consolidation process. Major (2000) investigated the laboratory consolidation behavior of debris-flow deposits resulting from gravitational loading and concluded that the excess fluid (pore) pressure, which drives transients of pore water pressure and effective stress, builds from the bottom to top rather than from top to bottom (upward rather than downward). He also presented a consolidation analysis and showed that the excess pore water pressure (fluid pressure) does not dissipate substantially even over the lab scale life time of a natural debris flow.

An accurate prediction of the time rate of consolidation is difficult to obtain due to the uncertainty

related to the factors affecting the consolidation process (Duncan, 1993; Hong and Shang, 1998; Zhou et al., 1999). Chang (1985) used a probabilistic analysis to examine the variability of one dimensional consolidation solutions, and calculated the time rate consolidation with both conventional and probabilistic methods. The required time to reach different degrees of consolidation varies by the method used. For higher degree of consolidation, the conventional method results in shorter consolidation times compared to the probabilistic method.

In this chapter, the consolidation time rate of fine coal refuse (FCR) has been investigated using samples of FCR obtained from an active FCR impoundment in eastern Kentucky, USA. FCR is a by-product of the coal mining process, and is usually mixed with water and a flocculant and is hydraulically placed behind impoundments constructed primarily with coarse coal refuse. The flocculant is added to promote rapid settling of the solids once the slurry is placed in the impoundment. There are more than 1170 tailing dams in US, of which ~700 are coal refuse impoundments (U.S Army Corps of Engineers, 2017) with hundreds of these impoundments in the Appalachia region. These on-site impoundments are essentially tall dams (200-800 feet tall) behind which the FCR is allowed to settle and dewater. When the fine refuse slurry is hydraulically discharged from the top of the starter dike, the location and rate at which the particles settle depends on the particle size, with the larger FCR particles settling first, and the finer particles remaining in suspension. The fine refuse then becomes the foundation for the second stage of embankment construction with additional coarse refuse used to construct the next dike followed by an additional stage of slurry placement. Construction continues in this manner to reach the permitted height of impoundment. One of the most critical concerns of impounded mine waste material is the rate at which the FCR consolidates or compresses, and whether or not the materials are prone to destabilization, i.e. flow. Destabilization of the FCR has led to fatalities and environmental disasters.

It is generally assumed that the fine refuse in these impoundments will consolidate over time due to the overburden weight of the materials above, losing some of the fluid-like properties that it possessed when initially placed. This consolidation process decreases the volume of the slurry, as the water is squeezed out, with the water pressure in the pores between solid particles decreasing over time. This consolidation and dissipation in pore pressure is accompanied by an increase in strength. Yet, the consolidation behavior of fine coal slurry has not been fully investigated. There are limited observations of the characteristics of slurry in place and its variation with depth within slurry impoundments (Hegazy et al., 2004; Zeng et al., 1998). Furthermore, there is no generally agreed upon model for the consolidation behavior of these materials, which would define under what conditions they are being consolidated.

In this study, traditional consolidation tests were conducted on in situ FCR samples obtained from a range of depths behind an impoundment. The consolidation response of the in situ samples was compared with companion samples of fresh liquid slurry pre-consolidated to stresses corresponding to the depths of

the recovered in situ samples. To study the consolidation process beginning from the time of placement as slurry to the formation of a particle skeleton similar to that observed in situ, an additional investigation was conducted in slurry columns at low solids content and increasing to higher stresses resulting in a solid state. The results from the above measurements were used to compare the time rate of consolidation using three methods: (1) the traditional Terzaghi 1-D infinitesimal strain method, (2) a finite strain approach (Cargill, 1984), and (3) a new model which incorporates the large variations of the coefficient of consolidation (C_v) that were measured when the samples were consolidated from a slurry. Since the time rate of consolidation depends on the selected value of coefficient of consolidation (C_v), a reasonable value for C_v must be identified to predict a more accurate time for consolidation. In this chapter, the variability of C_v in FCR slurry and its influence on time rate of consolidation is discussed.

5.3 EXPERIMENTAL OBSERVATIONS AND METHODS

5.3.1 OBSERVATIONS OF UNDER-CONSOLIDATED IN SITU SAMPLES OF FCR

Laboratory consolidation testing was carried out as part of the geotechnical investigations of the fine coal refuse impoundment in this study. Eight undisturbed FCR samples were collected from approximate depths of 28, 33, 36, 39, 42, 47, 53 and 59 meters behind an inactive impoundment (eastern Kentucky, USA) to study the consolidation response and time rate of consolidation of solid FCR. The water table was located at a depth of about 17 meters (55 feet). In addition, 8 companion samples were pre-consolidated from fresh FCR slurry to compare the consolidation behavior of in situ and fresh FCR. The fresh FCR slurry was collected from the discharge pipe as it was being placed behind an adjacent active FCR impoundment. The overburden pressure for preparation of samples from the fresh FCR slurry was estimated using the field measured unit weight of the coarse coal refuse overburden (17.3 kN/m³) and the solid FCR (16 kN/m³). The specific gravity of the fresh FCR solids is 2.21.

Figure 5-1 depicts an idealized representation of the FCR impoundment, based on the reported stages of construction from a cross-section drawing of the FCR impoundment. It is assumed that the FCR deposition follows this staging of the impoundment, and the time for consolidation due to the loadings from the stages above of only the 21 m thick layer of FCR behind Stage 1 is determined.
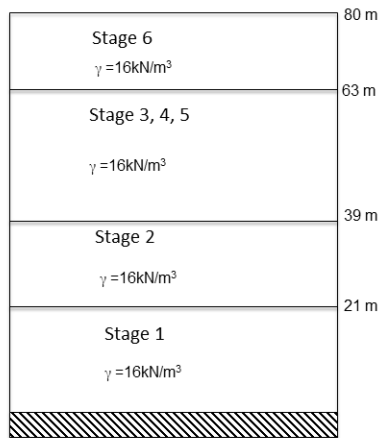
Figure 5-1. FCR deposition stages in the studied impoundment

It also assumed that the consolidation of the Stage 1 FCR is due to a surcharge from Stage 2. The loading sequence consisted of a simultaneous surcharge from Stages 3, 4 and 5 (which have the same crest elevation and hence the same FCR loading) at time = 5 years, and then the surcharge due to Stage 6 applied at time = 10 years was added to the top of existing layers. For this analysis, drainage was limited to the upper free surface providing one-way (or single) drainage (H_{dr} = 21m).

The undisturbed in situ samples were extruded from Shelby tubes obtained from the impoundment, where they had been in place for up to about 40 years. For each in situ sample, a companion fresh slurry sample was prepared in consolidation columns of length ~44 cm and diameter 10 cm. Vertical stresses were applied to the liquid slurry ranging from 365 kPa to 572 kPa, corresponding to the estimated overburden pressures for the companion in situ samples taken from the FCR impoundment.

Specimens for consolidation testing were prepared from both the Shelby tube samples and from the produced slurry samples by trimming with a standard consolidation ring of 65 mm (2.5 inch) diameter and 25 mm (1 inch) height. One dimensional consolidation tests were conducted according to ASTM-D2435/D2435M (2011).

The same loading and reading schedules were used to conduct 1-D consolidation tests on both the fresh slurry samples and the companion in situ samples. . The maximum loading stress was selected to be great enough to surpass the estimated pre-consolidated stress. The results of the consolidation tests of fresh and in situ FCR were compared in terms of pre-consolidation stress.

Figure 5-2 shows the variation of C_v values as a function of depth (equivalent consolidation stress) obtained from consolidation of the pre-consolidated fresh slurry samples and the companion in situ samples.

The C_v values were obtained based on Taylor's t_{90} method, and the reported C_v values for the fresh slurry samples were obtained from the loading at the median stress. The C_v values corresponding to each depth vary significantly for the in situ samples, and are an order of magnitude smaller than the C_v values from the fresh slurry samples.

A summary of the measured pre-consolidation stress from each of the consolidation tests is shown in Table 5-1. The depth for each of the in situ samples and the equivalent depths for each of the companion slurry samples are also shown. The measured pre-consolidation stresses were determined from the resulting consolidation curves according to the Casagrande construction for determining the pre-consolidation stress (Casagrande, 1936).

Figure 5-3 compares the measured pre-consolidation stresses from the in situ samples with that of the fresh slurry samples as a function of depth. It should be noted that the 1-D consolidation tests were conducted on the most competent samples trimmed from extruded Shelby tube samples. The consolidation specimens were selected from the areas in Shelby tube samples which were totally undisturbed and the pre-consolidation stresses shown in Figure 5-3 are maximum values and actual pre-consolidation values would be less than values shown in this Figure.

As shown in Figure 5-3, the fresh slurry samples generally follow the expected increase in pre-consolidation stress with depth (and the pre-consolidation stress is nearly equal to the calculated overburden pressure), and as indicated in Table 5-1, have values of OCR approaching 1 (normally consolidated). However, all of the in situ samples have measured pre-consolidation stresses that are much less than the calculated overburden pressure and have OCR values much less than 1 (ranging from 0.08 to 0.55). This suggests that the in situ samples are still undergoing consolidation, or are under-consolidated. As shown in Figure 5-2, the C_v values for the in situ samples are an order of magnitude smaller than the C_v values from the fresh slurry samples. This is consistent with (Duncan, 1993) who stated that the C_v for a given clay is about an order of magnitude larger at pressures below the pre-consolidation pressure at it is at pressures above the pre-consolidation pressure.

In situ samples — Cv (m2/year)

Fresh FCR samples — Cv (m2/year)
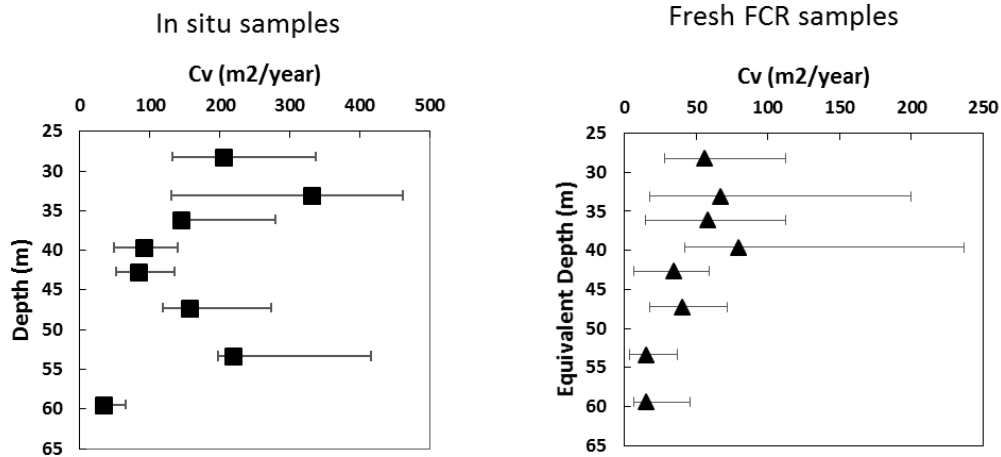
Figure 5-2. Variation of C$_v$ values with depth in fresh FCR and In situ FCR

Table 5-1. Results of Consolidation Tests on In Situ and Fresh FCR Slurry Samples

Sample Type	Depth (of in Situ samples) or Equivalent depth (corresponding to slurry consolidation stress) (m)	Imposed consolidation pressure (for slurry samples) or Calculated Overburden pressure (based on depth for in situ samples) (kPa)	Observed Pre-consolidation pressure (kPa)	Over-consolidation Ratio (OCR)
Fresh Slurry	28	365	360	0.97
In situ			134	0.37
Fresh Slurry	33	393	312	0.79
In situ			216	0.55
Fresh Slurry	36	420	336	0.80
In situ			58	0.14
Fresh Slurry	41	441	384	0.87
In situ			202	0.46
Fresh Slurry	44	462	480	1.04
In situ			38	0.08
Fresh Slurry	47	490	432	0.88
In situ			192	0.39
Fresh Slurry	53	531	490	0.92
In situ			1778	0.33
Fresh Slurry	59	572	495	0.87
In situ			216	0.38
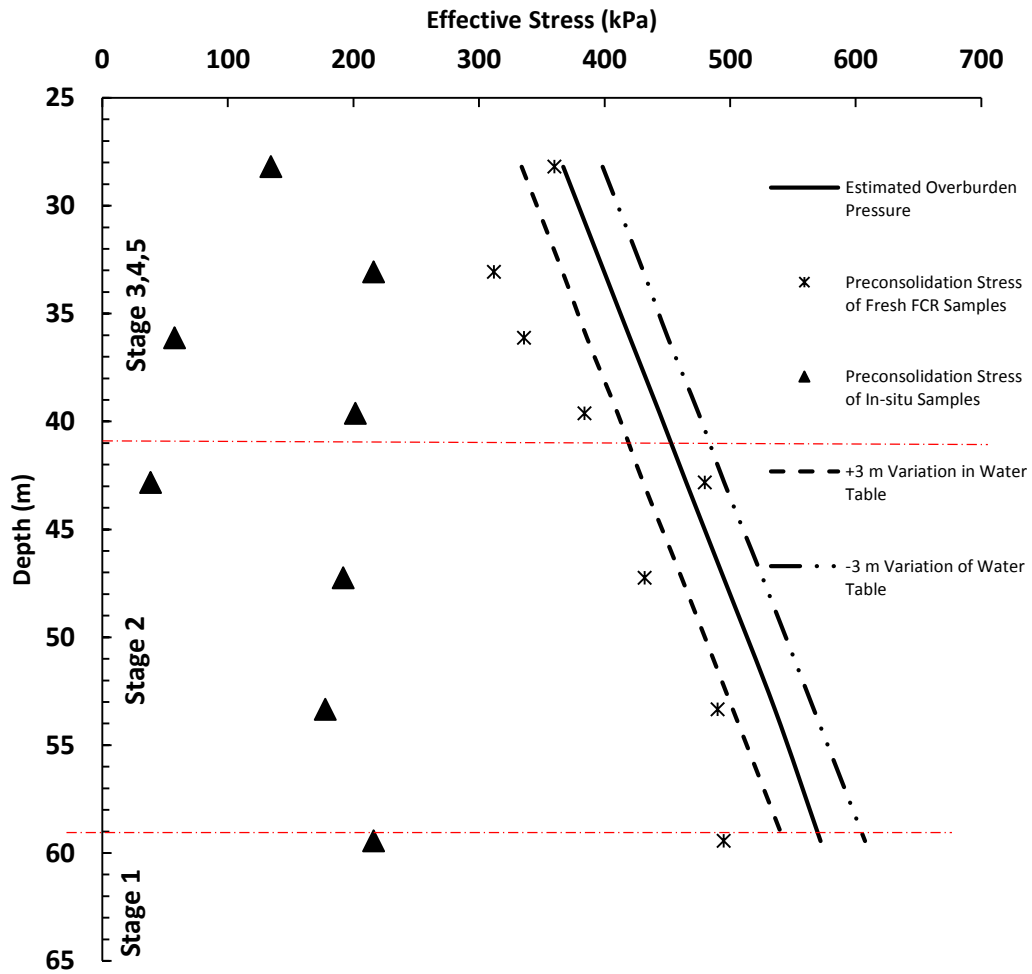
Figure 5-3. Pre-consolidation Stresses of FCR Slurry and In Situ Samples Compared with Effective Overburden Stress. The heights of the various stages of construction are also shown.

The small values of OCR are consistent with the observation of "fluid-like" material in split spoon samples from the same impoundment (Figure 5-4). As shown, there are multiple locations in the impoundment where "fluid-like" material can be seen which further suggests that the consolidation process is still underway even after many decades. This is consistent with study conducted with Zeng et al. (1998) and Zeng and Globe (2008) where they reported observing under-consolidated samples in an old inactive FCR impoundment. . Sangrey et al. (1979) studied under-consolidated sediments from Alaska coastal waters. They sampled continuous cores with the length of up to 8 meters in different areas and performed compression tests on the in situ samples. They reported samples with 10% average degree of consolidation, which had been in place for about 40 years. For most of the collected in situ samples, the OCR was very low and in some cases as low as 0.03-0.09 (Sangrey et al., 1979). Observations of under-consolidated materials consolidating under their self-weight have also been described by Holtz et al. (2011).

Figure 5-4. Observation of "Fluid-Like" material in in situ samples

In traditional geotechnical engineering practice, the mean value of C_v is usually used to predict the consolidation time rates. The value of C_v is a function of k and m_v (Equation 5-2)

$$C_v = \frac{k}{m_v \gamma_w}$$ **Equation 5-2**

in which k= coefficient of permeability, m_v= coefficient of volume compressibility, and γ_w = unit weight of water

As discussed by Duncan (1993), both k and m_v decrease as consolidation pressure increases, thus the changes nearly offset one another resulting in little effect of C_v. Conventional consolidation theory

89

(Terzaghi's Theory) assumes that the C_v. Value is constant over the consolidation period and it is necessary to pick a single value for C_v.when the conventional theory is used to calculate time rate of consolidation. However, in cases such as material placed as slurries, choosing a constant value of C_v is not straightforward and the C_v. varies over a wide range depending on the state of material (slurry vs. solid). As discussed by Duncan (1993) there are factors that complicates the selection of the value of C_v. One of the important factors to be considered in selection of C_v is preconsolidation stress. As discussed before, the C_v for a given clay is about an order of magnitude larger at pressures below the pre-consolidation pressure at it is at pressures above the pre-consolidation pressure. Therefore, if the effective stress in a clay deposit is smaller than preconsolidation stress, the value of C_v. will change greatly during the consolidation process meaning that it will increase by the increase of effective stress. The other important factor which affects the value of C_v. is length of drainage path. According to Taylor's method (Taylor, 1948) the C_v. can be calculated using Equation 5-3:

$$C_v = \frac{0.848\ D^2}{t_{90}}$$
Equation 5-3

where D is length of drainage path and t_{90} is time required to reach 90% of consolidation.

In many cases such as hydraulically place material, the length of drainage path decreases greatly during the consolidation process and it can decrease the value of C_v. significantly. The length of drainage path (D) at the beginning of consolidation of FCR slurry is order of magnitude larger than values of D after compression. Therefore, the accurate prediction of time rate of consolidation requires improved methods to estimate the C_v values. In this study, different values of C_v are used to predict consolidation time rate and a new method for predicting the time rate of consolidation of FCR slurry is presented.

5.3.2 *CONSOLIDATION OF FINE COAL REFUSE FROM SLURRY*

One dimensional tube consolidation tests on FCR slurry were performed to observe the consolidation process beginning with a liquid slurry. The effect of different pressure levels on the coefficient of consolidation (C_v) and consequently the time rate of the consolidation of the FCR was measured.

The as-received fresh liquid FCR slurry was poured into a consolidation tube made of Teflon with inner diameter of 100 mm (4inches) and length of about 500 mm (20 inches). Perforated plastic disks and filter paper were placed at each end to allow for double drainage. The loading started from 35 kPa and the settlement of the FCR slurry was monitored using a dial gage installed at the top of the loading rod (Figure 5-5). After reaching the end of primary consolidation, the stress was doubled and the same process was repeated for the new load. The process was repeated up to 550 kPa of vertical stress. The C_v value was calculated for each step of loading based on Taylor's square root of time method (Taylor, 1948). In these calculations of C_v , the actual decrease in the length of the drainage path was accounted for.

Figure 5-5. Consolidation Tube for FCR Slurry

Figure 5-6 presents the variation of C_v value with the applied consolidation pressure. The C_v value varies over a wide range as the applied pressure increases, from a low value during the period in which the material is primarily a fluid, to the higher values which reach the range of the solid samples discussed above. The lower values of C_v may be limited by the permeability of the filter paper on each end of the column.

Based on the C_v values obtained from tube consolidation, Equation 5-4 can be used to estimate the C_v value as a function of stress level on the FCR slurry samples.

$$C_v = -5\sigma'^2 + 0.05\sigma' + 1.3 \hspace{4cm} \textbf{Equation 5-4}$$

Since the time rate of consolidation is related to C_v, (Equation 5-1), the predicted time for consolidation can have a very wide range depending on the value chosen for C_v.
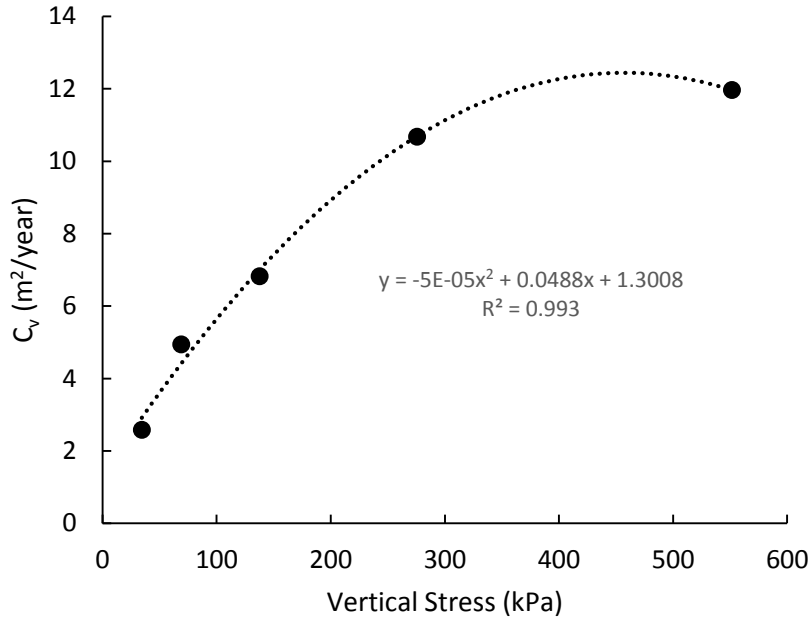
Figure 5-6. Variation of coefficient of consolidation with applied pressure

5.4 *DETERMINATION OF TIME RATE OF CONSOLIDATION*

The time rate of settlement for the FCR slurry as estimated from the traditional Terzaghi infinitesimal strain approach as is typically used for the consolidation of clay soils, is compared with the results obtained from the finite strain approach developed by Gibson et al. (1981) for soft sediments under the material self-weight, and by a new approximation method based on infinitesimal strain but with spatially and temporally variable values of C_v. The effect of the selected value of C_v on the time for consolidation is also investigated.

5.4.1 *TERZAGHI METHOD*

Equation 5-5 is a finite difference approximation to Equation 1, which has been used to obtain the excess pore water pressure as a function of depth, i, and time j as

$$u_{e_{i,j+1}} = \alpha u_{e_{i+1,j}} + (1 - 2\alpha)u_{e_{i,j}} + \alpha u_{e_{i-1,j}} \qquad \textbf{Equation 5-5}$$

where $\qquad \alpha = \dfrac{c_v \Delta t}{(\Delta z)^2}$

i: location increment $index$

j: time $increment\ index$ $\quad c_v$: Consolidation coefficient determined from consolidation tests

Δt: $time\ increment$

92

Δz: *Depth increment*

Equation 5-5 will be stable mathematically when the value of α is less than 0.5 and Δt and Δz each become small (Perloff and Baron, 1976).

5.4.2 FINITE STRAIN METHOD (GIBSON ET AL., 1981)

Gibson et al. (1981) developed a partial solution method for the case of a singly drained normally consolidated layer under the only the self-weight of the material. The dimensionless equation for the excess pore pressure E is:

$$\frac{\partial^2 E}{\partial z^2} + N\frac{\partial E}{\partial Z} = \frac{\partial E}{\partial T_{f.s}}$$ **Equation 5-6**

where

$$E(z,t) = \frac{e(z,t)}{e(0,0)}$$ **Equation 5-7**

$$Z = \frac{z}{l}$$

$$T_{f.s.} = \frac{gt}{l^2}$$ **Equation 5-8**

and $N = \lambda l(\gamma_s - \gamma_w)$

l is height of material solids where

$$l = \frac{h}{1+e_{00}}$$ **Equation 5- 9**

h is the layer thickness as deposited (slurry)

e_{00} is initial void ratio of the material at effective stress assumed initially zero throughout the layer

The initial conditions can be defined as:

$E(z,0) = 1 \,; 0 \leq Z \leq 1$

λ is linearization constant which can be calculated by fitting a curve in a form of Equation 5-9 to data generated from experimental consolidation testing:

$$e = (e_{00} - e_\infty)Exp(-\lambda\sigma') + e_\infty$$ **Equation 5-10**

where

e_∞ is void ratio at infinite effective stress

e_{00} is void ratio at zero effective stress.

The Gibson et al. (1981) curve fitting process was used to obtain the value for λ from the column consolidation of the liquid FCR slurry (Figure 5-5). Figure 5-7 compares the exponential void ratio-

93

effective stress relationship for two values of λ which bracket the experimental data ($\lambda = 0.02$ and $\lambda = 0.08$), from which the relationship with $\lambda = 0.08$ was found to give the best approximation.

Based on the picked λ value which best fits the experimental results ($\lambda = 0.08$), N can be calculated using following Equation:

$$N = \lambda l(\gamma_s - \gamma_w) = 0.08 \ m^2/kN \times 3.5m(16kN/m^3 - 10kN/m^3) = 1.68$$

Cargill (1984) used a computer program to solve Equation 4 with appropriate initial and boundary conditions for singly drained conditions and developed solution charts (Figure 5-8) to predict percent of consolidation.

Based on the calculated values for λ and N we can use Figure 5-8 to find Time factor ($T_{f.s.}$) corresponding to a degree of consolidation equal to 90%, and thus the time for consolidation can be calculated using Equation 5-11.

$$C_v = \frac{T_v H_{dr}^2}{t} \qquad\qquad \textbf{Equation 5-11}$$

The time for 90% consolidation is estimated from Figure 5-8 and assuming the effective layer thickness l is determined from in Equation 5-8 as:

$l = h/(1+e_{00}) = (21 \text{ m}/(1+5)) = 3.5 \text{ m}$

$$for \ \ C_v = g = 2.58\frac{m^2}{year} \ \ and \ U = 90\% \ \rightarrow T_{FS} = 0.6 \quad \rightarrow \quad 0.6 = \frac{2.58 \times t}{3.5^2} \quad \rightarrow \quad t = 2.84 \ years$$

$$for \ g = 11.97\frac{m^2}{year} \ \ and \ U = 90\% \ \rightarrow T_{FS} = 0.6 \quad \rightarrow \quad 0.6 = \frac{11.97 \times t}{3.5^2} \quad \rightarrow \quad t = 0.61 \ years$$

It should be noted that the above time rates are for consolidation under the self-weight of the material only, and this may be much higher in case of staged construction. Also, it can be seen that the time for consolidation is very sensitive to the value of the coefficient of consolidation(C_v) and since the C_v was observed to vary over a wide range, it may be necessary to consider the variation of C_v in prediction of consolidation time.

$$e = (e_{00} - e_{\infty})Exp(-\lambdaσ')$$
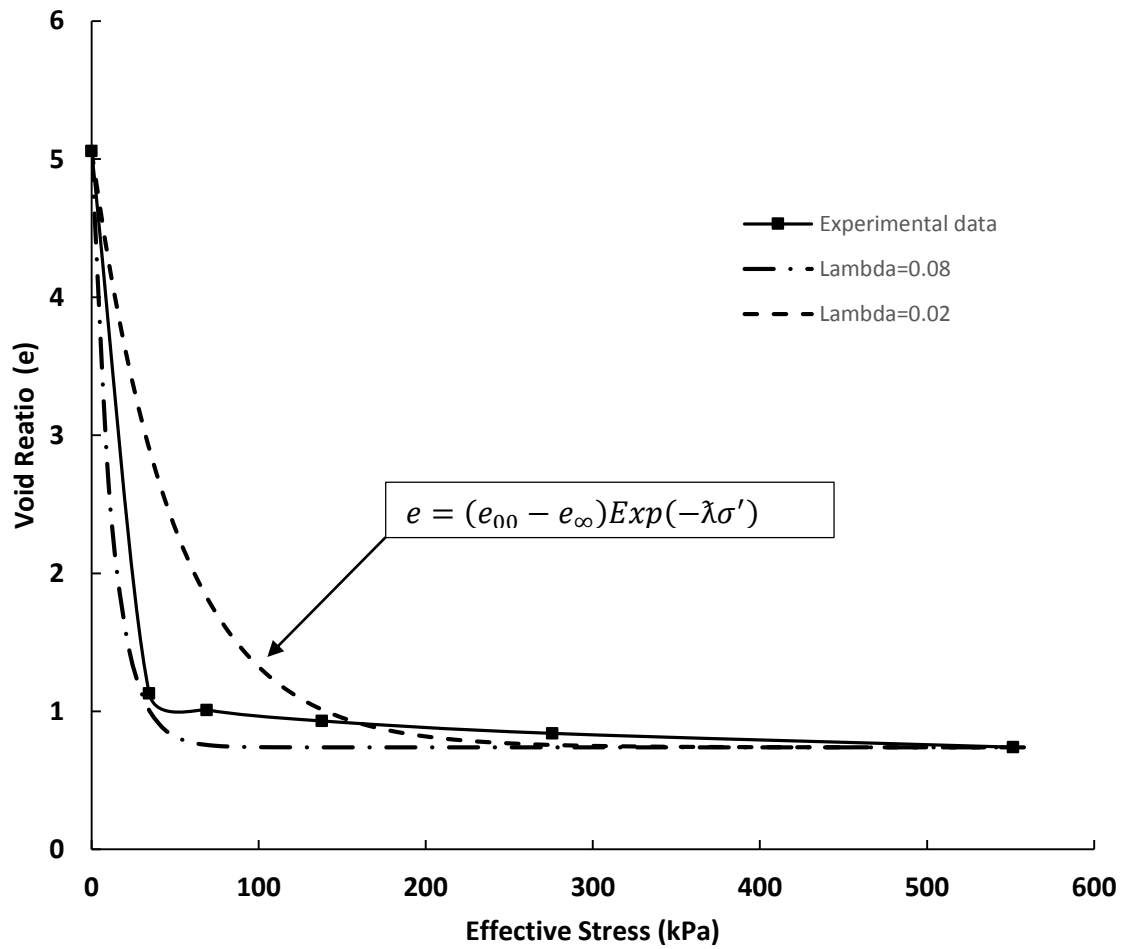
Figure 5-7. Exponential void ratio-effective stress relationship fitted to data from consolidation testing for as-received FCR slurry from eastern Kentucky
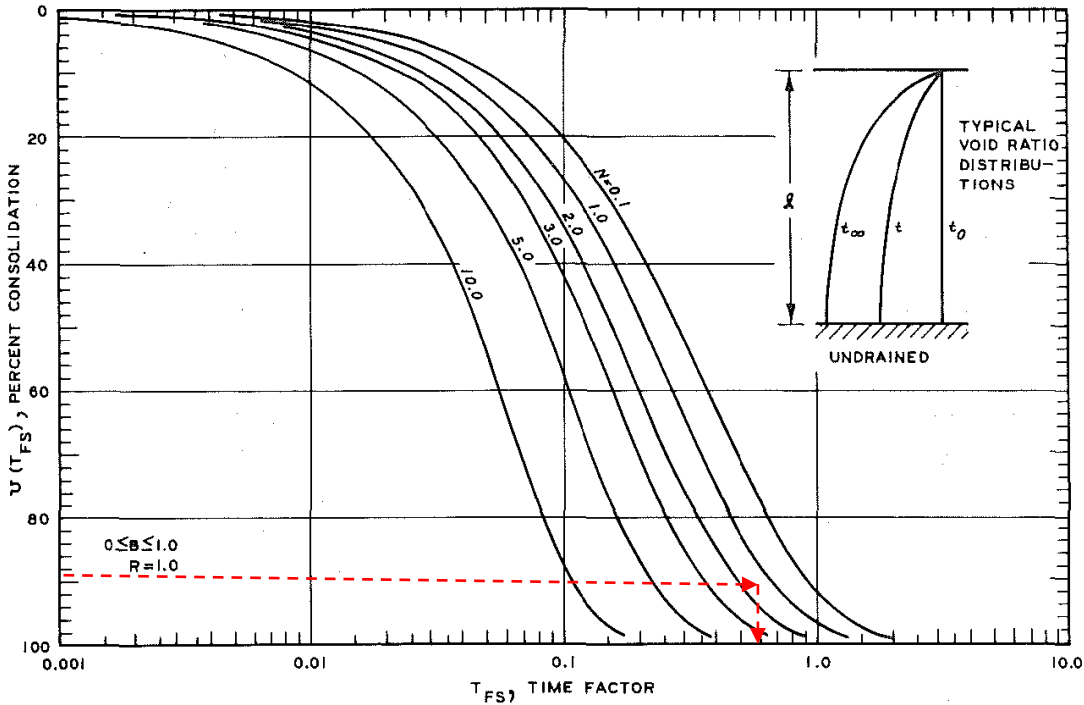
Figure 5-8. Degree of consolidation as function of dimensionless time factor for unconsolidated singly drained layers by finite strain theory (Cargill, 1984)

5.4.3 INFINITESIMAL STRAIN WITH SPATIAL AND TEMPORAL VARIATION OF C_v

As discussed before, the prediction of the time rate of consolidation is highly dependent upon the value selected for C_v. To investigate the effect of the stress dependent nature of C_v on the time rate of consolidation of the fresh FCR, the finite difference solution for Terzaghi's consolidation equation described above was modified to include the variation of C_v both with position and time to predict excess pore water pressure (Δu) versus time at various depths in the fine coal refuse impoundment.

For the case where C_v was assumed to be variable, the value of α (which is function of C_v) is recalculated for each time step Δt and each location Δz across the thickness of the FCR layer.

Thus Equation 5-4 becomes
$$\alpha_{j,i} = \frac{C_{vj,i}\Delta t}{(\Delta z)^2}$$

where j= time increment, i = the depth interval, $C_{vj,i}$ is the value of C_v from Equation 5-4 for the time increment j.

Since the C_v is a function of vertical effective stress (σ') (Equation 5-12), the effective stress should be calculated using following equation:

$$\sigma' = \sigma - u \qquad\qquad\qquad \textbf{Equation 5-12}$$

where

$\sigma: Total\ Stress$

$u: Excess\ pore\ water\ pressure$

$\sigma': effective\ stress$

Since the values of excess pore water pressure can be obtained from Equation 5-10, the σ' can be calculated for each time step at any location. In other words, the α value is unique for each time and depth and thus the excess pore water pressure is being calculated based on new α for each step. The value of C_v for each time step and position in the numerical calculation is changed based on the previously calculated value of the pore water pressure and effective stress. Figure 5-10 shows simplified flowchart of calculating excess pore water pressure at each time step.

A limitation of this method is that the thickness of the layer (or length of the drainage path) remains constant with time. However, the change in drainage path is incorporated indirectly in the measurements of the value of C_v.
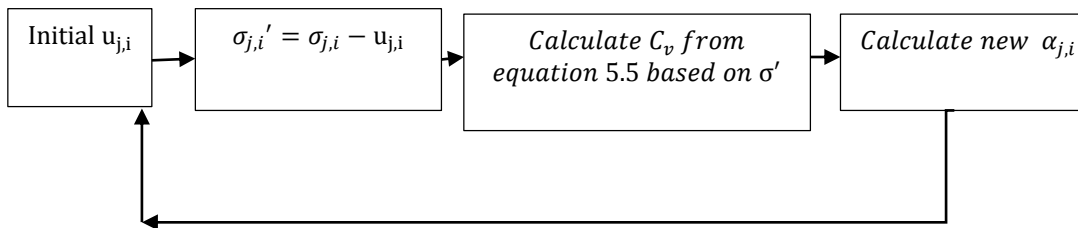
Figure 5-9. Flowchart of calculation of excess pore water pressure at each time step

5.5 RESULTS

The time rate of consolidation of the FCR was analyzed under two different loading scenarios: a) a single 21m thick layer of FCR consolidating under its own weight, and b) the 21 thick layer subjected to staged construction of 3 subsequent stages of FCR. The results from the three analytical models discussed above were compared, and the impact of various assumptions for the value of C_v investigated as well. Figure 5-10 shows the two loading scenarios schematically.

Figure 5-11 shows the effect of different C_v values on the time rate of consolidation for a single 21 m thick layer (Stage 1) of FCR due to the application of surcharge from Stage 2 (Figure-5-1) herein referred to as single stage loading. Terzaghi method and various C_v values, including the average from the solid in situ samples, the average from the companion consolidated fresh FCR samples, and the maximum and minimum values from the column slurry tests on fresh FCR.

In Figure 5-12 the time rate of consolidation for the Stage 1 using the finite strain method (Cargill, 1984) under the single stage loading. In both cases, the C_v values are assumed to be constant during the consolidation process.
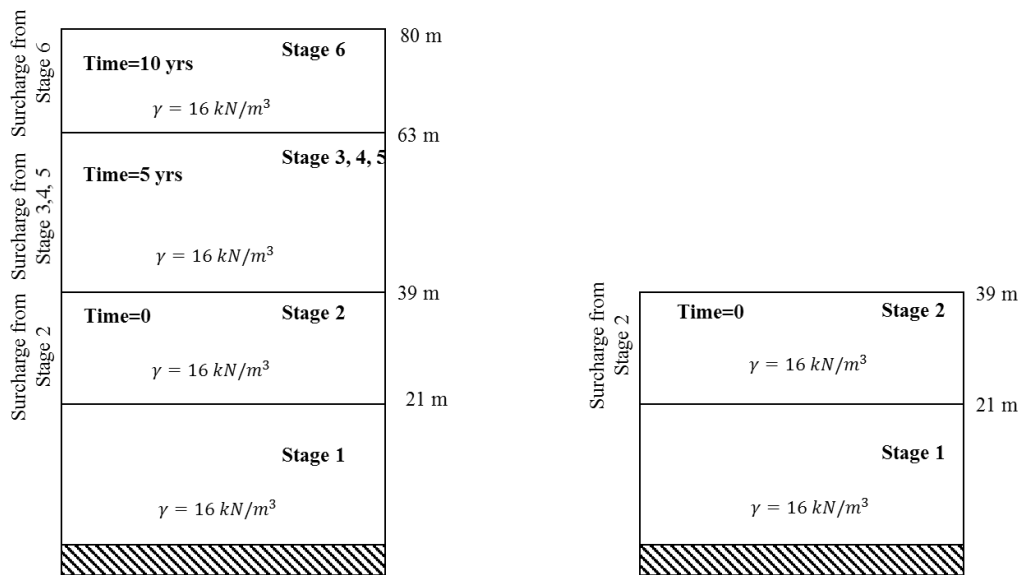
Figure 5-10. Two different loading scenarios used in this study to evaluate time rate of consolidation

98
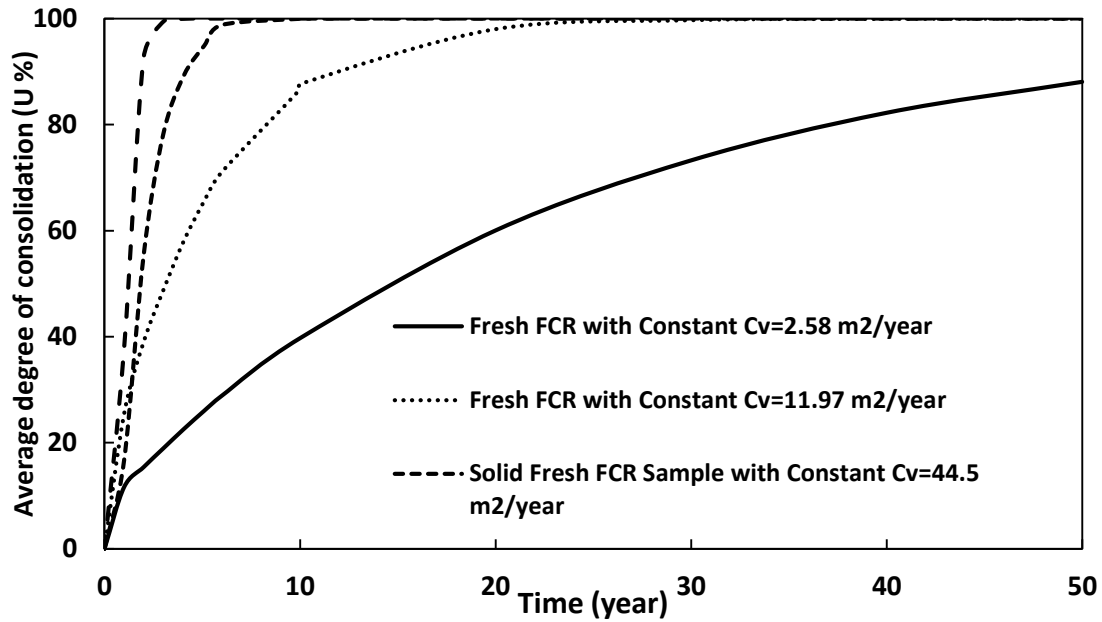
Figure 5-11. Time rate of consolidation of a single 21 m thick layer of FCR due to the single stage loading for various values of C_v using Terzaghi Method
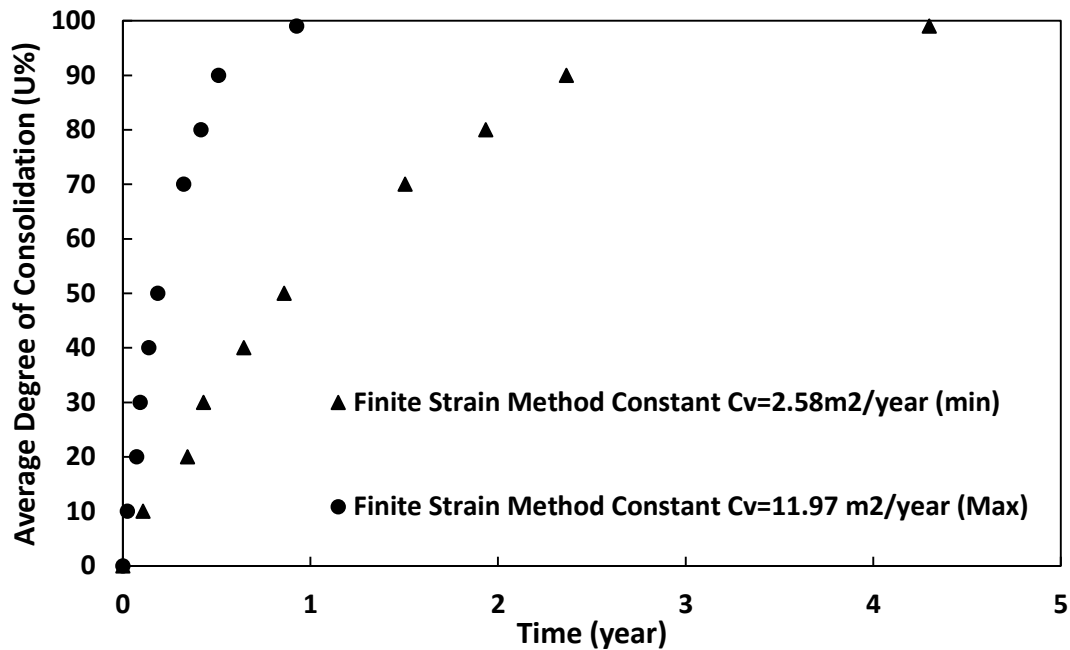
Figure 5-12. Time rate of consolidation of a single 21 m thick layer of FCR due to the single stage loading for various values of C_v using the (Cargill, 1984) finite strain method under self-weight

To illustrate the effect of the spatial and temporal variation of C_v, Figure 5-13 compares the time rate of consolidation of the same single stage loading with constant C_v values and variable C_v. The two results for constant C_v reflect the maximum and minimum C_v values obtained from the slurry column consolidation measurements.

Figure 5-14 presents the results from the variable C_v analysis in terms of the pore water pressure ratio, U_z, (excess pore water pressure divided by effective stress) for any location and time factor in a single drained FCR layer. It is assumed that the consolidation of the 21 m thick Stage 1 FCR is due to a surcharge from Stage 2, then 5 years later simultaneous surcharge from stages 3, 4 and 5 and then 10 years later another layer (Stage 6) was added to the top of existing layers. It can be seen in Figure 5-14 at the times t = 5.1 years and 10.05 years, which correspond to the addition of the upper stage surcharges, there is a reduction in the pore water pressure ratio, U_z, which disrupts the typical trend. To obtain average degree of consolidation for the entire layer, a numerical integration by the trapezoidal method was performed to calculate the area under the curves in Figure 5-14.

Figure 5-15 shows the average degree of consolidation of Stage 1 under the triple stage loading from stages 3, 4 and 5 at a time of 5 years, and then 5 years later at time of 10 years the application of Stage 6. The results from the variable C_v approach are compared with the Terzaghi method for constant C_v values corresponding to both the maximum and minimum values measured in the slurry column test.
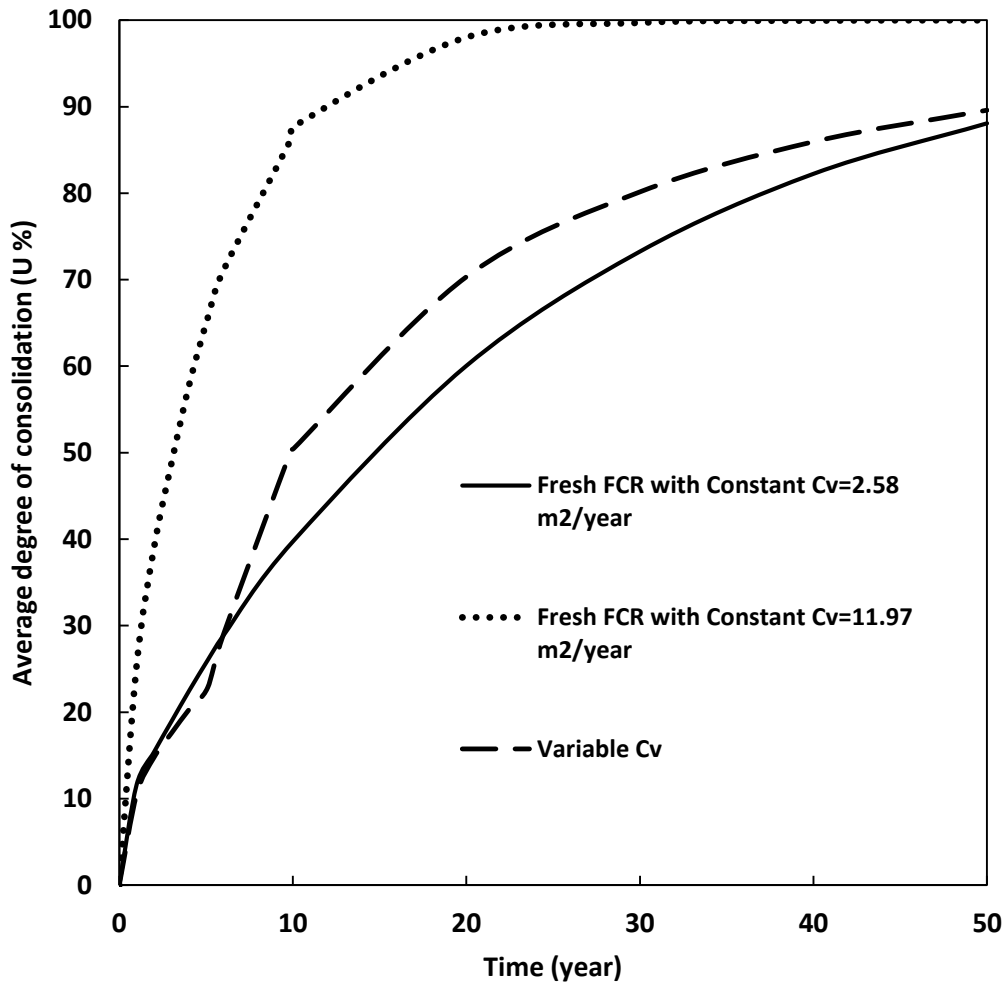
Figure 5-13. Time rate of consolidation of a single 21 m thick layer of FCR due to the double stage loading using the Terzaghi method with both constant and variable C_v
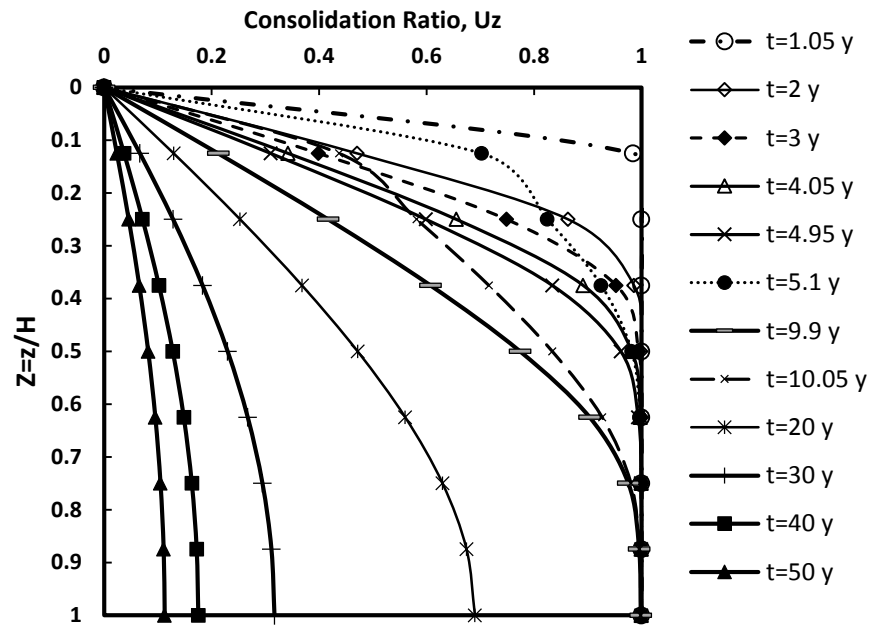
Figure 5-14. Consolidation ratio for any location and time in a single drained Stage 1 FCR layer under the triple stage loading using the variable C$_v$ method. The deviations occurring at times of t = 5.1 and 10.05 years correspond to the additional stages of loading.
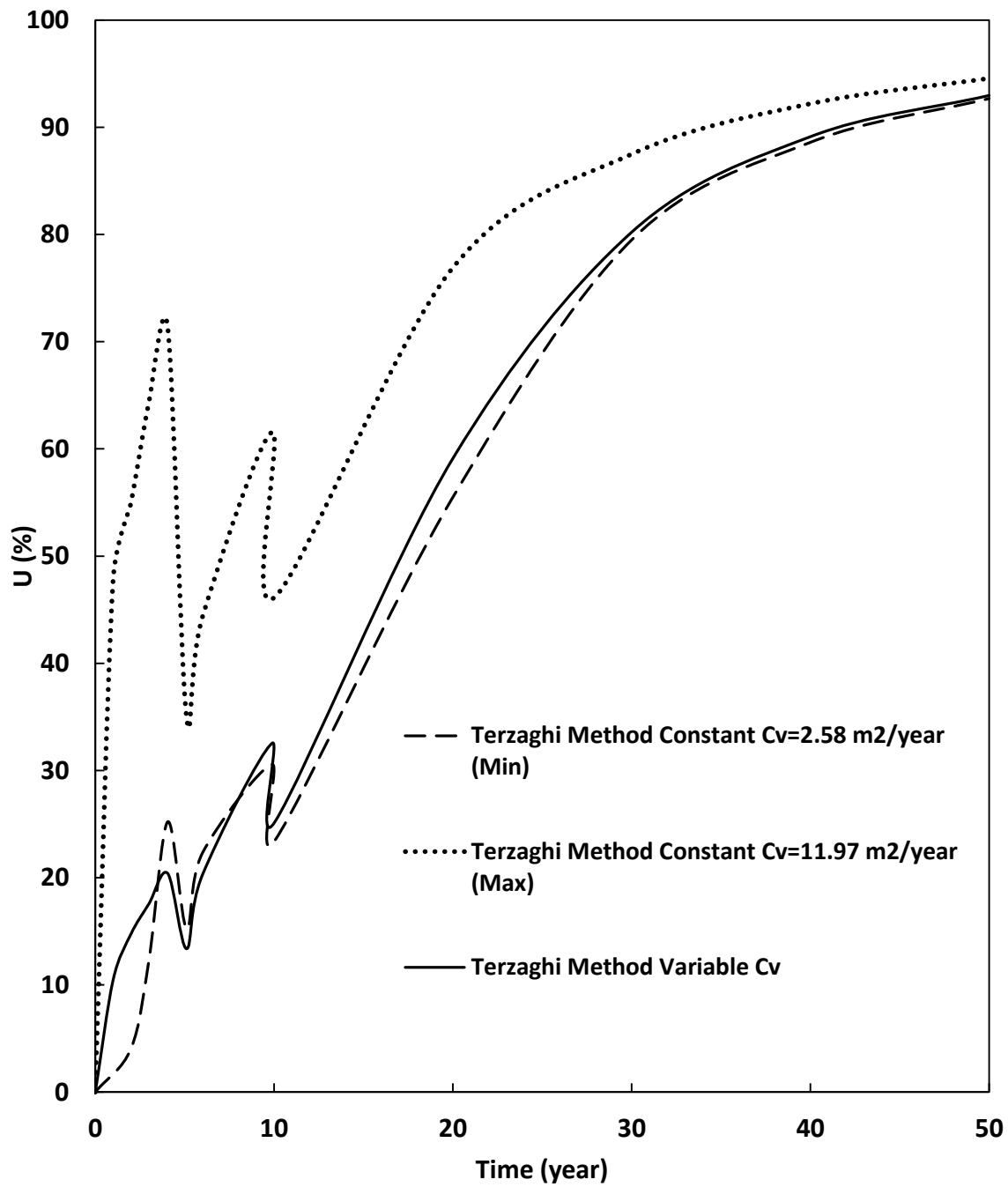
Figure 5-15. Time rate of consolidation of a single 21 m thick layer of FCR due to the triple stage loading using the Terzaghi method with both constant and variable C_v

5.6 DISCUSSION

Time rate of consolidation is directly related to the value of the coefficient of consolidation (C_v) and the selection of appropriate value(s) of C_v is not straight forward. A range of C_v values were obtained from solid samples taken in situ (Figure 5-2) which were an order of magnitude higher than the values measured from companion samples consolidated to similar stresses as the in situ samples. The in situ samples were found to be significantly under-consolidated, which may explain the differences in C_v when compared to the laboratory consolidated samples. Duncan (1990), referring to normally consolidated soils, suggested that for clay the value of C_v may be an order of magnitude larger at pressures below the pre-consolidation pressure and that it decreases greatly as the pre-consolidation pressure is reached. Although the FCR materials tend to be under-consolidated, the stress-dependent nature of C_v is important. As observed from the tests on FCR slurry in Figure 5-6, the C_v value for the FCR varies over a wide range depending on the state of the material (from slurry to solid), which reflects the effective stress state. The variation of C_v with effective stress was also reported by Duncan (1993) for San Francisco Bay mud (highly plastic organic clayey silt) where the value of C_v calculated using Taylor's method varied from 0.8 to 5.2 m²/year. Based on the results from Figure 5-11, when the C_v of solid in situ samples ($C_v = 157.8 \, m^2/year$) is used, the FCR layer reaches 100% of consolidation after about 3 years. The same degree of consolidation is reached after about 25 years when the maximum C_v from fresh slurry FCR ($C_v = 11.97 \, m^2/year$) is used. When the average C_v value for solid in situ FCR samples is used ($C_v = 157.8 \, m^2/year$), the time to reach the end of primary consolidation is even longer, reaching 90% after about 50 years. These differences in time rate of consolidation are even larger when comparing results from the different analysis methods (Figure 5-12). The Terzaghi method suggests it takes 25 years for the layer under the double stage loading to reach to 100% consolidation while the finite strain method (Gibson et al., 1981) suggests it takes less than a year for the same layer to reach to 100% consolidation (Figure 5-12).These big differences in time rate of consolidation emphasize the significance of picking an appropriate C_v. The FCR materials observed in situ were clearly not highly consolidated, based on the observed fluid like materials and the very low values of pre-consolidation stress measured in the lab, leading to the conclusion that the values of C_v obtained from the in situ samples could not be used for predicting the time rate of settlement.

As observed in Figure 5-15, at large times and degrees of consolidation, the variable C_v model yields similar results as that obtained with the traditional Terzaghi constant C_v approach. When a small value of C_v is used in the constant C_v approach, results similar to the variable C_v model are obtained. Significantly, in the case of the maximum C_v (=11.97 $m^2/year$) the FCR layer consolidates considerably faster than when the variable C_v or low value of C_v is used. The difference in the time rate of consolidation is much greater at the early stages. This is consistent with the experimental results in Figure 5-6 which

showed the value of C_v is function of effective stress (σ') and is increasing as the excess pore water pressure dissipates. In other words, as the slurry material reaches 90% consolidation, the assumption of constant C_v is reasonable value of the coefficient of consolidation has little effect on the degree of consolidation. This is because at large times the nature of the governing differential equation in the Terzaghi method assumes that the degree of consolidation asymptotically approaches 100% at time equal to infinity. In the case of the minimum value of C_v from the slurry consolidation test, ($C_v = 2.58\ m^2/year$) which represents the early stages of consolidation, the constant C_v produces a good approximation to the variable C_v method, although the variable C_v method gives a slightly faster rate for consolidation.

Based on the calculations from finite difference method, the Stage 1 FCR layer reached the average degree of consolidation of ~90% after 50 years of being placed.

While the predicted time for 90% consolidation is not affected much, the U% at early times is highly dependent on the value chosen for C_v. As time increases, the value of C_v approaches that of solids throughout and thus the difference in the calculations diminish. Although the length of the drainage path is held constant in the two infinitesimal strain calculations, shortening the drainage path would increase the rate of consolidation and hence difference would be smaller still.

One of the limitations of the traditional Terzaghi solution that it does not incorporate the change in the height of initial slurry. However, the height of Stage 1 which was used as a drainage path in this study, is the post consolidation height of the slurry in the impoundment which partially compensates the shortcoming of this method. Moreover, since the reduced values of drainage path are used to calculate the C_v values of increased effective stress, the value of C_v accounts for the change in sample height over the consolidation process, which indirectly incorporates in time rate calculation.

5.7 CONCLUSIONS

The consolidation of fine coal refuse has been investigated based on in situ sampling and laboratory measurements of the coefficient of consolidation from both solid and liquid slurry samples. These data are used to predict the time rate of consolidation using classical Terzaghi theory, a finite strain method, and a new method employing a spatial and temporal variable coefficient of consolidation. The results suggest that while the variable coefficient of consolidation method may best reflect the low degree of consolidation at early times when the material is still essentially slurry, a similar response can be obtained using the Terzaghi method with constant value of coefficient of consolidation obtained from measurements of the slurry consolidation at low stress levels. The low value of coefficient of consolidation has little effect on the degree of consolidation at large time due to the nature of the governing differential equation which assumes that the degree of consolidation asymptotically approaches 100% at time equal to infinity. The consolidation response of hydraulically placed slurry at early times is most important with respect to construction staging

and personnel safety. The results show that as the slurry material reaches 90% consolidation, the assumption of constant C_v is reasonable and the time to reach 90% is not highly dependent upon the value chosen for C_v, and the value of the coefficient of consolidation has little impact on the degree of consolidation.

The traditional Terzaghi method yields similar results as the variable C_v method, provided the minimum value of C_v from the slurry consolidation is in use, and the differences are greatest at early times.

5.8 REFERENCES

Bitzer, K., 1996. Modeling consolidation and fluid flow in sedimentary basins. Computers & Geosciences 22, 467-478.

Bryant, W.R., Hottman, W., Trabant, P., 1975. Permeability of unconsolidated and consolidated marine sediments, gulf of Mexico. Marine Geotechnology 1, 1-14.

Cargill, K.W., 1984. Prediction of Consolidation of Very Soft Soil. Journal of Geotechnical Engineering 110, 775-795.

Casagrande, A., 1936. The Determination of Pre-Consolidation Load and its Practical Significance, First International Conference on Soil Mechanics and Foundation Engineering, Cambridge, pp. 60-64.

Chang, C.S., 1985. Uncertainty of One‐Dimensional Consolidation Analysis. Journal of Geotechnical Engineering 111, 1411-1424.

Chilingarian, G.V., Rieke, H.H., Donaldson, E.C., 1995. Chapter 2 Compaction of argillaceous sediments, in: Chilingarian, G.V., Donaldson, E.C., Yen, T.F. (Eds.), Developments in Petroleum Science. Elsevier, pp. 47-164.

Duncan, J.M., 1993. Limitations of Conventional Analysis of Consolidation Settlement. Journal of Geotechnical Engineering 119, 1333-1359.

Elkateb, T., 2017. Stress-dependent consolidation characteristics of marine clay in the Northern Arabian Gulf. Ain Shams Engineering Journal.

Gibson, R.E., 1958. The Progress of Consolidation in a Clay Layer Increasing in Thickness with Time. Géotechnique 8, 171-182.

Gibson, R.E., Schiffman, R.L., Cargill, K.W., 1981. The theory of one-dimensional consolidation of saturated clays. II. Finite nonlinear consolidation of thick homogeneous layers. Canadian Geotechnical Journal 18, 280-293.

Hegazy, Y.A., Cushing, A.G., Lewis, C.J., 2004. Physical, mechanical, and hydraulic properties of coal refuse for slurry impoundment design. Geotechnical and Geophysical Site Characterization Vols 1 and 2, 1285-1291.

Holtz, R.D., Kovacs, W.D., Sheahan, T.C., 2011. An introduction to geotechnical engineering, 2nd ed. Pearson, Upper Saddle River, NJ.

Hong, H.P., Shang, J.Q., 1998. Probabilistic analysis of consolidation with prefabricated vertical drains for soil improvement. Canadian Geotechnical Journal 35, 666-667.

Karig, D.E., Ask, M.V.S., 2003. Geological perspectives on consolidation of clay-rich marine sediments. Journal of Geophysical Research: Solid Earth 108.

Major, J.J., 2000. Gravity-Driven Consolidation of Granular Slurries: Implications for Debris-Flow Deposition and Deposit Characteristics. Journal of Sedimentary Research 70, 64-83.

Perloff, W.H., Baron, W., 1976. Soil mechanics : principles and applications. Ronald Press Co., New York.

Sangrey, D.A., Cornell, U., Clukey, E.C., Molnia, B.F., 1979. Geotechnical Engineering Analysis of Underconsolidated Sediment from Alaska Coastal Waters, 11th Annual Offshore Technology Conference, Houston, pp. 677-682.

Schiffman, R.L., 1982. The consolidation of soft marine sediments. Geo-Marine Letters 2, 199.

Schiffman, R.L., Cargill, K.W., 1981. Finite Strain Consolidation of Sedimenting Clay Deposits, 10 th International Conference in Soil Mechanics and Foundation Engineering, Stockholm, pp. 239-242.

Taylor, D.W., 1948. Fundamentals of Soil Mechanics. John Wiley and sons, New York.

Terzaghi, K., 1943. Theoretical soil mechanics. J. Wiley & sons,; Chapman and Hall, limited., New York, London.

U.S Army Corps of Engineers, N.I.o.D., 2017. National Inventory of Dams

Zeng, X., Globe, J.A., 2008. Dynamic Properties of Coal Waste Refuse in A Tailings Dam. ASCE Geotechnical Special Publication, 181.

Zeng, X., Wu, J., Rohlf, R.A., 1998. Seismic Stability of Coal waste Tailing Dams. Geotechnical Earthquake Engineering and Soli Dynamics III 1, 950-960.

Zhou, W., Hong, H.P., Shang, J.Q., 1999. Probabilistic Design Method of Prefabricated Vertical Drains for Soil Improvement. Journal of Geotechnical and Geoenvironmental Engineering 125, 659-664.

CHAPTER VI
INFLUENCE OF FLOCCULANT ON THE UNDRAINED SHEAR STRENGTH

6.1   ABSTRACT

Flow behavior and the undrained shear strength response of fine coal refuse (FCR) specimens from an active impoundment in eastern Kentucky were investigated. The purpose of this study is to investigate the effect of added flocculant on the flow behavior and undrained shear strength of the FCR. The specimens were formed from fresh FCR slurry samples obtained from the slurry discharge pipe, as well as solids recovered from the same fresh FCR mixed with either distilled water or a sodium hexametaphosphate dispersant solution. The specimens were consolidated in columns over a range of low stresses to create soft, relatively low strength specimens. Specimens were prepared with different initial void ratios and moisture contents. Flow table tests as well as vane shear strength tests were performed to investigate the influence of the background solution type on the flow behavior and undrained shear strength. The results indicate that the nature of the background solution has a significant impact on the void ratio, flowability, and the undrained shear strength of the FCR. The flocculant present in the as-obtained fresh FCR slurry appears to contribute to higher resistance to flow and higher shear strength at higher values of moisture content and void ratios than the other background solutions at the same consolidation pressure. These tests illustrate the influence of particle associations on the undrained strength of fine coal refuse, and the impact of the flocculant on the shear strength of the FCR.

6.2   INTRODUCTION

Fine coal refuse (FCR) refers to the fines generated during the processing of raw coal. FCR is typically stored behind on-site impoundments constructed primarily with coarse coal refuse. The FCR is usually mixed with water and a chemical flocculant and then hydraulically placed by pumping the resulting slurry through a series of pipelines. Flocculants are added to the slurry in order to aggregate the fine FCR particles and accelerate settlement and subsequent consolidation after placement. As a result, the effective particle size distribution of the deposited FCR is altered (Jedari et al., 2017), potentially impacting the material properties such as rheology, consolidation time, and void ratio.

Destabilization of the impounded FCR (e.g. flow) is one of the major concerns regarding this material. Undrained shear strength of the FCR is one of the important parameters that is directly related to the resistance to flow. Undrained shear strength can be linked to the flow potential of the fine-grained soils. Flow potential is often described in the context of the Atterberg limits. Atterberg limits are used to distinguish the liquid state from the plastic state, with the liquid limit defining the water content at which a fine-grained material will begin to flow. The Atterberg limits are also compared to the field water content conditions using the liquidity index (LI) to assess the current material state.

The liquid limit can be correlated to the shear strength of soils. Skempton (1957) established a

relationship to correlate undrained shear strength to the corresponding overburden pressure and the plasticity index. He found that the undrained shear strength has a direct relationship with plasticity index (PI) and it increases with the increase in PI and with having plasticity index of a normally consolidated clay deposit, the variation of undrained shear strength with depth can be estimated. Casagrande (1958) related shear strength with liquid limit of a soil and suggested the average value of the shear strength of soils at the liquid limit to be 2.65 kN/m^2. Norman (1958) used a miniature laboratory vane shear device to measure shear strength of five soils at their respective liquid limits and reported that the strength ranged from 0.8-1.6 kN/m^2. Youssef et al. (1965) conducted a series of tests on a number of remolded clays from Egypt. The shear strengths of remolded samples were measured at the moisture content near to their respective liquid limits and found that the shear strength at the liquid limit ranges from 1.3-2.4 kN/m^2. Mesri (1975) showed that the mobilized undrained shear strength can be expressed independently from plasticity index. He estimated the ratio of mobilized shear strength of soft clays to overburden pressure to be equal to 0.22. Wroth and Wood (1978) linked the results of index tests of the soil and shear strength and correlated these results with liquidity index and compression index. They concluded that the estimation of shear strength depends only on the liquidity index and proposed an equation to correlate liquidity index and undrained shear strength. Leroueil et al. (1983) correlated undrained cohesion with liquidity index and linked the liquidity index of sensitive clays to their undrained shear strength. They showed that there is a nonlinear relationship between undrained shear strength and liquidity index. Yılmaz (2000) evaluated shear strength of fine-grained alluvial soils from different locations in Turkey and provided an empirical relationship between undrained shear strength and liquidity index showing that the undrained shear strength decreases exponentially with increase of liquidity index. Kuriakose et al. (2017) predicted the shear strength of saturated clays from India based on the liquid limit and moisture content.

Flocculants are added to the FCR slurry prior to placement to accelerate particle sedimentation. The effect of the flocculant on the mechanical response of FCR is not yet fully understood. However, many investigations have focused on the influence of flocculation on the shear strength of fine-grained soils (Beier et al., 2013; Sridharan and Prakash, 1999 among others). They showed that the flocculation increases the undrained shear strength of the fine-grained soil by altering the fabric of the soil. Yu (2014) performed direct shear tests on FCR samples collected from two impoundments (West Virginia and Kentucky) and observed that the in situ moisture content of impounded FCR plays a critical role in the shear strength of the coal refuse material. As water content increases, the undrained shear strength of FCR decreases. Hegazy et al. (2004) estimated the shear strength of FCR using laboratory and in situ tests. They determined drained shear strength parameters using consolidated isotropic undrained compression (CIUC). They also measured undrained shear strength of the FCR by the depth and concluded that the undrained strength is increasing with depth and overburden pressure. However, they did not study the effect of flocculant on the strength

111

behavior of the FCR.

The purpose of this study is to correlate a simplified flow measurement with undrained shear strength to potentially identify the conditions under which FCR is likely to flow. In this study, a series of modified flow table tests were conducted on consolidated fresh fine coal refuse prepared with three different background solutions: (1) the supernatant of the as-obtained FCR slurry containing a chemical flocculant, (2) distilled water, and (3) a dispersant solution. The undrained shear strength of the same specimens were obtained using a laboratory vane shear device. The results from the flow table tests were then correlated with the undrained shear strength in an attempt to identify the undrained shear strength that corresponds to onset of flow for FCR.

6.3 EXPERIMENTAL METHODS

6.3.1 FLOW TABLE TEST

A standard flow table test (ASTM-C230/C230M, 2014) was modified to evaluate flow behavior of FCR. The standard flow table (Figure 6-1) is designed for characterizing the consistency of mortars to be used in hydraulic cement. According to the ASTM standard, flow is determined as percent increase in diameter after a conically-shaped specimen is subjected to a required number of cam-actuated ½-inch table drops at a fixed rate (25 drops in 15 seconds). For this study, the conical mold was replaced with a cylindrical mold that can accommodate cylindrical specimens obtained by consolidating fresh FCR slurry. The standard flow table test method was modified to develop a flow index of FCR as a function of material properties and loading conditions.

The measurements were conducted on fresh FCR slurry obtained from an active coal mine impoundment in eastern Kentucky. To prepare the specimens, the FCR slurry was consolidated in consolidation tubes using selected applied pressures ranging from 28 kPa (4 psi) to 206 kPa (30 psi). These low values of consolidation pressure were selected to characterize the low strength of the materials at the boundary of flow and at water contents approaching the liquid limit. These pressures are very low compared to the overburden pressures in the slurry impoundment near the sampling source (365 kPa to 738 kPa). Because FCR is typically placed with a flocculant, different background solutions were used to prepare the specimens prior to strength testing to observe the effects of background solution. The background solutions in this study were (1) the supernatant fluid of as-obtained fresh FCR containing a polymer flocculant, (2) distilled water, and (3) a dispersant solution (sodium hexametaphosphate solution at 40 g $(NaPO_3)_6$ /liter water). These three solutions were selected to be consistent with the study of rheology and particle and floc size distribution of fresh FCR presented in Chapter 4 of this study.

The liquid slurry specimens were consolidated using consolidation tubes similar to those described

in Chapter 5 to prepare fresh slurry specimens for consolidation testing. In this case however, the PVC consolidation tubes were fitted with a removable base connected to the consolidation tube with a coupling. This allowed for the specimen to be tested directly in the removable base, minimizing specimen disturbance and eliminating the need for extruding the specimen from the tube (Figure 6-2). The diameter and height of the removable base were 100mm (4 inches) and 150mm (6 inches), respectively. The upper part of the PVC tube was long enough (~ 500mm) to accommodate enough slurry to create a consolidated specimen approximately equal to the height of the removable base.

For the as-obtained condition, the clear supernatant water (no solids) of the as-obtained slurry was decanted before pouring the remaining suspension directly into the consolidation tube. This increased the initial solids content of the slurry and resulted in a water content of approximately 110%. For the remaining test cases with different background solutions, the supernatant of the as-obtained slurry was decanted to recover as much solids as possible. The FCR solids were dried overnight in a standard oven (110 °C) and then ground with a mortar and pestle. The dried material was then mixed with enough background solution so that the final slurry had approximately the same moisture content as the decanted FCR (~110%). The dispersant background solution specimens were prepared by first soaking the solids in a sodium hexametaphosphate solution at 40 g $(NaPO_3)_6$ /liter water for 24 hours. Enough distilled water was then added to bring the slurry to a moisture content of approximately 110%. Sodium hexametaphosphate is a common dispersant and is used in the hydrometer analysis method (ASTM D422 Standard Test Method for Particle-Size Analysis of Soils). Sodium hexametaphosphate breaks down any larger aggregated or flocculated structures into individual grains, and disperses particles by providing both cationic and anionic species that bind to charged sites on the particles, rendering the particle neutral in charge. The particles then remain dissociated (Wintermyer and Kinter, 1955). A similar procedure was used to prepare the distilled water specimens; the dried solids were soaked in distilled water for 24 hours prior to placing the material in the consolidation columns at an initial moisture content of ~110%.

Each of the three prepared slurries was poured into the consolidation tube to a predetermined level so that the initial consolidated height would be consistent between the tested cases. A porous disk and filter paper were placed at the top and bottom of the tube to allow the sample to drain freely at the top and bottom during consolidation without losing a significant amount of solids. A dial gage installed at the top of the loading rod was used to record settlement of the specimen with the time. The desired consolidation pressure was applied to the specimen until reaching the end of primary consolidation as estimated by the Taylor square root of time method (Taylor, 1948). Since the focus of this study was to investigate the behavior at relatively high water contents and low shear strengths to capture threshold "flow" behavior of the FCR, the range of applied pressures to consolidate the slurry specimens was purposefully selected to be low. Based on previous observations, consolidation stresses ranging from 28 kPa to 206 kPa were selected to create

very soft slurry specimens.

The prepared specimens were each used for both undrained shear strength measurements and flow table testing. Once the specimen was consolidated to the selected stress, the removable base containing the specimen was detached from the consolidation column and trimmed so that the material surface was flush with the top of the removable base. The undrained shear strength was measured first with the specimen contained in the removable base. Then, the flow table tests were performed on the same specimens after extruding from the removable base and cutting by the use of a stainless steel mold.

FCR slurry was consolidated in a PVC tube with the inner diameter of 100 mm to stresses of 28kPa, 41 kPa, 55 kPa, 69 kPa, 83 kPa, 110 kPa, 138 kPa, 138 kPa, 138 kPa and 206 kPa. After the end of primary consolidation was reached for each stress, a lubricated stainless steel cutting cylinder mold with an inner diameter of 2.8" and height of 3.5" was carefully pushed into the specimen. The specimen-filled cutter was then placed on the center of the flow table and the specimen carefully extracted from the cutter. To minimize the friction between the flow table surface and the specimen, a Teflon sheet was used on the surface of the flow table. The cam was then rotated at a speed required for a rate of about 25 table drops in 15 seconds as per ASTM- C230. Cam rotation continued until at least one point on the specimen circumference reached a predetermined circular outline with diameter of 6 inches (Figure 6-3) at which point the test was stopped.
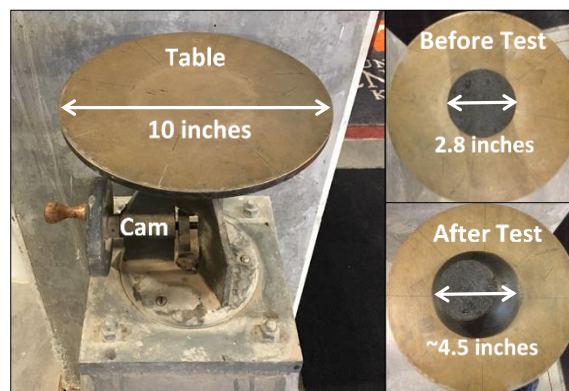
Figure 6-1. Flow table and preliminary flow test on FCR slurry
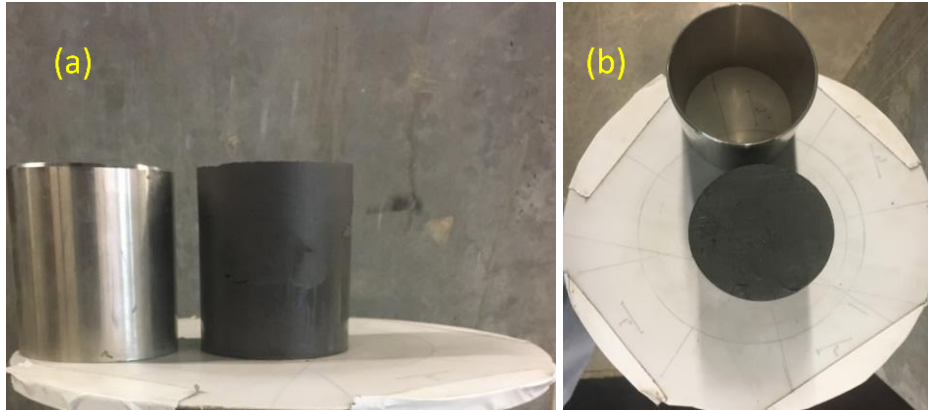
Figure 6-2. FCR cylindrical specimen prior to the flow table test (a) side view (b) Top view

Figure 6-3. FCR specimen at the end of the flow table test indicated by the specimen edge reaching the 6" diameter mark. (a) side view (b) plan view

6.3.2 VANE SHEAR TESTS

The undrained shear strengths of fine coal refuse under selected conditions were measured using the standard vane shear test (ASTM-D4648/D4648M, 2016; BS-1377, 1990). In this method of shear strength measurement, a torsional load is applied through a calibrated spring to a vane inserted into the material. Vane shear tests may be used to measure the undrained shear strength of undisturbed and remolded specimens and is an effective method to measure the strength of very soft materials. The device used for this study is a VJ Tech Laboratory Vane Apparatus (VJT5300). The shear strength capacity of the device can be modified by choosing among four different springs with various stiffness and vane sizes, and the measurable shear strength range is from 0 to 90 kN/m^2 (kPa). The laboratory vane shear device used in this study is shown in Figure 6-4. A motor attachment was used to automate all measurements.

The undrained shear strength (C_u) of the specimen was measured using two different vane sizes: a 12.7 mm (0.5-inch) diameter vane and a 25.4 mm (1.0-inch) diameter vane. There were four sets of springs with various stiffness to measure C_u. The appropriate spring set was selected depending on the estimated stiffness of the consolidated slurry. Table 6-1 provides the range of measureable C_u for each spring.

Figure 6-4. Laboratory vane shear apparatus

116
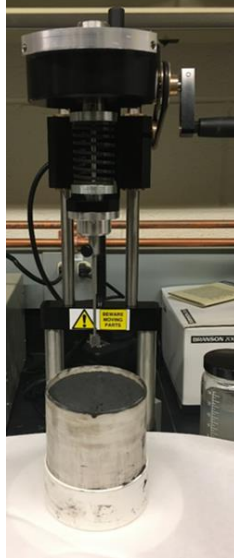
Figure 6-5. Vane shear test conducted on a consolidated FCR specimen in the removable base of the consolidation tube. The vane shown has a diameter of 12.7mm (0.5 inches).

Table 6-1. Range of Measurable Strength for the Vane Shear Device Springs

General Descriptive Term for Strength	Suggested Spring No.	Maximum Shear Stress (kN/m^2)
Very Soft	1 (Weakest)	20
Soft	2	40
Soft to Firm	3	60
Firm	4 (Stiffest)	90

For some initial specimens, the C_u measurements were conducted 3 times using the 12.7mm (0.5 inch) diameter vane at different locations in the specimen and 1 measurement with the 25.4mm (1 inch) diameter vane near the center of the specimen. The average value of all 4 values was reported. Since the measured values of C_u were not significantly affected by the size of the vane used, the measurements of subsequent specimens were conducted using only the smaller vane with 12.7mm diameter. The British Standard recommends the center to center distance of the vanes to be more than 2.3 times the vane diameter. All measurements performed here adhered to this recommendation.

The following procedures were used for measuring the undrained shear strength using the vane shear device. First, the specimen container was placed at the base of the vane apparatus, and the specimen axis was aligned with axis of the vane. Second, the pointer on the device was lined up with the zero position to ensure that no backlash in the mechanism for applying the torque. Third, the vane assembly was then lowered until the bottom of the vane just touched the surface of the specimen. Fourth, the vane was gently, but steadily pushed into the specimen to the required depth. According to the British Standard, the top of the vane should be at a distance no less than four times the blade width below the surface. Fifth, after pushing the vane into the specimen, the torque was applied using the motorized system at a rate of approximately 12 degrees per minute, and the maximum angular deflection of the torsion spring was recorded. The same procedure was repeated for multiple measurements of each specimen. Equation 6-1 was used to calculate the C_u of each specimen.

$$C_u = \frac{T}{\pi[\frac{d^2 h}{2} + \beta\frac{d^3}{4}]}$$
<div align="right">**Equation 6-1**</div>

where:

$\beta = \frac{2}{3}$ for uniform mobilization of undrained shear strength

T is the torque measured by the vane shear apparatus

d: diameter of the vane

h: height of the vane

Figure 6-6 shows the vane shear measurement locations for the FCR specimens. The first measurement was performed at center of the prepared specimen followed by four more measurements between the center and edge of the specimen.
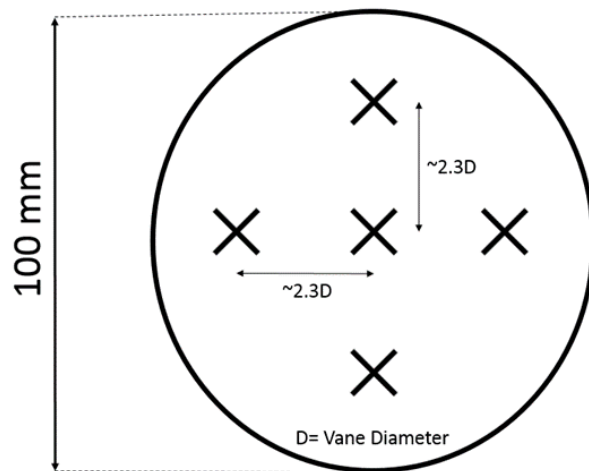
Figure 6-6. Schematic (plan view) of vane insertion locations on the prepared FCR specimen surface

6.4 RESULTS

6.4.1 FLOW TABLE TESTS

Figure 6-7 shows the influence of background chemistry on moisture content under various consolidation pressures and subsequent impact on FCR flowability. The number of drops at which the specimen touched the 6" circle is defined as "N_6 ". Despite the scattered N_6 values for the distilled water and dispersant solutions, for the as-received FCR specimens, two distinct trendlines with two different slopes are observed (best-fit lines derived assuming linear trends). The change in slope from moisture content < 40% to moisture content > 40% indicates an abrupt change in flow behavior. This "breakpoint" for the as-obtained FCR specimens may be attributed to a threshold for flow, above which the material begins to flow. This threshold occurs at a moisture content greater than liquid limit (LL=35.9%).

Figure 6-8 shows the variation of flowability with the applied consolidation pressure.

119
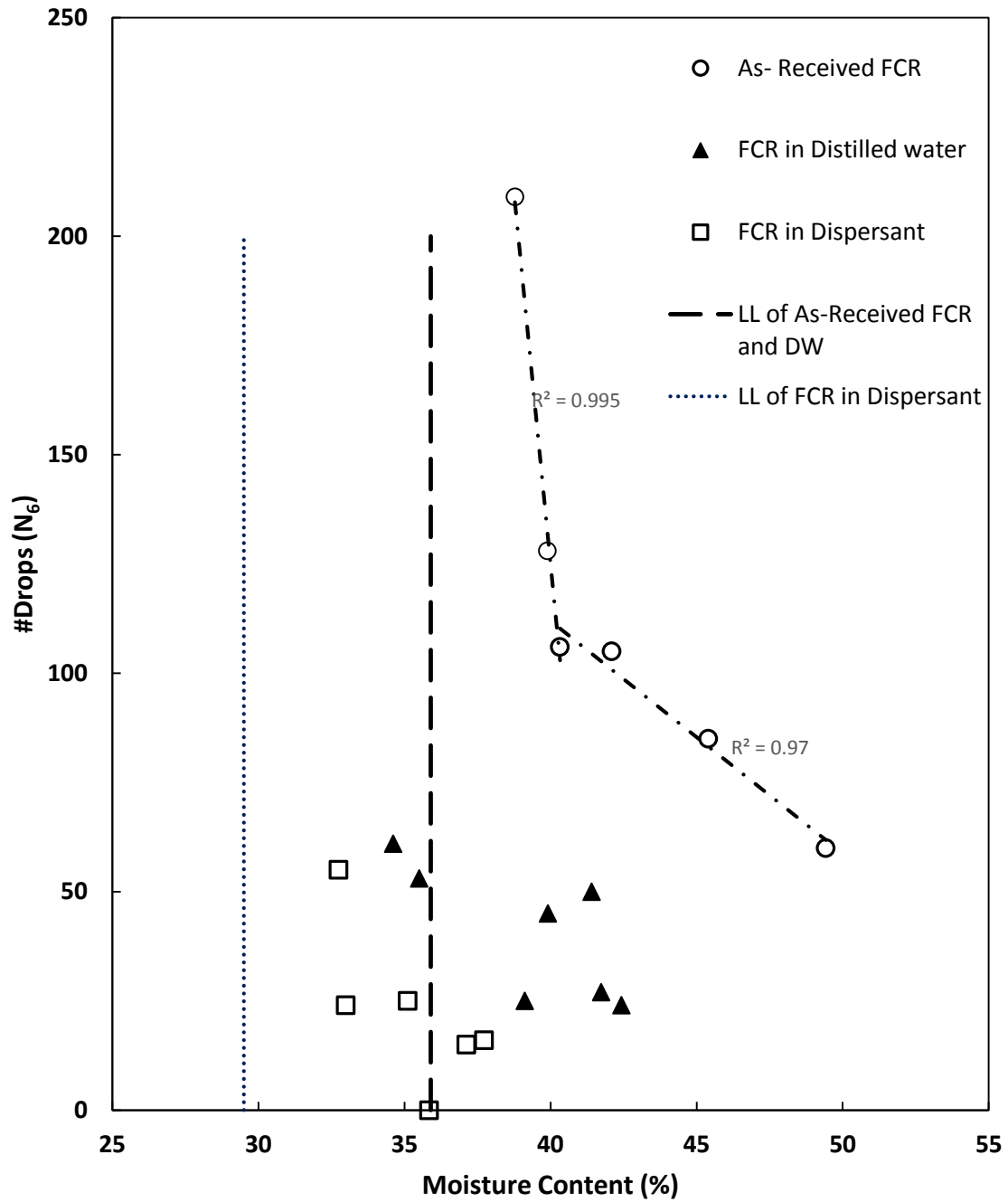
Figure 6-7. Variation of flowability with moisture content of FCR with different background solutions
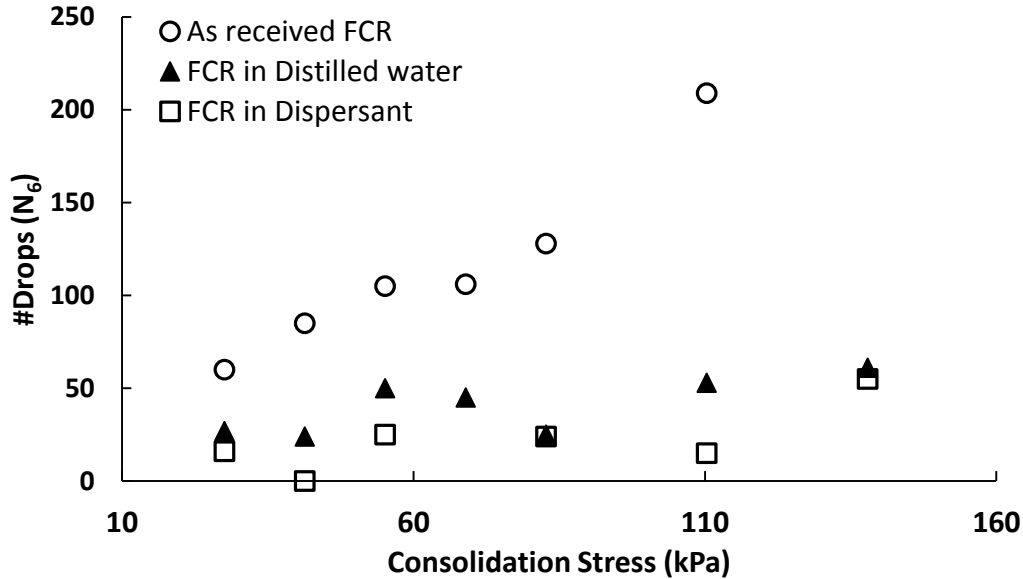
Figure 6-8. . Variation of flowability with applied consolidation stress

6.4.2 VANE SHEAR TESTS

Figure 6-9 shows the average undrained shear strength values of specimens prepared with different background solutions. For all consolidation stresses, the undrained shear strength of the as-received FCR in supernatant solution (with flocculant) is greater than that for both dispersant and distilled water cases. Note the sharp decrease in shear strength for the specimens consolidated at below about 83 kPa (12 psi).

These specimens are very soft and have low strength. For reference, vane shear measurements were conducted on selected common products and summarized in Table 6-2. For example, creamy peanut butter has a C_u of about 12 kPa.

Figure 6-10 shows the variation of the average values of the undrained shear strength of the FCR with different background solutions as a function of the void ratio. The specimens prepared using the dispersant solution and distilled water have lower void ratio values even at higher consolidation pressures. This confirms the lower void ratio values in the more dispersed specimens. In specimens with the dispersant, the void ratio does not significantly vary at higher pressures. The inter-particle spacing cannot be further decreased in this dispersed particle system, likely hindered by the relatively high sodium hexametaphosphate concentration in the pore water at this solids content creating a thixotropic material (observed to be "gel-like"). Thus, no significant further decrease in void ratio is expected, even at high stress levels.

121
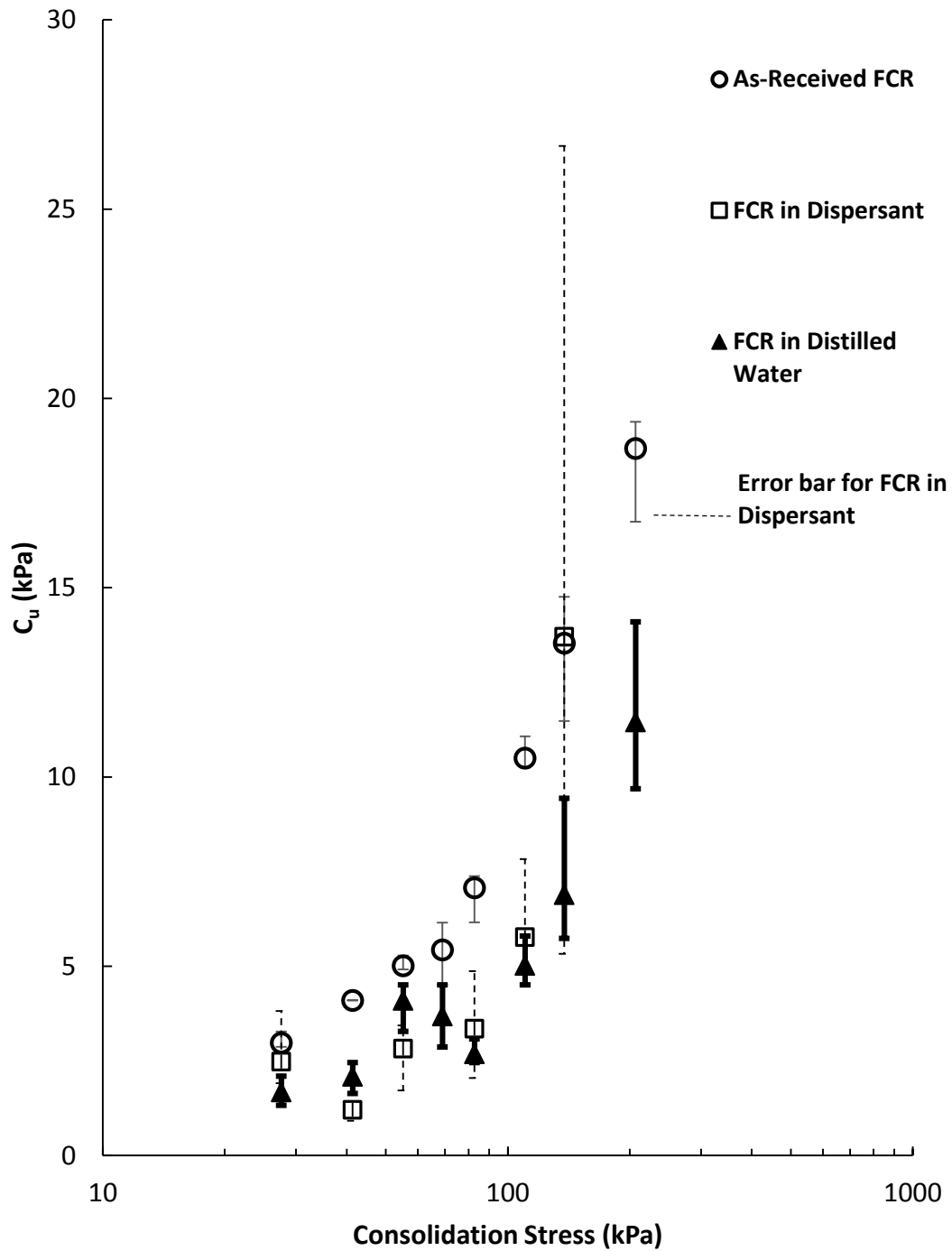
Figure 6-9. Undrained shear strength of FCR in different background solutions. The symbols indicate the mean value, and the error bars indicate the minimum and maximum measured shear strength of each specimen using the vane shear device.

Table 6-2. Undrained shear strength of some known food products as distinctive of softness of FCR

Food Product Name	Greek Yogurt (Kroger)	"Cheese Whiz" Sauce (Kroger)	Petroleum Jelly (Kroger)	Crisco Shortening	Creamy Peanut Butter (ALDI)
C_u (kPa)	0	0.38	1.34	4.5	11.8
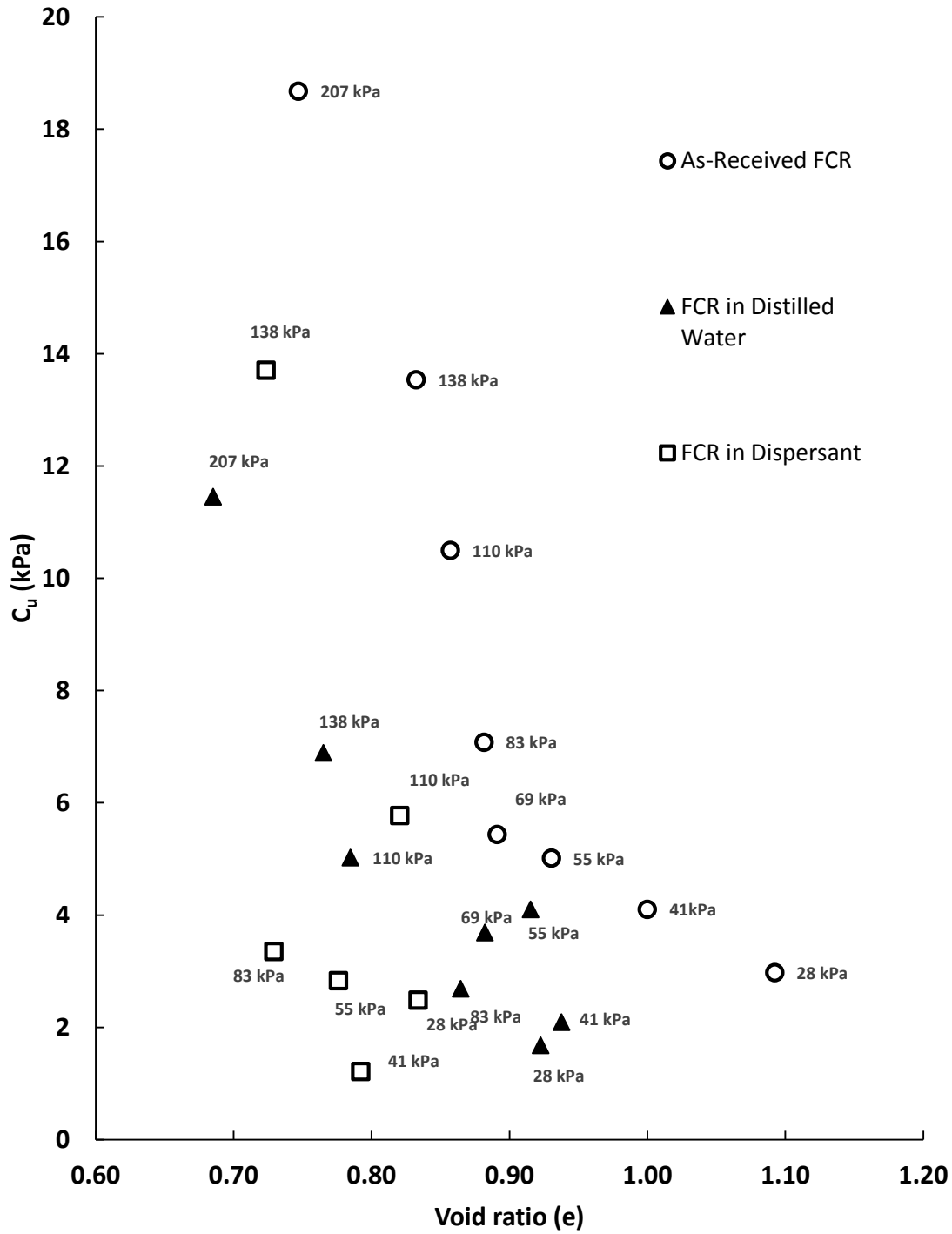
Figure 6-10. Variation of undrained shear strength with void ratio of FCR specimens prepared with different background solutions under various loading conditions. Value of consolidation stress is shown next to data points.

Figure 6-11 shows the effect of background chemistry on variation of moisture content under various consolidation pressures and the impact of that on the undrained shear strength of the FCR. Also shown are the liquid limit (LL) for the FCR with flocculant and the LL for the FCR with the dispersant solution and with distilled water (approximately equal). For a point of reference, Youssef et al. (1965) suggested that the average value of shear strength of soil at its liquid limit is between 1.3 and 2.4 kPa. For the as-received FCR, there is a breakpoint at w=40.3% which can be attributed to flow. The breakpoint happens at a moisture content greater than correspondent liquid limit (LL=35.9%). This indicates that even at moisture contents greater than liquid limit, the FCR has an undrained shear strength greater than what is suggested in traditional soil mechanics (Kuriakose et al., 2017; Wroth and Wood, 1978; Youssef et al., 1965).

Skempton (1957) presented a relationship between normalized undrained strength (ratio of undrained strength to the corresponding overburden pressure) and plasticity index of a soil as (Equation 6-2):

$$\frac{C_u}{P} = 0.11 + 0.0037 \, (PI) \qquad \qquad \textbf{Equation 6-2}$$

where C_u is undrained shear strength, P is overburden pressure and PI is plasticity index.

Mesri (1975) showed that the mobilized undrained shear strength can be expressed independently from plasticity index as Equation 6-3:

$$C_u(mob) = 0.22 \, P \qquad \qquad \textbf{Equation 6-3}$$

Figure 6-12 shows the normalized values of undrained shear strength $(\frac{C_u}{P})$ of the FCR in different background solutions. The normalized values of C_u are compared to the predicted values by Mesri (1975) For all three background solutions.
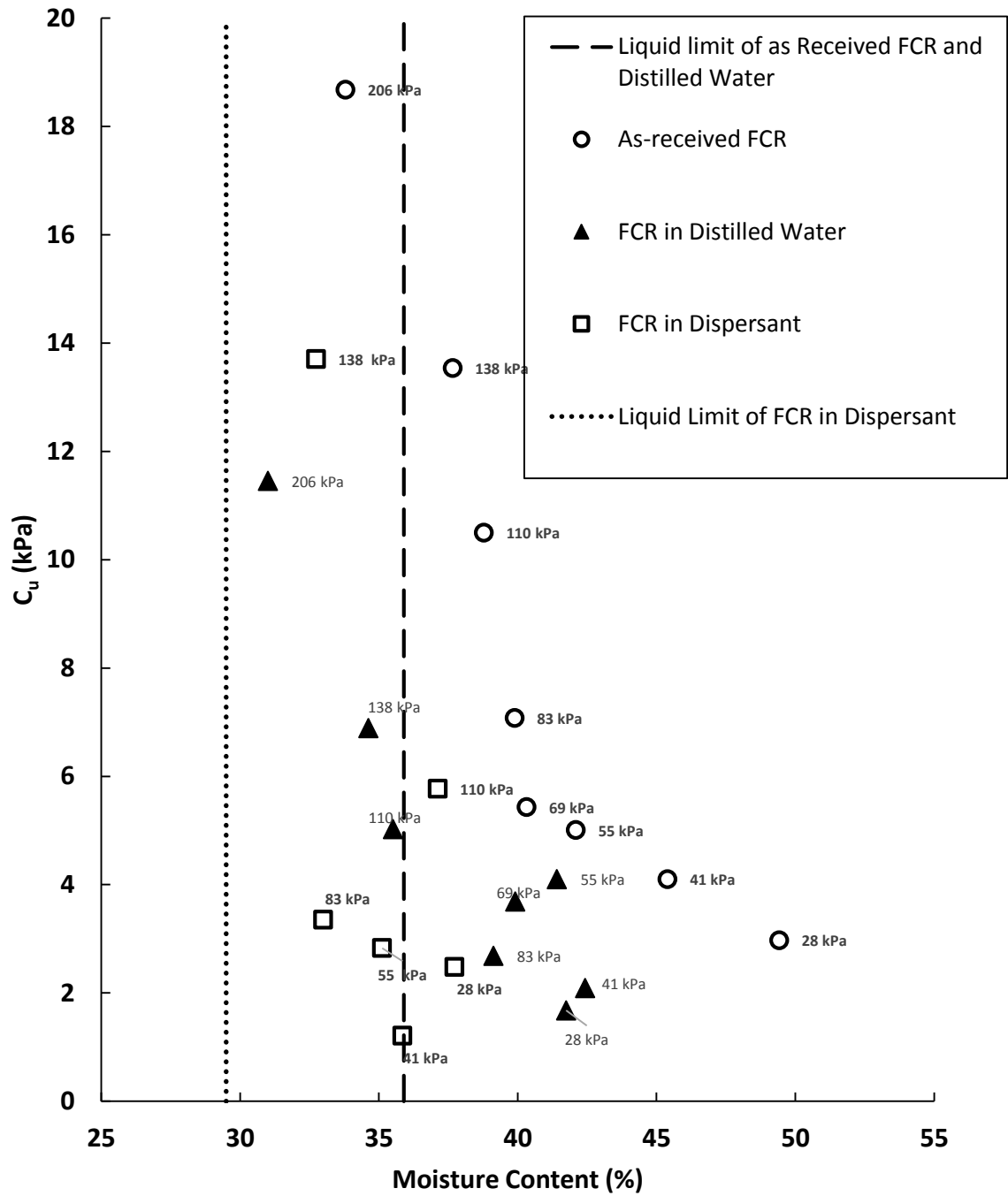
Figure 6-11. Variation of undrained shear strength with moisture content of FCR specimens prepared with different background solutions under various loading conditions. Value of consolidation stress shown next to data points.
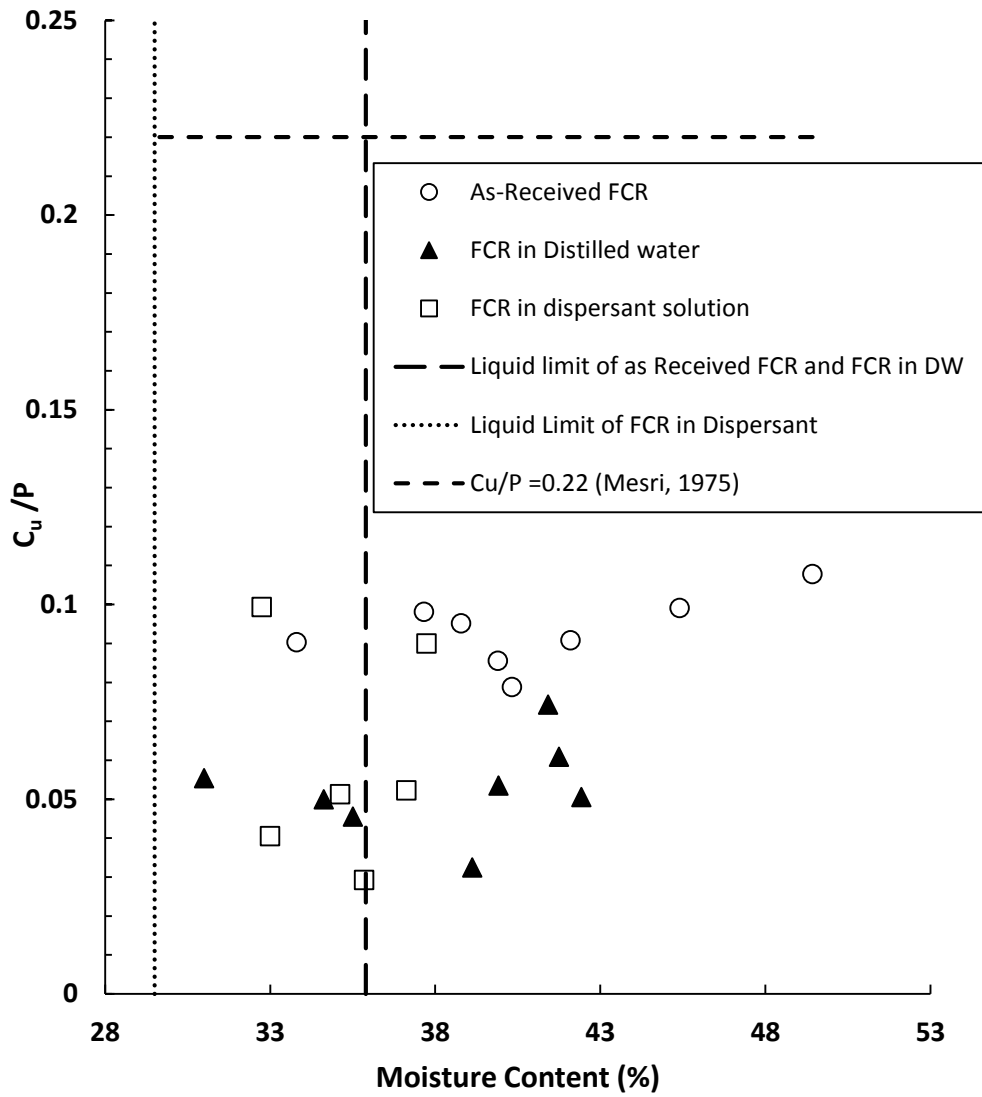
Figure 6-12. Normalized values of undrained strength ($\frac{C_u}{P}$) with moisture content for the FCR in different background solution and their comparison with C/P ratio (Mesri, 1975)

Table 6-3 presents the Atterberg limits of the FCR in different background solutions. The predicted $\frac{C_u}{P}$ values for each background solution using Equation 6-1 is also given.

Figure 6-13 compares the correlation between liquidity index and undrained shear strength from literature with the FCR in different background solutions. Correlations of undrained shear strength and liquidity index of remolded clays from Egypt (Wroth and Wood, 1978; Youssef et al., 1965), sensitive clays (Locat and Demers, 1988), soft alluvial clays from Turkey (Yılmaz, 2000) ,and soft marine clays from India (Kuriakose et al., 2017) are also compared with the experimental data of this study. For the same liquidity index, FCR has higher undrained strength. Further, in case of the as-received FCR, the undrained shear strength is greater even for the cases in which the liquidity index is greater than 1.

Table 6-3. Atterberg limits of the FCR in different background solutions

FCR Background Solution Case	Liquid Limit (LL)	Plastic Limit (PL)	Plasticity Index (PI)	C_u/P (Skempton, 1957)
As-Received FCR	35.8	24.3	11.5	15.26%
FCR in Distilled water	35.7	23.9	11.8	15.48%
FCR in Dispersant	29.5	16	13.5	16%
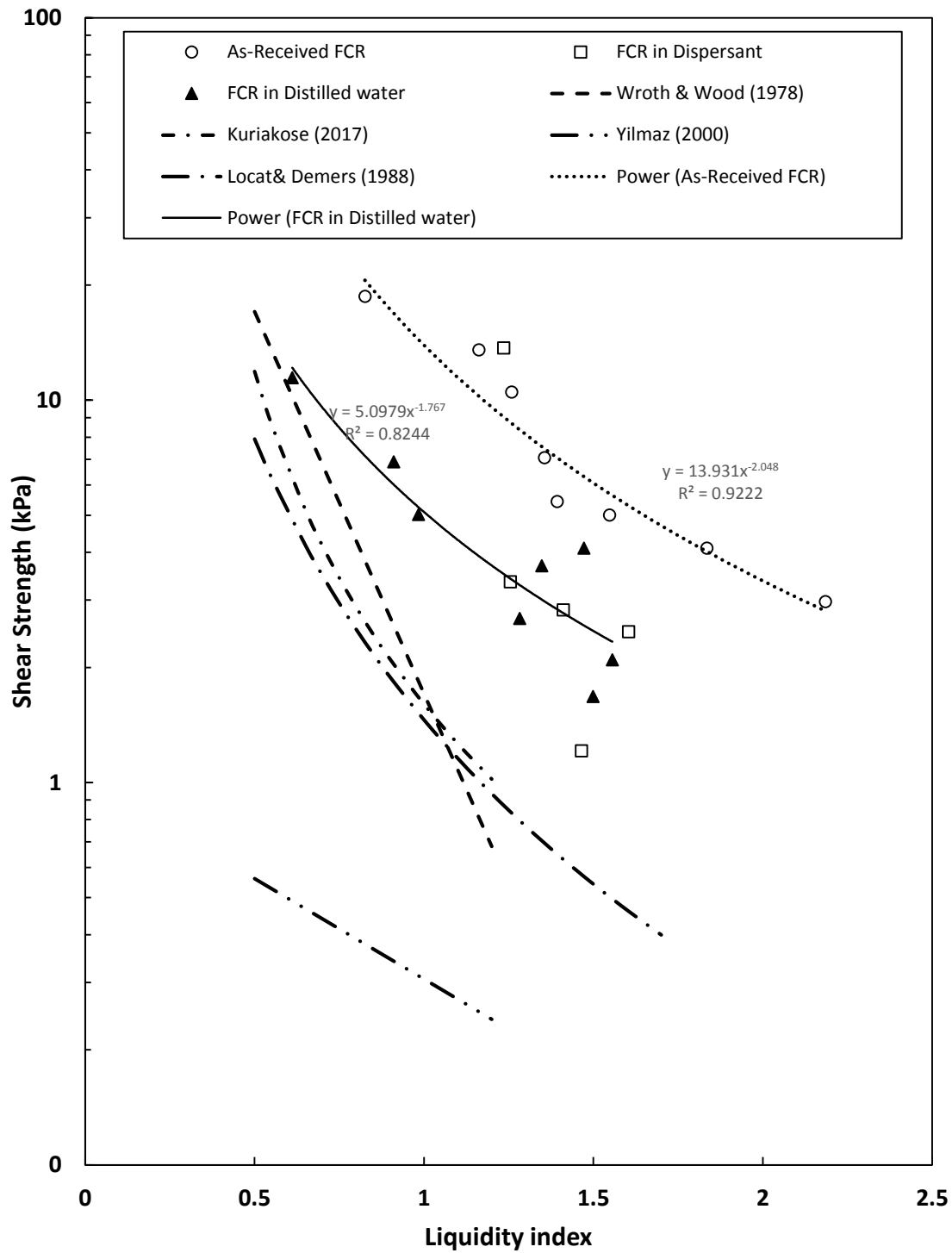
Figure 6-13. Correlation between liquidity index and undrained shear strength. FCR values are compared with data found in the literature

6.5 DISCUSSION

The flow table results suggest that as-received FCR tends to have higher resistance to flow compared to the FCR in either distilled water or dispersant (Figure 6-7). For the as-received FCR, there appears to be an observable threshold at which the number of drops (N_6) increases sharply above this threshold. In other words, this breakpoint indicates that flow is much more likely to occur when the overburden stress is less than about 69 kPa. The breakpoint occurs at the moisture content of about 40%, which is larger than the corresponding liquid limit (LL=35.8%). Thus, even at the moisture contents greater than LL, flow does not happen. The undrained shear strength of the as-received FCR at the threshold is about 5.4 kPa, which is about two times greater than the predicted undrained shear strength for fine-grained soils at their liquid limit (Casagrande, 1958; Youssef et al., 1965)

Figure 6-14 shows the variation of flow with 3 different background solutions. Here, flow is defined as the number of drops required for the any point of the specimen circumference to touch a pre-drawn 6" circle, N_6. The as-obtained FCR specimens have higher N_6 values compared to both the distilled water and dispersant cases. Thus, the flocculant appears to increase the resistance to flow. On the other hand, the FCR specimens in dispersant solution have the lowest resistance to flow for most stress cases tested here.

From the results in Figure 6-14, the number of drops can be correlated to the corresponding undrained shear strength using curve fitting with a reasonable approximation.

Figure 6-12 shows the as-received FCR has a higher sensitivity to the overburden pressure than the FCR in distilled water and dispersant solution. However, the sensitivity of FCR in all of the background solutions are less than the predicted C_u/P values by Skempton (1957) and Mesri (1975). This could be related to the inter-particle interactions due to the particle-level arrangement, or fabric.

The results from vane shear tests suggest that the soil structure affects the undrained shear strength, with the strength decreasing as the background solution changes from flocculated, to distilled water, to dispersant (Figure 6-10). A flocculated particulate system tends to have a higher void ratio, higher compressibility, higher hydraulic conductivity, and higher shear strength than a dispersed one (Lambe and Whitman, 1969). These observations are consistent with those of specimen consistency from the consolidation tests described in chapter 5.
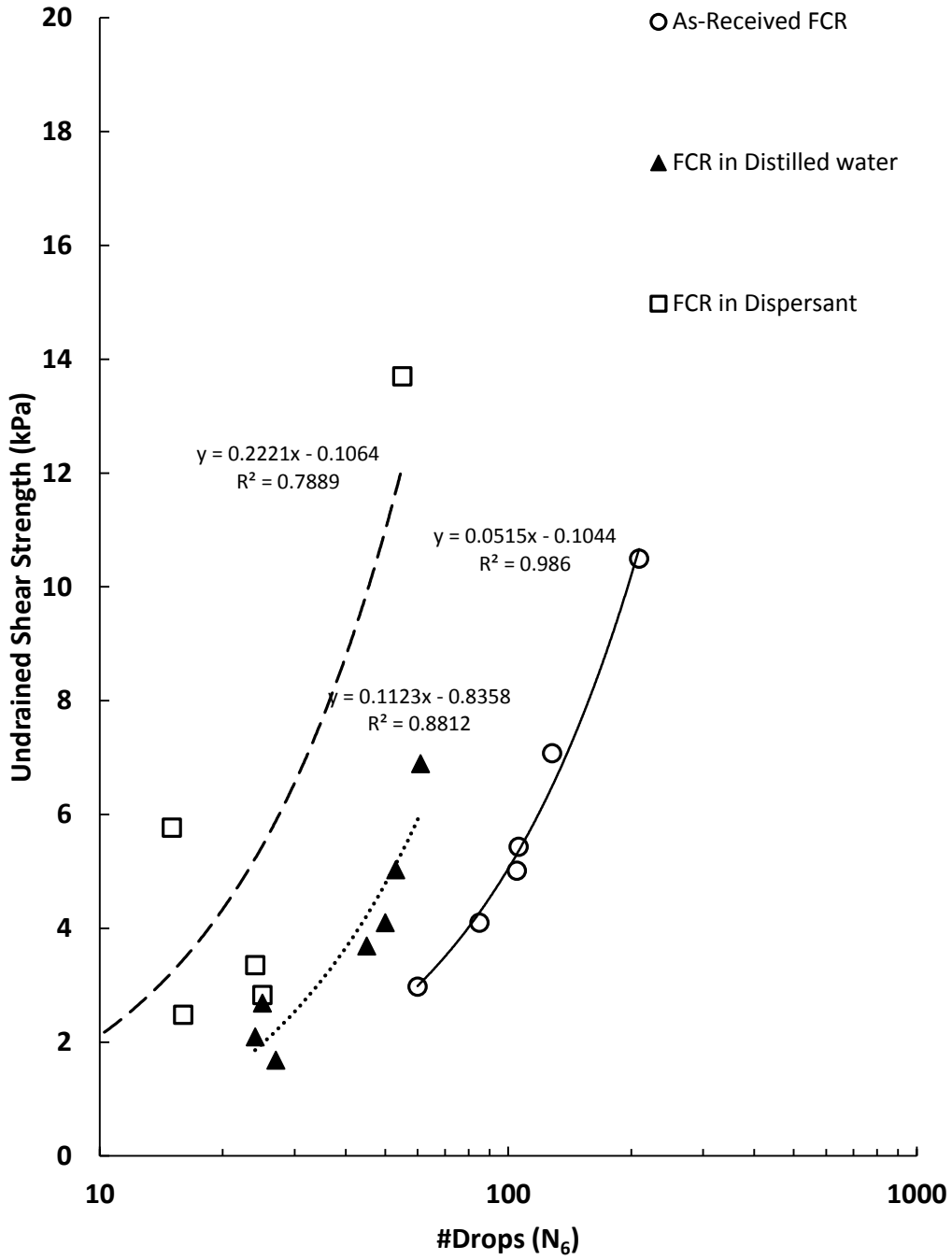
Figure 6-14. Correlation between flowability and undrained shear strength of the FCR in different background solutions

The material properties are a function of the particle-level arrangement, or fabric. Two common fabric types are dispersed and flocculated in which the particles either remain as individual units or bind together to form larger structures, respectively. Fabric, in part, determines the mechanical properties such as shear strength, compressibility, and hydraulic conductivity (Mitchell and Soga, 2005). A summary of the known relationships between clay particle fabric and selected soil properties is shown in Figure 6-15. In nature, the difference in clay particle associations (dispersed vs. flocculated) depends on the surrounding pore fluid chemistry, namely pH and ionic concentration. These associations can be altered by purposefully exposing the materials to chemical additives. For example, the compressibility of clays can be significantly reduced by adding salt, which changes the soil fabric from flocculated to dispersed by reducing the inter particle spacing (Di Maio et al., 2004)

Polymer flocculants are another type of chemical additive used to manipulate particle interactions. The fine particles in FCR slurries tend to remain as individual particles in suspension, i.e. dispersed. These dispersed particles take a very long time to settle (weeks to months). Polymer flocculants are used to bind these particles creating larger formations that settle at a faster rate. These loosely bonded particle structures are called flocs. The mechanism(s) by which the polymer binds to the particle surface depends on the particle surface characteristics (existence of charged sites) and the polymer type, anionic (negatively charged), cationic (positively charged), or non-ionic. The bond types include Coulombic, dipole, hydrogen bonding, and van der Waals. Flocs form when the polymer molecules bind to the surface sites of two or more particles as shown in Figure 6-16 (Hunter, 2001). In order to easily distribute the polymer flocculant into a slurry system, the polymer should be water-soluble. Thus, these flocculants are likely to be highly hydrophilic.

FCR specimens with flocculant (as-received FCR) tend to resist more against flow compared to the FCR in distilled water and dispersant solution. The results of flow table tests shows that there is a reasonable correlation between numbers of drops to reach 6" circle (N_6) and undrained shear strength (C_u). Table 6-4 summarizes the correlation between N_6 and C_u. With these correlations, the undrained shear strength of FCR can be estimated indirectly by conducting the simplified modified flow table test.

Clay Particle-Level Arrangement

	Dispersed	Edge-to-Face Flocculated
Permeability :	low	high
Compressibility :	low	high
Shear resistance :	high or low	very high
Water retention :	low	high
Surface area :	low	high

Impact on Material Properties
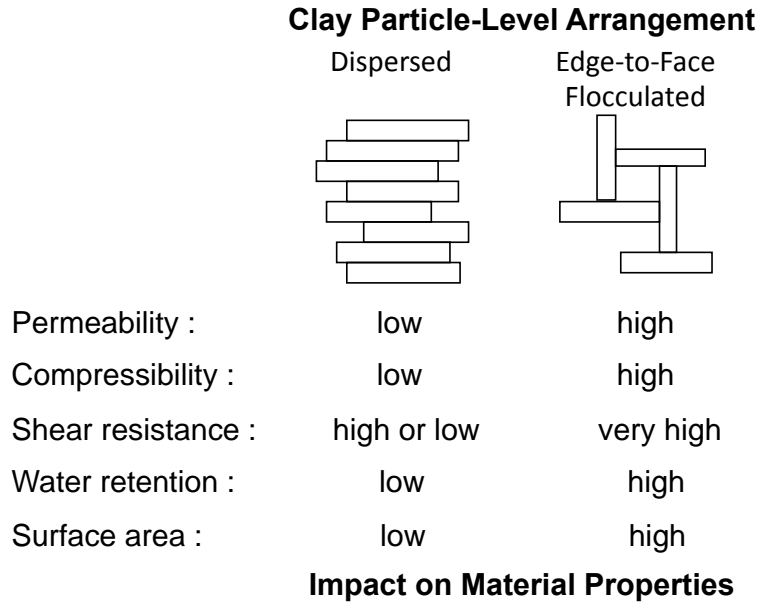
Figure 6-15. Relationship between clay particle fabric and selected material properties.
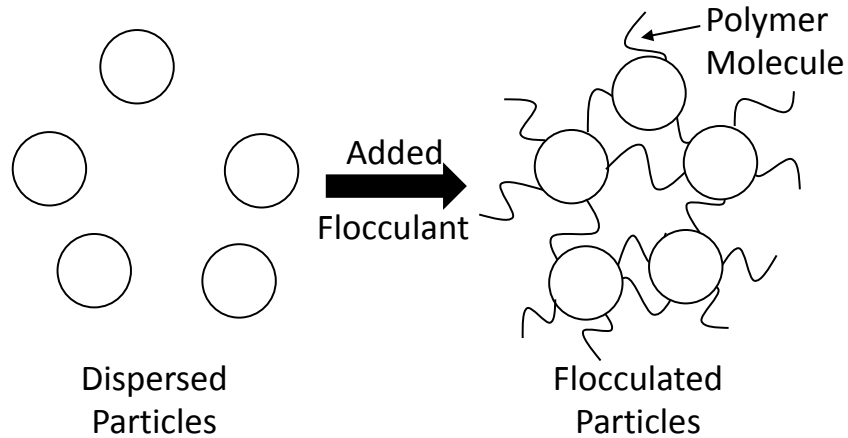
Figure 6-16. Floc formation from dispersed particles induced by a polymer flocculant.

Table 6-4. Correlation equations between flowability and undrained shear strength of the FCR in different background solutions.

FCR Background Solution Case	Correlation Equation	R^2 value
As-Received FCR	$C_u = 0.051N_6 - 0104$	0.986
FCR in Distilled water	$C_u = 0.11N_6 - 0.84$	0.881
FCR in Dispersant Solution	$C_u = 0.22N_6 - 0.106$	0.788

For all consolidation stresses, the undrained shear strength of the as-received FCR in supernatant solution (with flocculant) is greater than that for both dispersant and distilled water cases (Figure 6-9).

The FCR specimens in dispersant have lower undrained shear strength than the FCR with flocculant. Yet, in several tested cases the moisture contents of the dispersant-mixed FCR are lower than the as-received FCR (with flocculant) liquid limit. This observation from Figure 6-11 is counter to the typical relationship between moisture content and shear strength, i.e. strength decreases with increasing moisture content. However, the different background solutions used here highlight the sensitivity of FCR to the surrounding fluid chemistry. Subsequent determination of the liquid limit of the FCR with distilled water and flocculant found that the change in background solution reduced the LL from ~36% to 29.5%. One likely reason for this is the dispersed structure of the FCR after exposure to the dispersant solution, which decreases the amount of water the particulate system can hold.

For all of the FCR specimens in different background solutions, the normalized values of undrained shear strength ($\frac{C_u}{P}$) are less than corresponding values predicted by Skempton (1957) and Mesri (1975) (Table 6-3 and Figure 6-12). The average $\frac{C_u}{P}$ for the as-received FCR specimens, FCR in distilled water and dispersant solution is 9.3%, 5.28% and 6.2% respectively, while the predicted values by Skempton (1957) are 15.3%, 15.5% and 16% respectively. This shows that the FCR has lower sensitivity to the overburden pressure compared to fine-grained soils.

The FCR with dispersant specimens exhibited thixotropic properties at lower pressures. One potential reason for the observed thixotropic behavior of FCR in the dispersant solution may be that the concentration of the dispersant agent increases when the solid content of the slurry increases with increasing consolidation pressure. The inter-particle repulsive forces induced by the dispersant limits the decrease in inter-particle spacing, and particles maintain a minimum distance from one another. This is consistent with the observed lower undrained shear strength and higher flowability of the FCR in the dispersant solution. This may also explain the lower moisture content of FCR in dispersant at the same stress level compared to distilled water and as-received FCR.

The correlation between liquidity index (LI) and undrained shear strength (C_u) shows a reasonable link between them in as-received FCR and the FCR in distilled water while there is not any visible trend for the FCR in dispersant solution (Figure 6-13). Comparison of the correlations in literature which are based on fine-grained soils, and the results from this study show that the FCR tends to have higher undrained shear strength at the same corresponding liquidity index compared to the fine-grained soils presented by other researchers (Kuriakose et al., 2017; Locat and Demers, 1988; Wroth and Wood, 1978; Yılmaz, 2000).The FCR has larger undrained strength and in case of the as-received FCR, the undrained strength is higher even in liquidity indices larger than 1.

6.6 CONCLUSIONS

The flowability varies with the type of background solution used to prepare the FCR specimens (Figure 6-12). At similar moisture contents, the number of drops required for the specimen to reach the 6" diameter mark (N_6) is higher for the as-received case (with flocculant) than the distilled water and dispersant cases. This observation is consistent with the vane shear test results in that the FCR with flocculant had a higher undrained shear strength compared to the FCR in distilled water and dispersant solutions. The polymer flocculant binds the particles together and creates resistance to flow in the FCR. In case of the FCR in the dispersant solution, higher flowability was observed compared to the FCR in distilled water and flocculant solution (as-received FCR) at the same moisture content.

There is a good correlation between N_6 and the undrained shear strength (C_u) of the as-received FCR (Figure 6-13). Also for other background solutions there are reasonable correlations and it can be used to estimate the undrained shear strength of FCR indirectly only by conducting flow table test.

The polymer flocculant which is added to the as-received FCR alters the properties of the FCR by bonding the particles together (Figure 6-16) and forming the flocs increases the undrained strength and consequently increases the resistance of the FCR against flow.

The as-received FCR has a greater sensitivity to the consolidation pressure than the FCR in distilled water and dispersant solution in which the flowability remains almost constant with increase of applied consolidation pressure. The FCR with dispersant specimens exhibited thixotropic properties at lower pressures. One potential reason for the observed thixotropic behavior of FCR in the dispersant solution may be that the concentration of the dispersant agent increases when the solid content of the slurry increases with increasing consolidation pressure. The inter-particle repulsive forces induced by the dispersant limits the decrease in inter-particle spacing, and particles maintain a minimum distance from one another. This is consistent with the observed lower undrained shear strength and higher flowability of the FCR in the dispersant solution. This may also explain the lower moisture content of FCR in dispersant at the same stress level compared to distilled water and as-received FCR.

Vane shear tests conducted on slurry specimens consolidated to relatively low stress levels demonstrated that at very low consolidation stresses, the FCR has low undrained strength, only slightly greater than that typically attributed to the liquid limit. However, as the consolidation stress increases, a sharp increase in the strength was observed. This response was observed for slurry specimens prepared with the flocculant, with distilled water, and with a dispersant. The undrained shear strength decreased according to the following order of background fluids: flocculant, distilled water, and dispersant. This suggests that tests on fresh slurry with flocculant overestimate the undrained shear strength (or resistance to flow) relative to in situ samples in which the flocculant may no longer be viable, and thus the fabric is transitioning into a more dispersed structure. These results also suggest that the liquid limit may not coincide with the increase

135

in strength or water content above which the strength decreases abruptly, and that the LL determined from samples with flocculant may not represent the LL of FCR if the flocculant loses its effectiveness. The flow table results indicate that the flocculant in the FCR slurry makes the material less susceptible to flow due to the polymer-particle associations. On the other hand, under applied loads the inter-particle spacing cannot be further decreased when there is dispersant in particle system. This is likely due to the relatively high dispersant concentration in the pore water at this solids content creating a thixotropic material (observed to be "gel-like"). Thus, no significant further decrease in void ratio is expected, even at high stress levels, which makes the FCR more flowable when dispersant is added. The role of the flocculant with respect to the resistance to flow is important in considerations of the long-term stability of these impounded refuse materials.

6.7 REFERENCES

ASTM-C230/C230M, 2014. Standard Specification for Flow Table for Use in Tests of Hydraulic Cement.

ASTM-D4648/D4648M, 2016. Standard Test Methods for Laboratory Miniature Vane Shear Test for Saturated Fine-Grained Clayey Soil. American Society for Testing and Materials.

Beier, N., Wilson, W., Dunmola, A., Sego, D., 2013. Impact of flocculation-based dewatering on the shear strength of oil sands fine tailings. Canadian Geotechnical Journal 50, 1001-1007.

BS-1377, 1990. Methods of Test for Soils for Civil Engineering Purposes, BS 1377, "Determination of shear strength by the laboratory vane method", pp. 1-3.

Casagrande, A., 1958. Notes on the design of liquid limit device. Geotechniqe 8, 84-91.

Di Maio, C., Santoli, L., Schiovone, P., 2004. Volume Change Behavior of Clays: the Influence of Mineral Composition, Pore Fluid Composition, and Stress Rate. Mechanics of Materials 36, 435-451.

Hegazy, Y.A., Cushing, A.G., Lewis, C.J., 2004. Physical, mechanical, and hydraulic properties of coal refuse for slurry impoundment design. Geotechnical and Geophysical Site Characterization Vols 1 and 2, 1285-1291.

Hunter, R.J., 2001. Foundations of Colloid Science, 2nd ed. Oxford University Press, New York.

Jedari, C., Palomino, A.M., Cyr, H.J., Drumm, E.C., Boles, D., 2017. Grain and Floc Size Distribution Analysis of Fine Coal Refuse Slurry, Proceeding of 19th International Conference on Soil Mechanics and Geotechnical Engineering. ISSMGE, Seoul, Korea, pp. 403-406.

Kuriakose, B., Abraham, B.M., Sridharan, A., Jose, B.T., 2017. Water Content Ratio: An Effective Substitute for Liquidity Index for Prediction of Shear Strength of Clays. Geotechnical and Geological Engineering 35, 1577-1586.

Lambe, T.W., Whitman, R.V., 1969. Soil Mechanics. John Wiley & Sons, New York.

Leroueil, S., Tavenas, F., Bihan, J.-P.L., 1983. Propriétés caractéristiques des argiles de l'est du Canada. Canadian Geotechnical Journal 20, 681-705.

Locat, J., Demers, D., 1988. Viscosity, yield stress, remolded strength, and liquidity index relationships for sensitive clays. Canadian Geotechnical Journal 25, 799-806.

Mesri, G., 1975. New design procedure for stability of soft clays. [Discussion.]. Geotechnical Engineering Division, ASCE 101, 409-412.

Mitchell, J.K., Soga, K., 2005. Fundamentals of Soil Behavior, 3rd ed. Wiley.

Norman, L.E.J., 1958. A comparison of values of liquid limit determined with apparatus having bases of different hardness. Geotechnique 8, 79-83.

Skempton, A.W., 1957. Discussion: Further data on the c/p ratio in normally consolidated clays, Proceedings of the Institution of Civil Engineers, pp. 305-307.

Sridharan, A., Prakash, K., 1999. Mechanisms controlling the undrained shear strength behaviour of clays. Canadian Geotechnical Journal 36, 1030-1038.

Taylor, D.W., 1948. Fundamentals of Soil Mechanics. John Wiley and sons, New York.

Wintermyer, A.M., Kinter, E.B., 1955. Dispersing Agents for Particle-Size Analysis of Soils. Highway Research Board Bulletin 95, 1-14.

Wroth, C.P., Wood, D.M., 1978. The correlation of index properties with some basic engineering properties of soils. Canadian Geotechnical Journal 15, 137-145.

Yılmaz, I., 2000. Evaluation of shear strength of clayey soils by using their liquidity index. Bulletin of Engineering Geology and the Environment 59, 227-229.

Youssef, M.S., El Ramli, A.H., El Demery, M., 1965. Relationships between shear strength, consolidation, liquid limit, and plastic limit for remoulded clays, The 6th International Conference on Soil Mechanics and Foundation Engineering, Montreal, pp. 126-129.

Yu, H., 2014. Geotechnical Properties and Flow Behavior of Coal Refuse under Static and Impact Loading, Civil engineering. Case Western Reserve University, Cleveland, OH.

CHAPTER VII
CONCLUSIONS AND RECOMMENDATIONS FOR FUTURE STUDIES

Fine coal refuse is a by-product of the coal mining process, and is usually mixed with water and a flocculant and is hydraulically placed behind impoundments constructed primarily with coarse coal refuse. The rate at which the FCR consolidates is one of the most critical characteristics of impounded mine waste material related to destabilization, i.e. flow. The general assumption is that the fine refuse in these impoundments will consolidate over time due to the overburden weight of the material above, losing some of the fluid-like properties that it possessed when initially placed. This consolidation process decreases the volume of the slurry, as the water is squeezed out, with the water pressure in the pores between solid particles decreasing over time. This consolidation and dissipation in pore pressure is accompanied by an increase in strength. Yet, the consolidation behavior of fine coal slurry has not been fully investigated. There are limited observations of the characteristics of slurry in place and its variation with depth within slurry impoundments. Furthermore, there is no generally agreed upon model for the consolidation behavior of these materials, which would define under what conditions they are being consolidated.

The results of this study give a better understanding of the consolidation behavior and undrained shear resistance of the hydraulically placed FCR behind impoundments. In this chapter the conclusions of this study are summarized and some recommendations for future studies have been made.

7.1 CONCLUSIONS RELATED TO THE FIELD EXPLORATION OF AN EXISTING SLURRY IMPOUNDMENT

In this study, the in situ characteristics of FCR in an inactive impoundment were investigated through a geotechnical exploration to a depth of about 60 m. Results show that in spite of being hydraulically placed, the FCR materials are very heterogeneous and the grain size distribution curves indicated there are two major groups of material referred to as "sandy" and "silty" fine coal refuse. The Atterberg limits of the FCR from different depths found scattered values for moisture content, liquid limit and plastic limit, and in some zones values of liquidity index which were greater than 1 suggesting the potential of local flowable material. Despite being in place a long time allowing for consolidation (approximately 40 years), some thin "fluid-like" zones were observed in the split-spoon. The SPT blow counts (N_{60}-values) in the FCR range from 7 to 15 blows per foot suggesting medium to stiff material consistency, which does not reflect the presence of the observed thin layers of very soft material, nor the WOT materials recorded or the measured liquidity index values greater than 1. It appears the stiffer and coarser FCR materials produce N-values which represent the material consistency over the length of the sampler, and may obscure the presence of the short intervals of very soft material. This suggests the SPT is not an effective means to investigate slurry placed materials if the intent is to identify thin zones of very soft, potentially flowable under-consolidated materials.

A series of grain size distribution measurements using traditional hydrometer tests and laser diffraction analysis were performed on fine coal refuse and kaolin suspensions to investigate the capability of each method for capturing the effective grain size distribution as a function of background chemistry. The results show that (1) the background solution chemistry influences the FCR floc stability and alters the grain size distribution over time and (2) the D_{90}, D_{50}, and D_{10} values obtained from the two methods are not in agreement, with larger D_{90} values reported from hydrometer analysis. The differences between the values obtained highlight one important limitaion of hydrometer analysis, which is the assumption the effective grain size distribution remains constant with time. If grain size changes during the hydrometer analysis, the initial readings represent a different sample than the final readings and may not be comparable. In other words, the hydrometer test may not accurately measure effective grain size distribution over the measurement period.

Laser diffraction offers several advantages over hydrometer analysis including a short measurement period, small sample size requirement, and the ability to measure a wide range of particle sizes in the same analysis. This study highlights another advantage of the PSA method, the ability to accurately measure changes in particle size over time within the same sample. The ability to capture real-time flocculation or deflocculation means this technique can be applied to grain size distribution studies of FCR slurries, and other comparable materials, in their as-placed condition without any pretreatment. This method has the ability to capture dynamic particle interactions over the time.

Based on the particle size analyses, the background solution composition has a significant influence on the formation of flocs in FCR suspensions and thus the effective grain size distribution. However, the effective grain size distribution may also change over time even for the same background solution. These findings are relevant to the overall stability of FCR in impoundments in that particle associations and the presence of a flocculant have a significant impact on the macro-scale properties of FCR, such as consolidation behavior and flow potential.

Three flow models were selected to identify the best fit for predicting the flow behavior of FCR suspensions and identify the presence of flocs: Newtonian/Bingham plastic model, power law model, and the Casson model. The models that best describe the FCR suspensions tested for this study are the (near) Newtonian/Bingham plastic model, with both ideal and non-ideal behavior, and the power law model. Within each model, flocculation was evident in the distilled water and supernatant cases, while very little to no flocculation was observed for the dispersant and as-received suspensions. Note that the as-received material contains a flocculant in the supernatant. Yet, the influence of the flocculant on viscosity was not

significantly different than the distilled water case.

7.3   CONSOLIDATION AND TIME RATE OF SETTLEMENT OF THE IN SITU AND FRESH SLURRY FCR

The consolidation of fine coal refuse has been investigated based on in situ sampling and laboratory measurements of the coefficient of consolidation from both solid and liquid slurry samples. These data are used to predict the time rate of consolidation using classical Terzaghi theory, a finite strain method, and a new method employing a spatial and temporal variable coefficient of consolidation. The results suggest that while the variable coefficient of consolidation method may best reflect the low degree of consolidation at early times when the material is still essentially slurry, a similar response can be obtained using the Terzaghi method with constant value of coefficient of consolidation obtained from measurements of the slurry consolidation at low stress levels. The low value of coefficient of consolidation has little effect on the degree of consolidation at large time due to the nature of the governing differential equation which assumes that the degree of consolidation asymptotically approaches 100% at time equal to infinity. The consolidation response of hydraulically placed slurry at early times is most important with respect to construction staging, impoundment closure, and personnel safety. The results show that as the slurry material reaches 90% consolidation, the assumption of constant C_v is reasonable and the time to reach 90% is not highly dependent upon the value chosen for C_v, and the value of the coefficient of consolidation has little impact on the degree of consolidation.

The traditional Terzaghi method yields similar results as the variable C_v method, provided the minimum value of C_v from the slurry consolidation is in use, and the differences are greatest at early times.

7.4   UNDRAINED SHEAR STRENGTH AS MEASURED BY VANE SHEAR TESTING AND THE EFFECTS OF FLOCCULENT

The flowability varies with the type of background solution used to prepare the FCR specimens. At similar moisture contents, the number of drops required for the specimen to reach the 6" diameter mark (N_6) is higher for the as-received case (with flocculant) than the distilled water and dispersant cases. This observation is consistent with the vane shear test results in that the FCR with flocculant had a higher undrained shear strength compared to the FCR in distilled water and dispersant solutions. The polymer flocculant binds the particles together and creates resistance to flow in the FCR. In case of the FCR in the dispersant solution, higher flowability was observed compared to the FCR in distilled water and flocculant solution (as-received FCR) at the same moisture content.

There is a good correlation between N_6 and the undrained shear strength (C_u) of the as-received

142

FCR Also for other background solutions there are reasonable correlations and it can be used to estimate the undrained shear strength of FCR indirectly only by conducting flow table test.

The polymer flocculant which is added to the as-received FCR alters the properties of the FCR by bonding the particles together and forming the flocs increases the undrained strength and consequently increases the resistance of the FCR against flow.

The as-received FCR has a greater sensitivity to the consolidation pressure than the FCR in distilled water and dispersant solution in which the flowability remains almost constant with increase of applied consolidation pressure. The FCR with dispersant specimens exhibited thixotropic properties at lower pressures. One potential reason for the observed thixotropic behavior of FCR in the dispersant solution may be that the concentration of the dispersant agent increases when the solid content of the slurry increases with increasing consolidation pressure. The inter-particle repulsive forces induced by the dispersant limits the decrease in inter-particle spacing, and particles maintain a minimum distance from one another. This is consistent with the observed lower undrained shear strength and higher flowability of the FCR in the dispersant solution. This may also explain the lower moisture content of FCR in dispersant at the same stress level compared to distilled water and as-received FCR.

Vane shear tests conducted on slurry specimens consolidated to relatively low stress levels demonstrated that at very low consolidation stresses, the FCR has low undrained strength, only slightly greater than that typically attributed to the liquid limit. However, as the consolidation stress increases, a sharp increase in the strength was observed. This response was observed for slurry specimens prepared with the flocculant, with distilled water, and with a dispersant. The undrained shear strength decreased according to the following order of background fluids: flocculant, distilled water, and dispersant. This suggests that tests on fresh slurry with flocculant overestimate the undrained shear strength (or resistance to flow) relative to in situ samples in which the flocculant may no longer be viable, and thus the fabric is transitioning into a more dispersed structure. These results also suggest that the liquid limit may not coincide with the increase in strength or water content above which the strength decreases abruptly, and that the LL determined from samples with flocculant may not represent the LL of FCR if the flocculant loses its effectiveness. The flow table results indicate that the flocculant in the FCR slurry makes the material less susceptible to flow due to the polymer-particle associations. On the other hand, under applied loads the inter-particle spacing cannot be further decreased when there is dispersant in particle system. This is likely due to the relatively high dispersant concentration in the pore water at this solids content creating a thixotropic material (observed to be "gel-like"). Thus, no significant further decrease in void ratio is expected, even at high stress levels, which makes the FCR more flowable when dispersant is added. The role of the flocculant with respect to the resistance to flow is important in considerations of the long-term stability of these impounded refuse materials.

7.5   KEY CONCLUSIONS

- The standard penetration test (SPT) is not an effective means to investigate slurry placed materials if the intent is to identify thin zones of very soft, potentially flowable under-consolidated materials.

- Although the influence of solution chemistry on fabric is well-known for clay mineral particle systems, these same dependencies of fabric on the surrounding fluid composition have not been considered for the silt-sized manufactured (non-clay mineral) FCR particles. The particle-level structure, flocculated or dispersed, of FCR was shown to be strongly controlled by the background solution composition.

- The flocculant added to the FCR just prior to placement in the impoundment may degrade over time. This is suggested by two distinct observations: a) apparent grain size changes due to floc breakage during laser diffraction testing and b) much lower void ratios measured in the in situ samples relative to fresh slurry samples at similar consolidation stresses. Thus, flocs formed during the initial mixing and placement of FCR may breakdown into individual particles as the flocculant ages, with corresponding changes in behavior.

- The prediction of the time rate of consolidation for slurry placed FCR is made difficult by the wide range of values found for the coefficient of consolidation, C_v. As the slurry material reaches 90% consolidation, the assumption of constant value of C_v is reasonable and the time to reach 90% is not highly dependent upon the value chosen for C_v due to the nature of the governing differential equation. Hence, the value of the coefficient of consolidation has little impact on the degree of consolidation at large times.

- Because the construction, final closure, and subsequent safety of FCR impoundments is dependent upon the consolidation of the FCR at lower times or degrees of consolidation, values of C_v obtained from column slurry tests such as those conducted here may be required. Similarly, the use of a variable C_v approach may lead to better predictions of degree of consolation at early time.

- The traditional Terzaghi method yields similar results as the variable C_v method, provided the minimum value of C_v from the slurry consolidation is in use, and the differences are greatest at early times.

- Liquid limit may not adequately predict the potential for flow, but the vane shear test and flow table test may provide a more rational and repeatable threshold measurement.

- The undrained shear strength of the FCR decreases according to the following order of background fluids: flocculant, distilled water, and dispersant. This suggests that tests on fresh slurry with flocculant overestimate the undrained shear strength (or resistance to flow) relative to in situ samples in which the flocculant may no longer be viable, and thus the fabric is transitioning into a more dispersed structure.

- The as-received FCR has a greater sensitivity to the consolidation pressure than the FCR in distilled water and dispersant solution in which the flowability remains almost constant with increase of applied

consolidation pressure

- Fresh slurry material properties may not be a good proxy for understanding the material properties of FCR impounded for many years due to changes in particle association.

7.6 RECOMMENDATIONS FOR FUTURE WORK

a) In a FCR slurry, the low solids content in the early stages of consolidation result in a magnitude of vertical strain that is large relative to the final FCR thickness, and the change in void ratio and variation of the permeability is significant during the consolidation process. Assuming that the slurry consolidation is one dimensional and the drainage is allowed from both the top and bottom, the consolidation or solidification begins at the upper and lower boundaries of the slurry and the gradient of pore pressure varies across the sample. As the consolidation process continues, the thickness of solidified areas at the top and bottom of the sample increases as depicted in the schematic of Figure 7-1. The consolidation process is thus controlled by the permeability of the more solid material at each the top and bottom of the layer. When the two solid regions combine, there is finally effective stress build-up throughout the layer. Prior to this solidification/consolidation across the entire layer, a zone of fluid-like material may form due to the much lower permeability of material at the upper and lower boundaries which may lead to trapping of slurry material in between those boundaries. This mechanism might prevent dissipation of excess pore water pressure (fluid pressure) even over the life time of the impoundment. This can lead to the formation of thin layers of fluid-like material which may be susceptible to flow or destabilization.

b) The formation of filter cakes of finer FCR adjacent to coarser layers and their impact on the dissipation of pore water pressure can be studied in future research.

c) The influence of flocculant on the consolidation properties of FCR is another interesting topic which can be studied further. Similar to the vane shear tests, consolidation testing on samples consolidated with distilled water and dispersant could be conducted and the response examined with respect to the flocculant samples. Furthermore, the aging of the flocculant can also be addressed.
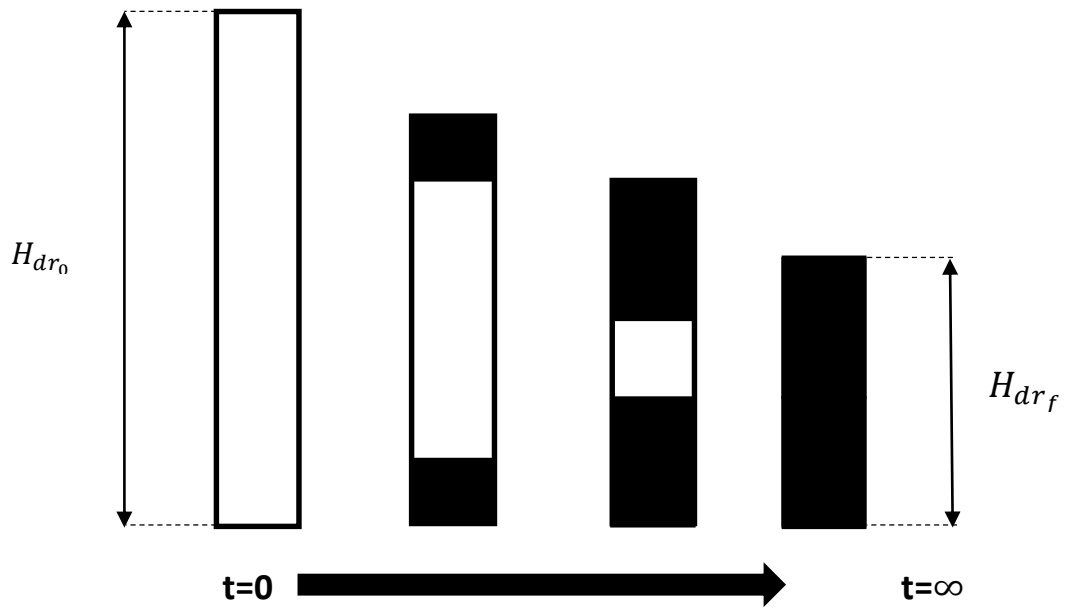
Figure 7-1. Schematic of the 1-D consolidation process of slurry. White zones depict slurry with low solids content and dark filled zones correspond to more solid areas for which Terzaghi's consolidation theory may be valid.

VITA

Cyrus Jedari is from Tabriz, Iran. He has a Bachelor's degree in Civil Engineering, from Mohaghegh Ardebili University and a Master's degree in Geotechnical Engineering from Kharazmi University. He joined University of Tennessee as a Ph. D. student in August 2015 and started his research from then. During his education at the University of Tennessee, he received a summer graduate research fellowship award. He has presented his research at International Foundations Congress and Equipment Expo (IFCEE 2018, Orlando). Also his research has been presented at 19th International Conference on Soil Mechanics and Geotechnical Engineering, Seoul, South Korea.